9-3-2020 1:00 PM

Developing a model to assess the contribution of cytokeratin 19-expressing cells during multipotent stromal cell-induced islet regeneration

Brianna Ananthan, *The University of Western Ontario*

Supervisor: Hess, David A., *Robarts Research Institute*

A thesis submitted in partial fulfillment of the requirements for the Master of Science degree in Physiology and Pharmacology

Abstract

Previously, pharmacological activation of Wnt-signaling in human bone marrow-derived multipotent stromal cells (hMSC) generated conditioned media (CM) that promoted β-cell regeneration in streptozotocin-treated mice. Ductal-derived endocrine progenitors, which have been shown to generate β-cells following pancreatic injury, represent a candidate for the 'signal-receiving cell'. Ductal (CK19+) cells from mice pancreata obtained by purification of live Dolichos Biflorus Agglutinin lectin+ cells and cultured in minimal media supplemented with Untreated, Wnt-activated, or Wnt-inhibited CM demonstrated a significantly increased proportion of EdU+/CK19+ cells following 48-hours of supplementation but no endocrine phenotype acquisition. Lineage-tracing CK19-CreERT;Ai9(RCL-tdT) mice treated with tamoxifen (single dose) demonstrated specific labeling of pancreatic CK19+ cells. Streptozotocin treatment (60 mg/kg/day, 5 days) resulted in decreased β-cell mass, islet density, and insulin+ cell frequency, as well as impaired glucose tolerance and increased pancreatic leukocyte infiltration. This model will be used in future studies to lineage-trace CK19+ cell contribution during hMSC CM-induced islet regeneration.

Keywords: Multipotent Stromal Cell, Conditioned Media, Cell-free Therapy, Islet Regeneration, Diabetes, Cytokeratin 19, Ductal Cell, Lineage Tracing, Streptozotocin.

Summary

Type 1 diabetes is characterized by the destruction of insulin-producing β-cells in pancreatic islets, leaving patients unable to control their blood glucose. Regeneration of lost β-cells represents a promising treatment strategy. Our lab pioneered the use of transplanted human bone-marrow derived mesenchymal stem cells (MSC) to stimulate islet regeneration in mice with β-cell destruction. Pharmacological activation of the Wnt-pathway in MSC cultures generated a concentrated protein mixture (CM) that consistently reduced blood glucose levels in mice with diabetes. However, the identity of signal-receiving cells that mediate islet regeneration within the pancreas remains unknown. Recently, regeneration of β-cells from pancreatic duct cells has been demonstrated. Treating isolated pancreatic duct cells with MSC CM increased their replication compared to minimal culture conditions but did not stimulate expression of other pancreatic cell proteins. We also characterized a specialized mouse model designed to follow the fate of duct cells. This model will be used in future studies to investigate ductal cell contribution to islet regeneration following CM injection. These studies contribute to the development of 'cell-free' regenerative medicine therapies for diabetes.

Co-Authorship Statement

The following contains material from a manuscript in preparation co-authored by Brianna Ananthan, Gillian Bell, Dr. Tyler Cooper, and Dr. David Hess. Brianna Ananthan performed all experimental work presented in this thesis in the lab of Dr. David Hess. Gillian Bell helped with animal care, experimental conceptualization, and technique training. Dr. Tyler Cooper assisted with experimental conceptualization. Dr. David Hess contributed to the design and interpretation of all experiments.

Acknowledgements

Firstly, I would like to express my deep appreciation for my supervisor, Dr. David Hess, for fostering a supportive lab environment and teaching me a multitude of valuable academic and life skills. From my start in the lab as a fourth-year student, your guidance and encouragement have increased my passion for science and research as a learner, collaborator, and community member. Thank you for your ongoing support and patience through the challenges and breakthroughs. The skills developed and lessons learned under your supervision will be ones that will stick with me for a lifetime.

I would like to thank the members of my advisory committee: Dr. Samuel Asfaha, Dr. Cheryle Séguin, and Dr. Lina Dagnino for your insight and technical expertise which helped advance my project every step of the way.

Thank you, Gillian Bell, for teaching me so many techniques from cell culture to animal care from the beginning. Your expertise and support were instrumental in my path as a graduate student. Your willingness to lend a helping hand at every step has been so inspirational.

I would like to thank all of the members of the Hess lab who provided insight and support throughout my thesis work, including Sarah Krause, Yehia Moharrem, Christopher Leclerc, Fiona Serack, and Dr. Tyler Cooper. I would also like to thank Sarah and Yehia for the many caffeine runs which helped me push through long days. Thank you to Kristin Chadwick at the London Regional Flow Cytometry Facility for her services in cell sorting and flow cytometry troubleshooting.

I would also like to thank Canadian Institutes of Health Research and the Juvenile Diabetes Research Foundation for providing funding for my work as a graduate student.

Finally, I would like to thank my family for their wisdom and emotional support throughout these two years. To my siblings, Jason, Meghan, Joshua, and Matthew, thank you for always listening and providing perspective through the ups and downs. To my partner, Jason, thank you for riding this rollercoaster with me with a big heart and open arms. To my parents, I cannot even begin to express my appreciation for the unconditional support you've given me over the years in all of my pursuits. I love you all.

Table of Contents

List of Figures

List of Abbreviations

7-AAD – 7-Aminoactinomycin D

ADP – Adenosine diphosphate

ANOVA – Analysis of variance

APC – Adenomatous polypsosis coli gene product

ARX – Aristaless related homeobox

ATP – Adenosine triphosphate

AUC – Area under the curve

AX - Alloxan

BB - Biobreeding

BSA – Bovine serum albumin

CAB – Citric acid buffer

CD – Cluster of differentiation

CK1 – Casein kinase 1

CK19 – Cytokeratin 19

CM – Conditioned media

DBA – Dolichos Bifluoros Agglutinin

DM – Diabetes mellitus

DMEM/F-12 - Dulbecco-s Modified Eagle Medium/Ham's F-12

DMSO – Dimethyl sulfoxide

DNA-PK – DNA-dependent protein kinase

EdU – Ethynyldeoxyuridine

EGF – Epidermal growth factor

EMT – Epithelial-to-mesenchymal transition

Ezh2 - enhancer of zeste 2 polycomb repressive complex 2

FACS – Fluorescence activated cell sorting

FGF – Fibroblast growth factor

GIP – Glucose-dependent insulinotropic peptide

GLP – Glucagon-like peptide

GLUT – Glucose transporter

GPCR – G-protein coupled receptor

GSK3β – Glycogen synthase kinase-3β

hESC – Human embryonic stem cells

HFD – High-fat diet

HGF – Hepatocyte growth factor

HLA – Human leukocyte antigen

hMSC – Human multipotent stromal cells

Hnf1b – Hepatocyte nuclear factor 1 homeobox B

IDF – International Diabetes Federation

IFN-γ – Interferon-γ

IGF-1 – Insulin growth factor 1

IL-1β – Interleukin 1β

iPan – Intrapancreatic

iPSC – Induced pluripotent stem cells

IRS – Insulin receptor substrate

ISCT - International Society for Cellular Therapy

MAF - v-maf musculoaponeurotic fibrosarcoma oncogene homologue

MFI – Mean fluorescence intensity

MHC – Major histocompatibility complex

MSC – Multipotent stromal cells

NGF – Nerve growth factor

Ngn3 – Neurogenin 3

Nkx6.1 – NK6 homeobox 1

NOD – Non-obese diabetic

PAX – Paired box

PBS – Phosphate buffered saline

PDC – Pancreatic ductal cell

Pdgfr - platelet-derived growth factor receptor

PDX-1 – Pancreatic and duodenal homeobox 1

PERK – Pancreatic endoplasmic reticulum kinase

Pft1a – Pancreas-specific transcription factor

Polypeptide – PP

RNA-seq – Ribonucleic acid sequencing

ROS – Reactive oxidative species

SCID – Severe combined immunodeficient

SD – Standard deviation

SEM – Standard error of the mean

STZ - Streptozotocin

T1D – Type 1 diabetes

T2D – Type 2 diabetes

TCF/LEF – DNA-bound T-cell factor/lymphoid enhancer factor

Th – T helper

TNF-α – Tumor necrosis factor-α

VEGF – Vascular endothelial growth factor

Wnt+ - Wnt-stimulated

Wnt- - Wnt-inhibited

1.0 Introduction

1.1 Functions of the Pancreas

The pancreas, a digestive organ located in the upper left abdominal cavity, is composed of exocrine and endocrine tissue. Exocrine cells, including acinar and ductal cells, aid in the digestion of food passing from the stomach into the small intestine. Acinar cells synthesize proenzymes, which become activated in the duodenum to break down proteins, carbohydrates, and lipids. Ductal cells secrete bicarbonate to neutralize acidic chyme from the stomach as it passes into the duodenum. Endocrine cells, organized in clusters called islets of Langerhans, synthesize and secrete hormones via the portal vein system to regulate glucose homeostasis[1].

1.1.1 Human Pancreas Development

During human fetal development, the pancreas arises from interactions between the endodermal epithelium and surrounding mesenchyme[2]. Pancreatic organogenesis begins with the formation of the pancreatic and duodenal homeobox 1 (Pdx1)- and pancreas-specific transcription factor (Ptf1a)-expressing dorsal and ventral buds from the endoderm-derived primitive gut epithelium at gestational day 26[3–5]. Subsequently, fusion of these buds forms the definitive pancreas with an interconnected ductal network[3]. As the left ventral bud regresses, later becoming the inferior head of the pancreas, the right ventral bud fuses with the dorsal bud during gut rotation at 6-7 weeks of gestation, giving rise to the majority of the pancreas[4]. Between gestational days 45 and 47, the pancreatic epithelium undergoes active growth, proliferation, and branching morphogenesis into the surrounding mesenchyme, controlled by NOTCH, fibroblast growth factor (FGF), and epidermal growth factor (EGF) signaling[3,4]. Compartmentalization of the pancreatic tip and trunk occurs at around gestational week 7, with proacinar/tip cells expressing GATA4 and bipotent endocrine/ductal progenitor cells expressing *Sox9,* NK6 homeobox 1 (*Nkx6.1),* hepatocyte nuclear factor 1 homeobox B (*Hnf1)b,* and *Pdx1*[4,6,7].

Exocrine tissue, comprised of acinar and ductal cells, makes up >95% of the pancreas[8]. Acinar-specific gene expression of digestive enzyme precursors and other factors mark a distinct commitment at around gestational weeks 11-15, including chymotrypsinogen, trypsinogen, protease, elastase 1, and subsequently amylase after gestational week 23[4]. Acinar cells are connected to ductal tissue through centroacinar cells/terminal duct cells[8]. Duct cells transport these pancreatic zymogens and secrete bicarbonate to neutralize gastric acid into the duodenum[8]. Continued expression of *Sox9* and *Hnf1b* and expression of differentiated ductal cell markers including cytokeratin 19 (CK19), carbonic anhydrase 1, mucin 1, and cystic fibrosis membrane conductance regulator mark ductal commitment from trunk progenitors at gestational week 11[4,8]. However, it remains unclear whether differentiated ductal cells retain the ability to give rise to endocrine cells that bipotent trunk precursor cells possess.

The endocrine compartment, which makes up 2-3% of the pancreas, is composed of hormone-secreting cells including insulin-secreting β-cells (65-80%), glucagon-secreting α-cells (15-20%), somatostatin-secreting δ-cells (3-10%), polypeptide (PP)-secreting PP cells (3-5%), and ghrelin-secreting ε-cells (<1%)[9–14]. Transient expression of the transcription factor Neurogenin 3 (*Ngn3*) and paired box (PAX)6 expression mark commitment of bipotent trunk progenitors to an endocrine lineage fate[3,10,15]. As endocrine cells commit to their specific lineages, each cell type expresses a unique set of transcription factors. When endocrine cells commit to an α-lineage, they express aristaless related homeobox (ARX) and glucagon, but not paired box 4 (PAX4) or PDX1[15]. On the other hand, β-cells express PDX1, NKX6.1, v-maf musculoaponeurotic fibrosarcoma oncogene homologue (MAF)A, PAX4, and insulin, but not ARX[15]. It is thought that reciprocal inhibition between ARX and PAX4 expression may mark a key checkpoint in specification between α- and β-cell identity, respectively[16–19]. The first endocrine cell type to appear is insulin-expressing cells at gestational week 7.5, followed by glucagon- and somatostatin-expressing cells[4]. Differentiated endocrine cells migrate away from the ductal epithelium and organize into clusters called islets of Langerhans which form during gestational week 10 and obtain a vascular network by gestational week 14[4,8]. The majority of α-, β-, and δ-cells within the human pancreas are single hormone expressing after birth[4]. Bi-hormonal expression of insulin and glucagon in approximately 20-40% of α- and β-cells has been noted between gestational week 9 and 16, which significantly declined by gestational week 21 and was predominantly undetectable in the adult pancreas[4,15].

1.1.2 Glucose Homeostasis and Regulation of Insulin Secretion

The human body requires a consistent supply of glucose during all states: well-fed, starvation, exercise, rest, or stress[20]. For example, the human brain requires 6 grams of glucose per hour to maintain basic function[20]. The islets of Langerhans play a crucial role in maintaining normoglycemia through secretion of antagonistic hormones, insulin and glucagon, to prevent deleterious consequences of hyperglycemia and hypoglycemia. After a meal, absorption of carbohydrates causes blood glucose levels to rise. In response to elevated exogenous glucose concentrations, circulating blood glucose is taken up from capillaries within and surrounding islets by the low affinity facultative glucose transporter (GLUT) 2 (K_m=17 mmol/l), located on pancreatic β-cells[14,21,22]. Upon entry into the cell, this glucose enters glycolysis to increase the ratio of adenosine triphosphate (ATP) to adenosine diphosphate (ADP)[14]. An increased ATP/ADP ratio leads to closure of ATP-sensitive potassium (K^+)-channels and subsequent depolarization of the β-cell membrane[14]. Upon depolarization, voltage-dependent calcium (Ca^{2+}) -channels facilitate the influx of Ca^{2+} ions, which triggers fusion of insulin-containing vesicles with the plasma membrane and release of vesicle contents into the blood in a biphasic manner[14,23]. Circulating insulin is taken up primarily by the liver, muscle, and adipose tissue to facilitate insulin-dependent uptake of exogenous glucose via GLUT4 from the blood, promoting anabolic processes such as glycogenesis and lipogenesis[14,24–26]. Conversely, when blood glucose levels are low, such as during a fasting state, α-cells secrete glucagon which signals hepatocytes to mobilize glucose via glycogenolysis to restore normoglycemia.

Insulin secretion is affected by additional external regulators. Incretin hormones, including glucagon-like peptide (GLP)-1 and glucose-dependent insulinotropic peptide (GIP) amplify insulin secretion[27]. GLP-1 and GIP are released by enteroendocrine L-cells and K-cells, respectively, following nutrient entry into the intestine following oral ingestion[28–33]. Pancreatic β-cells can increase the rate of insulin translation in response to the presence of nutrients, regulated in part by pancreatic endoplasmic reticulum kinase (PERK) and eukaryotic initiation factor 2a[22,34–36]. Conversely, short-chain fatty acids exhibit an inhibitory effect on insulin secretion as a result of reduced ATP/ADP ratio following oxidation[14,37]. The stress hormone norepinephrine also inhibits insulin secretion by binding to G-protein coupled receptor (GPCR)-linked α_2-adrenergic receptors, causing hyperpolarization of β-cells[38–40]. Proper regulation of insulin secretion and

function is critical for energy homeostasis. β-cell dysfunction, a hallmark of diabetes mellitus (DM), leads to aberrant glucose homeostasis and long-term complications.

β-cell mass can be dynamic to meet bodily demands and maintain glucose homeostasis during pregnancy and weight gain. Studies have shown a linear correlation between β-cell mass and body weight and/or body mass index in mice, rats, and humans[41–44]. β-cell mass is dictated by the balance between β-cell production (through replication or neogenesis), β-cell death, and β-cell volume changes (hypertrophy or atrophy)[44].

1.2 Diabetes Mellitus

The earliest known report of DM dates back to 1552 BC when Egyptian physician Hesy-Ra described a disease characterized by frequent urination and rapid weight loss[45]. Between the fifth and sixth centuries, Sushrant recorded an association of these symptoms with sweet-tasting urine in Indian literature[46]. Since then, the emergence of chemical analysis as a diagnostic tool and the study of endocrinology have improved our understanding of diabetes pathology[46].

Diabetes results from the destruction of insulin-producing β-cells in the pancreas as a consequence of autoimmune attack (Type 1) or insulin insensitivity (Type 2), leaving patients unable to control blood glucose[47]. The International Diabetes Federation (IDF) the prevalence of diabetes in adults to be 463 million in 2019, which is projected to increase to 700 million by 2045[48]. The annual economic burden of diabetes and its cardiovascular co-morbidities has been estimated at $825 billion in a systematic review by the Non-communicable Diseases Risk Factor Collaboration[49]. This load is placed on patients and their families, their health infrastructures, and national economies[49]. *Thus, there exists an irrefutable need to develop curative therapies for diabetes.*

1.2.1 Type 1 Diabetes

Type 1 diabetes (T1D) is an autoimmune disease resulting in the selective destruction of pancreatic β-cells by T-lymphocytes[22]. Typically diagnosed in juvenile patients, T1D is characterized by the inability to synthesize and secrete insulin endogenously[50]. The extent of β-

cell loss at the presentation of clinical symptoms varies between individuals and is dependent on age and cellular pattern of infiltrating cells during insulitis[51–54]. T1D accounts for <15% of total DM cases, with a worldwide prevalence of 1.1 million in children aged 0-19 in 2019[48,55]. The worldwide incidence of T1D has been estimated to increase 3% annually, with the greatest increase observed in children aged 0-4[55].

Apoptosis of β-cells in T1D results from immune antibody binding and cellular reactivity to endogenous islet antigens. T-cell and macrophage islet infiltration and subsequent release of inflammatory cytokines, including interleukin-1β (IL-1β), interferon-γ (IFN-γ), and tumor necrosis factor-α (TNF-α), result in T-cell activation and β-cell destruction[22,56–61]. Following autoantibody generation, cluster of differentiation (CD) 4+ naïve T helper (Th) 0 cells polarize towards an inflammatory Th1 phenotype. Th1 cells presented with islet self-antigens by antigen presenting cells promotes β-cell destruction through release of cytokines and subsequent recruitment of pro-inflammatory (M1) macrophages and CD8+ cytotoxic T-lympocytes[22,62–66]. Activated T-lymphocytes then mediate direct β-cell destruction through the pore-forming perforin-dependent pathway or induce apoptosis via Fas/Fas ligand interactions[67]. Mutations in the human leukocyte antigen (HLA) gene, encoding cell surface antigens that facilitate interaction with immune cells, correlate to an increased risk in developing T1D[68–70]. Environmental factors including infant nutrition, vitamin D deficiency, gut microbiota, and viral infections may contribute to the development of T1D in individuals with genetic predispositions[71]. Our understanding of the underlying causes and progression of T1D is growing with use of advanced technologies including artificial intelligence, however, characterization of the disease in humans is complicated by the latency between the onset of the autoimmune disease process and presentation of clinical symptoms, as well as limited availability of human pancreas tissue for study[72–74].

1.2.2 Type 2 Diabetes

Glucose homeostasis in the body depends on insulin secretion by pancreatic β-cells and normal body cell responses to insulin receptor binding and subsequent glucose uptake[75]. During Type 2 diabetes (T2D) pathogenesis, the response to insulin becomes defective, leading to dysregulated glucose balance and metabolism. Of the 463 million people estimated to have diabetes by the IDF, individuals aged 20-79 with T2D overwhelmingly dominate this estimation[48].

Approximately 50% of adults living with diabetes are unaware of their condition because there is a long pre-detection period (3-7 years) during which blood glucose levels are elevated but symptoms are not clinically diagnosed[48,55]. Thus, early detection is crucial in improving outcomes associated with T2D and associated complications[48,55]. In developed countries, the annual incidence of T2D is estimated at 6.7-7 per 1000 individuals per year[55].

Also termed non-insulin-dependent diabetes, the development and progression of T2D is marked by deterioration in the ability to respond to elevated blood glucose levels over several years. Progression towards a diabetic state is characterized by a reduction in insulin sensitivity, leading to decreased glucose uptake by effector cells[76]. When the energy balance in the body is chronically skewed towards excess calories, fat accumulates in subcutaneous tissue[77]. When the storage capacity of this tissue is exceeded, fatty acids are stored in tissues such as the liver, muscles, and in the pancreas[77]. Fat accumulation in liver and muscle tissue contributes to impaired glucose uptake in response to insulin as a result of impaired insulin receptor tyrosine kinase activity, while fat in the pancreas contributes to further β-cell dysregulation[77–79]. Studies suggest that this impaired insulin response also stems from dysfunctional glucose storage processes, including decreased skeletal muscle glycogenesis and increased gluconeogenesis despite hyperinsulinemia[76,77,79]. Following initial insulin resistance, compensatory mechanisms in response to the increased metabolic load, including β-cell mass expansion and increased secretion of insulin by β-cells will occur but cannot be sustained over time[77,80]. Chronic hyperglycemia depletes insulin-containing vesicles, reducing the capacity of β-cells to respond to new glucose. Glucotoxicity, which is correlated with an increase in reactive oxidative species (ROS), also causes stress on β-cells, subsequently leading to β-cell hypertrophy and increased risk of apoptosis[81]. As T2D progresses, the rate of β-cell apoptosis exceeds the rate of β-cell replication and neogenesis, leading to a decline in total β-cell mass[80].

Aberrant innate immunity activation also plays a role in the progression of T2D. Increased levels of circulating innate immune acute-phase circulating factors, including C-reactive protein, serum amyloid A, α-1-acid glycoprotein, sialic acid, and IL-6, have all been observed in T2D patients[82]. Increased circulating inflammatory cytokines can exacerbate insulin resistance. For example, TNF-α activates c-Jun NH_2-terminal kinase which inhibits insulin signaling through serine phosphorylation of insulin receptor substrate (IRS)-1 and IRS-2 and stimulation of suppressor of cytokine signaling proteins, which bind and facilitate degradation of IRS-1 and IRS-2[83].

Genetic predispositions also predict susceptibility to T2D. As a polygenic disease, in which single mutations can have protective or deleterious effects, scientists have been working to identify candidate genes to characterize the genetic components in patients with T2D[84]. Single nucleotide polymorphisms in genes including peroxisome proliferator-activated receptor γ (PPARG), potassium inwardly rectifying channel subfamily J member 11 (KCNJ11), Wolfram syndrome 1 (WFS1) gene, and HNF1b are associated with development of T2D[84]. In individuals with genetic predispositions, environmental factors including high-fat diet, reduced physical activity, age, pollutants, and exposure to a diabetic environment in utero contribute to an increased risk of T2D[85–87]. Consequences of chronic hyperglycemia and fat accumulation in organ tissues include cardiovascular disease, retinopathy, and neuropathy[88].

1.2.3 Animal Models to Study Diabetes

Animal models of diabetes allow for study of spontaneous or induced pathology that resembles one or more aspects of the disease in humans[89]. Both T1D and T2D are multifactorial diseases in which polygenic and environmental components contribute to disease progression.

1.2.3.1 Models for T1D

To study autoimmune T1D, the non-obese diabetic (NOD) mouse is commonly used. In NOD mice, insulitis starts at approximately 4-5 weeks of age with lymphocytes surrounding islets followed by infiltration of an unusually high number of CD4+ and CD8+ T-cells[89]. Immune cell influx ultimately results in destruction of >90% of β-cells and hyperglycemia by weeks 24-30 of age[89]. As in humans, NOD mice develop autoantibodies to insulin, glutamic acid decarboxylase, and the tyrosine phosphatase ICA512[89]. Major histocompatibility complex (MHC) alleles are also important factors in disease progression in these mice, similar to humans[89]. Although clinical symptoms typically present in human patients, including hyperglycemia, glycosuria, polydipsia, and polyuria, manifest in NOD mice, they have a higher resistance to ketoacidosis and can survive up to 2-4 weeks without exogenous insulin[89].

The Diabetes-prone biobreeding (BB) rat has MHC gene susceptibility to autoimmune diabetes and develops islet-specific and glutamic acid decarboxylase autoantibodies[89,90]. Insulitis within this rat model is similar to human pathogenesis with Th1-lymphocytes predominating infiltration[91]. At 8-16 weeks of age, rats become hyperglycemic, lack insulin, and exhibit polyuria and polydipsia[89]. Similar to humans, BB rats are prone to ketoacidosis and need exogenous insulin treatments to survive[91]. However, this rat model has depressed levels of CD4+ T-cells and almost non-existent CD8+ T-cells[91], which compromises its acceptability as a model for human T1D diabetes.

Chemical agents have also been used to model diabetes. Streptozotocin (STZ) and alloxan (AX) target pancreatic β-cells via GLUT2 transporter specificity and mediate β-cell death through ROS and free radical mechanisms[89]. STZ, a nitrosourea related antibiotic and antineoplastic agent produced by Streptomyces achromogenes, induces DNA alkylation and fragmentation within β-

cells, leading to β-cell destruction and insulin-dependent diabetes[89]. Although these chemical agents cause hyperglycemia and insulinopenia, they do not recapitulate the autoimmune aspects of T1D[89,92–94].

1.2.3.2 Models for T2D

Spontaneous mouse models of T2D contain genetic mutations that make mice susceptible to the development of diabetic-like symptoms. Among these are the ob/ob and db/db mouse strains with mutations in the leptin and leptin receptor genes, respectively[89]. The ob/ob genotype is characterized by excessive appetite, low energy expenditure, and obesity starting at approximately 4 weeks of age[89]. Following insulin resistance from hyperphagia and obesity, hyperinsulinemia ensues[89,95]. Ob/ob mice derived from the C57BL/6J strain develop mild hyperglycemia, while similar mice derived from the C57BL/KS strain develop severe diabetes which may be lethal[89,95]. Db/Db mice also develop hyperphagia, obesity, insulin resistance, and hyperinsulinemia before developing hyperglycemia by 8 weeks of age as a result of β-cell failure[89,96].

Non-spontaneous models of T2D include C57BL/6J mice fed a high-fat diet (HFD). HFD induces system metabolic alterations consistent with T2D. Disease progression is marked by obesity, insulin resistance, subsequent hyperglycemia, and lipid accumulation[97]. ROS production as a result of chronic hyperglycemia causes apoptosis of β-cells and subsequent reduction in β-cell mass[98,99]. Mice fed a HFD also exhibit increased systolic blood pressure compared to those fed a low-fat diet[100]. Similar to human T2D pathogenesis, low level chronic inflammation, including within the cardiovascular system, has been identified in HFD mice, which has been attributed to immune responses that are more often Th1-mediated[99]. However, a standardized protocol for this model has yet to be established.

1.3 Therapeutic Approaches to Treat Diabetes Mellitus

Scientific and technological advances have played a critical role in developing effective treatments for diabetes. Identifying targets and strategies for long term, sustainable treatments has been crucial in the advancement of patient care. Treatments for diabetes have primarily focused on insulin therapy, gene therapy, cell replacement, and regenerative approaches. Before these treatments became available, physicians promoted fasting and calorie-restricted diets for diabetes to improve glucosuria and acidosis, and delay negative outcomes in children with diabetes[101,102]. Starting with the discovery of insulin in 1920, finding a curative therapy for diabetes has seemed more within reach[102].

1.3.1 Drug Treatments

Exogenous insulin therapy has become a common treatment for patients with T1D and for some with T2D. In 1920, Frederick Banting, an orthopedic surgeon, had the idea to isolate pancreas extracts to treat depancreatized dogs that developed diabetes[102]. Following intravenous injection of what Banting and Charles Best termed ‘isletin’, the blood glucose levels of these dogs decreased[102]. After J.B. Collip joined the group in 1921, the team purified isletin for human use, and the first injection was given to a 14-year-old boy in 1922[102]. Improvements in methodology for purification over the ensuing years has led to consistent positive clinical outcomes. Subsequent development of more potent insulin and short- and long-acting analogs, has led to improved physiological control of diabetes symptoms and reduced complications[102]. Today, insulin therapy is given through injections or via an insulin pump and can either be used alone or alongside other oral medications to control symptoms. There are many different types of exogenous insulin available with differing pharmacokinetic properties, as well as various delivery methods, so finding the most suitable therapy for each patient is paramount in maintaining their health. However, patients on insulin therapy must continuously monitor their blood glucose and injections must be given on a regular basis lifelong.

Other pharmacological agents and combination therapies have also been used to control blood glucose and other symptoms in patients with diabetes. Metformin is a biguanide that increases insulin sensitivity by phosphorylating GLUT-enhancer factors and inhibits hepatic gluconeogenesis[103,104]. Additionally, in combination with an effective treatment plan, metformin has been shown to help with weight loss as well as serum triglyceride and low density lipoprotein level reduction[105]. However, it does not affect the activity of β-cells. Sulfonylureas act on the ATP-sensitive potassium channels of β-cells to trigger insulin secretion[106]. Efficacy of sulfonylureas require the presence of residual β-cell mass and may contribute to exhaustion and death of those remaining β-cells[103]. While there has been tremendous progress in developing pharmacological therapies to manage diabetes, they cannot fully recapitulate the refined and complex processes of blood glucose homeostasis in healthy persons. Moreover, the cost of medication for patients represents a major hurdle for adherence to treatment[107].

1.3.2 Gene Therapy

Gene therapy refers to the replacement or silencing of dysfunctional genes to treat or prevent disease. Gene vectors in the form of lentiviruses, adenoviruses, liposomes, and naked DNA have been used for delivery of the insulin gene into various body tissues, including pancreatic, liver, fat, and muscle[103]. One genetic approach to delay the progression of autoimmune diabetes and destruction of β-cells targets the immune system itself. Inducing expression of proinsulin under control of the MHC class II promoter has been shown to prevent onset of T1D in NOD mice[108]. However, this strategy relies on early detection of immune reactivity to β-cells before clinical presentation of symptoms.

Another gene therapy approach has been the reprogramming of non-β-cells to replace lost β-cells through induced expression of β-cell specific transcription factors. For example, recombinant-adenovirus-mediated gene transfer of Pdx-1 to hepatocytes of STZ-treated mice considerably increased biologically active plasma insulin content and reduced hyperglycemia[109]. Pdx-1 is a crucial regulator in early pancreas morphogenesis and plays an important role in controlling glucose-dependent insulin expression in β-cells[110]. Reprogramming of pancreatic cells has also shown some success in recovering β-cell mass. *In vivo* delivery of adenoviral vectors carrying Ngn3, Pdx1, and MafA preferentially reprogrammed pancreatic exocrine cells into β-like

cells with indistinguishable morphology and gene expression from endogenous β-cells that could ameliorate STZ-induced hyperglycemia[111]. Pdx1 and MafA-carrying adeno-associated virus cassettes administered through the pancreatic duct reprogrammed α-cells into insulin-expressing β-cells to restore normoglycemia in in AX-treated or autoimmune NOD mice[112]. However, long-term effectiveness of cell reprogramming would have to be combined with treatment strategies to combat ongoing autoimmunity or increased metabolic load to improve survival of newly formed β-cells.

1.3.3 Cell Replacement Strategies

In 2000, James Shapiro and his team published their success in helping seven consecutive patients with T1D achieve insulin independence a year after islet transplantation via the Edmonton Protocol combined with glucocorticoid-free immunosuppressive therapy to reduce chances of graft rejection[113]. Islets isolated from multiple cadaveric donors matched for blood type and lymphocytotoxic antibodies were transplanted to recipients via the hepatic portal vein[113]. The immunosuppressive regimen included long-term sirolimus and tacrolimus use in combination with short-term dacluzimab administration[113]. However, ongoing autoimmunity, graft rejection, and adverse responses to immunosuppressive drugs ultimately contributed to rejection of donor islets[114115]. Since then, intensive research has focused on improving outcomes and graft survival for patients who have received islet transplants. Data from the Collaborative Islet Transplantation Registry indicates a 44% success rate in achieving insulin independence 3 years after surgery[116]. While there have been positive results in the field of allogeneic islet replacement therapy in controlling blood glucose and improving glycated hemoglobin levels in diabetic patients via the Edmonton Protocol[113], shortages of cadaveric donor islets[117–119], the necessity for lifelong immunosuppressive drugs[117–121], and modest success achieving long-term insulin independence[118,120] have proven to be major barriers to this treatment strategy.

To address the challenge of donor tissue availability, scientists have investigated alternate sources of β-cells for transplantation. One attractive source under investigation is pluripotent stem cells, including human embryonic stem cells (hESC) or induced pluripotent stem cells (iPSC). hESC, first derived from the inner cell mass of blastocysts by James Thompson and his team in 1998, can give rise to any cell type found in the body when given the appropriate signals[116,122]. iPSC, first described by Shinya Yamanaka in 2006, are reprogrammed adult fibroblast or somatic cells that have been reverted to a pluripotent state through introduction of factors including the transcription factors Oct3/4, Sox2, c-Myc, and Klf4 in culture[116,123]. Under stepwise differentiation protocols, iPSC can be pushed towards a β-cell lineage that express maturity markers (e.g. insulin, MafA, Nkx6.1, Pdx1) through guidance following developmental specification[124–128]. However, of the differentiated endocrine cells generated in culture, many are polyhormonal and lack glucose-dependent insulin secretory ability[116]. These cultures also contain other pancreatic cell types from various developmental stages[116]. While there has been success in reducing hyperglycemia in mice with chemically ablated β-cells, challenges in the application of this approach in clinical trials include immune response towards the encapsulation device[129,130], hypoxia following implantation[129–132], and impaired insulin release kinetics[132]. Ongoing research focussed on more efficient generation of insulin-producing β-like cells and encapsulation strategies to promote survival have been undertaken by companies such as Semma Therapeutics and ViaCyte[133].

1.3.4 Endogenous Regeneration of β-cells

Another strategy under investigation to restore β-cell mass focuses improvement of the microenvironment that causes β-cell death. Normally, the adult pancreas exhibits low rates of cell turnover and limited response to injury compared to other organs such as the liver or small intestine[134–136]. However, increased β-cell mass in response to pregnancy or obesity suggests that the endocrine pancreas may be stimulated to heal under diabetic conditions in the presence of a microenvironment that favours regeneration over destruction[134,137,138].

One method has targeted regulation of pathways that affect β-cell proliferation. Early in life, the primary mechanism of β-cell expansion is through self-replication[139,140]. However, the proliferative capacity of β-cells declines in an age-dependent manner with negligible detectable

levels in adults over 30 years old[141]. One goal within this field is to identify key regulators of β-cell proliferation that mediate this observed decrease in proliferation over time. An increase in expression of $p16^{Ink4a}$, a cyclin-dependent kinase inhibitor encoded by the *Cdkn2a* gene, in β-cells is strongly correlated with increased age[118,142]. $P16^{Ink4a}$ expression is inhibited by the epigenetic regulator histone-lysine N/methyltransferase enzyme encoded by enhancer of zeste 2 polycomb repressive complex 2 (Ezh2), which decreases its expression with age[143]. Increasing Ezh2 expression in a transgenic mouse model through direct upregulation or by indirectly targeting platelet-derived growth factor receptor (Pdgfr) signaling has shown success in achieving β-cell mass expansion through replication[143,144]. However, translation of findings in regulation of cell cycle proteins in humans is difficult, as cell-cycle proteins in rodent islets are different from those identified in human islets. High-throughput screens have identified compounds that can stimulate β-cell proliferation in human islets such as 5-iodotubercidin, harmine, and WS6[145–147]. While there has been progress in elucidating β-cell regulatory pathways and identifying stimulators of proliferation, clinically relevant β-cell mass restoration by β-cell replication alone has proven difficult to attain[136,148].

Another strategy to stimulate β-cell regeneration focusses on conversion of non-β-cells to β-cells *in situ*. Single-cell ribonucleic acid sequencing (RNA-seq) of human pancreata has revealed heterogeneity within cell populations with indication of intermediate stages between lineages, which could indicate potential plasticity within the human pancreas[149–152]. Investigation of this potential plasticity has been conducted by the Collombat, Herrera, and Bonner-Weir groups, among others[18,19,44,153–160]. Differentiation studies demonstrated induction of islet-derived fibroblast-like cells to hormone-expressing cells *in vitro* and transition between α- and β-cells following induction of lineage specific transcription factors in mouse models, suggesting previously unrecognized plasticity between mature endocrine cell types[16,18,19,159,161]. Expression of MafA and Pdx1 in Nng3+/glucagon+ cells resulted in their transition to β-cells in transgenic mice[159]. Following *Pax4*-mediated α- to β-cell transition, $Hnf1\beta^{+}$ duct-lining cells demonstrated transient activation of *Neurogenin 3*, an endocrine progenitor marker, before adopting an α- then β-cell phenotype and function[19,154,156]. Misexpression of Ngn3 in ductal cells stimulated reactivation of the endocrine lineage specification pathway, resulting in their transition into functional β-like cells in mice[154]. Supporting the hypothesis that β-cells can be generated from

ductal cells in the adult pancreas, 15% of insulin-expressing β-cells, which were not associated with other islet cells, have been found in or budding from ductules, paralleling β-cell lineage specification processes in the developing pancreas[162]. *These findings have generated interest in stimulating islet regeneration during diabetes if we can identify clinically relevant stimuli to modulate these regulatory pathways*. While Ben-Othman *et al.* reported that long term gamma-aminobutyric acid exposure[155] and Li *et al.* reported artemether[163] could modestly induce α- to β-cell transition, subsequent studies have failed to replicate their results[164,165].

1.4 Multipotent Stromal Cells

Stem and progenitor cells from various lineages have been highly studied as a promising source of therapeutic properties. Multipotent stromal cells (MSC), also referred to as mesenchymal stem cells, have received a high degree of attention in recent years due to their wide range of therapeutic actions. The first descriptions of MSC appeared in the 1970s by Friedenstein and his team[166]. Since then, investigation into the therapeutic potential of MSC has been of high interest based on their multipotency, secretory, and immunomodulatory functions. Derived from various sources within the body, MSC have been considered for therapies for a wide array of diseases including myocardial infarction, liver fibrosis, osteoarthritis, and diabetes, among others.

1.4.1 Properties and Characterization

The clear definition and criteria of MSC has long been debated. Many investigators have reported different methods for isolation, expansion in culture, and criteria for characterizing MSC, making comparison and applications of studies in different contexts difficult[167]. In response, the International Society for Cellular Therapy (ISCT) published their minimal criteria for defining MSC in 2006[167]. Their criteria include: plastic adherence; expression of cell surface markers CD105, CD73, and CD90 in ≥ 95% of cells in culture, as well as negative expression of CD45, CD34, CD14, CD11b, CD19 and HLA isotype DR in ≤ 2% of cells; and the capacity to differentiate into bone, fat, and cartilage *in vitro*[167]. MSC can be isolated from various human adult tissues, including bone marrow[168–170], adipose tissue[169,171], peripheral blood[172,173], lung tissue[174,175], and muscle tissue[176,177]. In response to the various tissue sources from which MSC can be derived, the ISCT recommended that descriptions of MSC be supplemented by the tissue origin as cells

from different tissues exhibit varied phenotype, functions, and secretory profiles[178]. For example, expression of Sox2, a marker associated with the maintenance of multipotency, self-renewal, and neurogenesis in early embryonic development, has only been associated with MSC derived from bone marrow[179]. MSC are highly proliferative *in vitro*, and those isolated from human bone marrow have been shown to maintain expression of the stem cell markers *Oct-4, Rex-1,* and *Sox-2* for at least 10 passages[177]. However, differences in MSC properties are donor dependent. Among different bone marrow donors of varying ages, there are differences in growth kinetics, osteogenesis, alkaline phosphatase activity, and secretory profiles[180–183]. With donor and tissue source variability, research geared towards more thorough characterization of MSC, including cell subpopulations, is ongoing.

1.4.2 MSC-Mediated Repair

MSC have shown great promise as a therapeutic tool for a wide range of diseases and disorders. As previously mentioned, one of the criteria for defining MSC is their multipotency. When MSC are placed in induction medias supplemented with specific factors, they can be pushed down osteogenic, chondrogenic, or adipogenic lineages, which has stimulated interest in tissue replacement strategies[184–186]. While these cells possess the capacity for *in vitro* multipotency under appropriate culture conditions, *in vivo* engraftment studies have been largely disappointing[187–189].

The benefits of MSC cell treatments have predominantly been attributed to indirect or paracrine mechanisms. MSC secrete a wide array of factors into the surrounding environment. The MSC secretome, which can be concentrated to generate conditioned media (CM), is comprised of soluble factors and extracellular vesicles, which together make up a regenerative microenvironment containing immunomodulatory, anti-apoptotic, pro-angiogenic, proliferative, and growth factors that facilitate tissue repair[187,190–192]. Important for tissue regeneration, the secretome has been shown to include anti-apoptotic growth factors including insulin-like growth factor 1 (IGF-1), tissue inhibitor of metalloproteinases 1 and 2, growth hormone, EGF, hepatocyte growth factor (HGF), and nerve growth factor (NGF)[180]. Immunomodulatory functions of MSC include promotion of a pro-regenerative macrophage phenotype, mobilization of macrophages to the site of injury, limiting degranulation of mast cells, inhibition of lymphocyte proliferation, decreasing lymphocyte proinflammatory cytokine synthesis, and increasing lymphocyte anti-

inflammatory cytokine synthesis[180]. MSC secrete vascular endothelial growth factor (VEGF) which stimulates migration and proliferation of endothelial cells to facilitate the formation of blood vessels[180,193,194]. Treatment using MSC CM has demonstrated regenerative effects in disease models including intervertebral disc injury, myocardial infarction, and neuronal damage in a preclinical setting, and bone regeneration and alopecia in clinical trials[195]. Key advantages of this approach include: (1) avoidance of immune incompatibility and tumorigenicity associated with stem cell administration, (2) MSC CM can be assessed for efficacy, safety, and dosage similarly to other pharmaceuticals, and (3) MSC CM can be stored long term without compromising effectiveness[187]. Use of CM also provides the opportunity to engineer production of specific factors through modulation of signaling pathways.

1.4.3 MSC as a Therapeutic Option for Diabetes

As documented in other tissues, MSC may have the ability to facilitate regeneration of pancreatic endorcrine tissue. MSC isolated from human bone marrow have been shown to reduce hyperglycemia, increase serum insulin, and stimulate islet regeneration following intravenous injection or intracardiac infusion in STZ-treated mice[196–200]. The immunomodulatory functions of MSC have also been shown to delay the onset of hyperglycemia and β-cell loss in mouse models of T1D[201]. Intravenous injection of bone marrow-derived human MSC (hMSC) also improved blood glucose levels and ameliorated insulin resistance by increasing GLUT4 expression in a rat model of T2D[202]. However, the mechanisms that mediate these therapeutic actions remain unclear. While focusing on the transdifferentiation potential of MSC initially sparked optimism in generating insulin-producing cells, low transdifferentation efficiency and engraftment rates have limited clinical feasibility exploiting this uncommon property[203]. Thus, many current studies investigating the therapeutic abilities of MSC for treating diabetes focus on paracrine factors. Paracrine factors secreted by MSC have been shown to modulate β-cell signalling pathways to promote survival and improve glucose-dependent insulin secretion[204–206].

Clinical trials using MSC to treat diabetes have focused primarily on harnessing their immunomodulatory properties. Clinically, these cells are an attractive therapeutic option because they can be isolated relatively non-invasively from various adult tissues including bone marrow and adipose tissue, or from perinatal tissues often discarded, such as the umbilical cord or placenta.

Additionally, their rapid expansion *in vitro* without significant loss in secretory regenerative ability add to their clinical applicability[203]. A number of these studies resulted in reduced insulin requirement, increased fasting C-peptide levels, and/or improved HbA1c with few reports of adverse events following transplantation into patients[203]. Some studies have also shown improvement of donor islet graft survival when transplanted in combination with MSC[203].

We have previously shown that transplantation of culture-expanded bone marrow-derived hMSC also demonstrated the capacity to reduce hyperglycemia and increase β-cell mass by stimulating the formation of small ductal-associated islet clusters via paracrine signals in mice with STZ-mediated β-cell ablation[198–200]. The modest short-lived increase in β-cell replication could not account for the robust increase in β-cell mass[199,200,207]. However, regenerative capacity was donor-dependent[199,200,208,209] and decreased with prolonged expansion[199,200]. Comparative global secretome analyses by mass spectrometry revealed regenerative hMSC ($hMSC^{R}$) exclusively secreted proteins associated with active canonical Wnt/β-catenin signaling, a pathway implicated in cell growth, proliferation, and differentiation[208]. In contrast, non-regenerative secretome samples ($hMSC^{NR}$) contained increased levels of Wnt-pathway inhibitors Dickopf-1/3[208].

The canonical Wnt/β-catenin signaling pathway has various functions in embryonic development and adult homeostasis, including involvement in cell proliferation, polarity, and differentiation[210]. The primary role of this pathway is to regulate nuclear levels of the transcriptional co-activator β-catenin. In the absence of signaling ligands, cytoplasmic β-catenin is constantly degraded by a destruction complex comprised of Axin, adenomatous polypsosis coli gene product (APC), casein kinasae 1 (CK1), and glycogen synthase kinase 3 (GSK3)[210]. CK1 and GSK3 phosphorylate β-catenin for ubiquitination and degradation by proteasomes[210]. This effectively prevents β-catenin from reaching the nucleus and target genes are repressed by the DNA-bound T cell factor/lymphoid enhancer factor (TCF/LEF) protein family[210]. On the other hand, activation of this pathway is achieved when a Wnt ligant binds to a Frizzled receptor and co-receptor, low-density lipoprotein receptor related protein 6/5[210]. Subsequent recruitment of Dishevelled results in inhibition of the aforementioned destruction complex, preventing phosphorylation of β-catenin[210]. Cytosolic β-catenin accumulates and travels to the nucleus where it interacts with TCF/LEF proteins to activate expression of target genes[210]. Apart from its

signalling functions, β-catenin also plays an important role in in cell-cell adhesions[211]. To assess the relevance of the Wnt-pathway to the regenerative capacity of hMSC, Wnt-pathway activation was mimicked in hMSC^{NR} cultures using treatment with the glycogen synthase kinase-3β inhibitor CHIR99021 for 24 hours in serum-free media before CM collection and concentration[207,208]. In the absence of Wnt ligands, GSK3 marks β-catenin for degradataion[212] (**Fig. 1.1**). Conversely, Wnt-pathway inhibition was achieved using IWR-1, which stabilizes Axin in the β-catenin inhibition complex and ultimately facilitates its degradation[213,214].

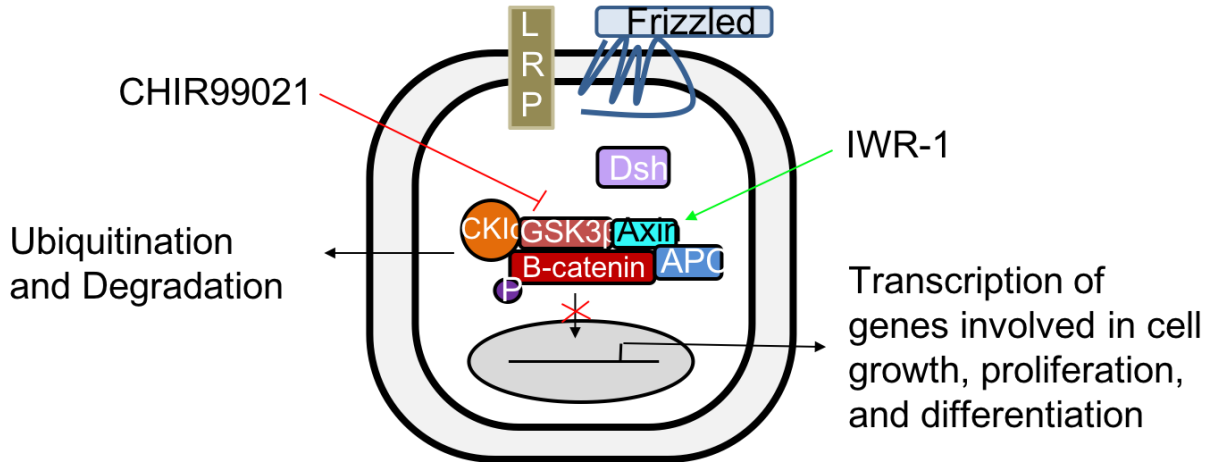

Figure 1.1 CHIR99021 and IWR-1 can be used to stimulate or inhibit the canonical Wnt/β-catenin pathway, respectively. When Wnt ligands bind to their appropriate Frizzled family receptor on the plasma membrane, an intracellular signal causes destabilization of the glycogen synthase kinase-3β (GSK3)/Axin/Adenomatous Polyposis Coli (APC) inhibition complex, preventing the ubiquitination and degradation of cytosolic β-catenin and permitting its translocation into the nucleus to affect transcription of genes involved in cell growth, proliferation, and differentiation. CHIR99021, a GSK3 inhibitor, activates the Wnt pathway by destabilizing the GSK3/Axin/APC inhibition complex, and facilitating nuclear translocation of β-catenin. IWR-1 stabilizes Axin, and by extension the GSK3/Axin/APC inhibition complex, to promote ubiquitination and degradation of cytosolic β-catenin.

When co-cultured with human islets for 7 days, Wnt-stimulated (Wnt+) CM enhanced β-cell survival and proliferation compared to Untreated CM or basal Roswell Park Memorial Institute media[208]. After injection into the pancreas of STZ-treated mice, Wnt+ CM consistently induced reversal of hyperglycemia, increased β-cell mass, and improved glucose tolerance compared to unconditioned media or Wnt-inhibited (Wnt-) CM injection following intrapancreatic (iPan) injection in STZ-treated mice[207].

While iPan-injection of *Wnt+ hMSC CM reliably rescues hyperglycemia and β-cell mass*, the identity of 'signal-receiving cells' within the pancreas that mediate islet regeneration remains unknown. Elucidation of the islet regenerative pathway and identification of the essential effectors that stimulate β-cell mass recovery will provide the foundation for a testable cell-free therapy and delivery method to reliably induce β-cell regeneration. $hMSC^{R}$ CM contains pro-angionenic factors, including FGF7, PDGF, and VEGF-A, which could produce a regenerative microenvironment that promotes islet vascularization[208]. Additionally, $hMSC^{R}$ secrete immunomodulatory factors, including TGF-β and stromal cell-derived factor 1 (CXCL12), compared to $hMSC^{NR}$, which secrete elevated levels of pro-inflammatory cytokines, including IL-1β, IL-6, and IL-8[208]. Collectively, iPan injection of Wnt+ hMSC CM creates a microenvironment that accelerates islet regeneration through its immunomodulatory, anti-apoptotic, pro-angiogenic, proliferative, and growth factors that facilitate tissue repair[187,190–192]. Proteomic analyses and RNA-sequencing of hMSC CM may prove to be useful tools in elucidating the key factors that differentiate regenerative versus non-regenerative samples. Treatment efficacy in strong pre-clinical models, including NOD mice or db/db mice, will direct future studies in clinical trials.

1.4.4 Elucidating the Islet Regenerative Cascade Induced by hMSC CM

Analyses of human pancreas donations from healthy and diabetic individuals have revealed that insulin-expressing cells budding from pancreatic ducts was more common than observation of enlarged islets, indicating more putative regions suggesting neogenesis compared to areas of β-cell replication or hypertrophy[43,44,215]. Additionally, expansion of islet-depleted ductal tissue *in vitro* in 3D Matrigel resulted in glucose responsive insulin secreting islet-like clusters budding from ductal clusters[160,216]. Lineage tracing studies have demonstrated transition of duct cells to functional β-like cells following transcription factor misexpression, β-cell ablation, or pancreatic

injury[153,154,156,217,218]. This proposed model suggests that ductal cells may act as facultative progenitors that contribute to β-cell neogenesis upon experience of stressful conditions. Following a dedifferentiation event including epithelial-to-mesenchymal transition (EMT) and transient re-expression of *Ngn3*, it is proposed that these cells transition to an α-cell phenotype before transitioning to β-like cells[153,154,156,217] (**Fig. 1.2**). Additionally, the Medalist Study, which followed 411 patients with T1D for ≥ 50 years, showed that 63.4% had C-peptide levels within the minimal or sustained range[219]. Furthermore, during a mixed-meal tolerance test, over half of individuals with C-peptide levels >0.17 nmol/l responded with a two-fold or greater increase compared to fasting levels[219]. Histological analyses of pancreatic sections from individuals who had passed away during the course of the study revealed steady state insulin+ β-cell proliferation[219]. These data support residual β-cell function in patients who have had T1D long-term. Thus, β-cell regeneration may be mediated by multiple cell populations, including pre-existing β-cells and facultative progenitors within the pancreas.

Following iPan injection, Wnt+ hMSC CM induced a regenerative cascade resulting in the emergence of neoislets associated with the ductal epithelium 4 days post-transplantation[207]. Histological analyses revealed detection of glucagon+ cells co-localized with β-cell markers insulin, MafA, or Nkx6.1[207]. Nuclear expression of Nkx6.1 and MafA in newly formed insulin+ islets suggested proper β-cell maturation[207]. Additionally, vimentin+ cell hyperplasia surrounding the ductal epithelium was observed following STZ-treatment with or without subsequent hMSC CM injection, which is consistent with a model of EMT by the ductal epithelium proposed by other groups[156,207,220]. However, the rate of β-cell proliferation could not account for the robust increase in β-cell mass. To address the question of whether these neoislets originate from ductal facultative progenitors following Wnt+ CM injection, we proposed to use a lineage tracing mouse model to follow the fate of pancreatic CK19-expressing ductal cells.

These lineage tracing mice have a Cre recombinase fused to a murine estrogen receptor ligand binding domain inserted upstream of the initiation sequence of the CK19 gene[221]. Expression of CK19, an intermediate filament protein, can ben seen in the adult lung, oral cavity, stomach, small intestines, and within the pancreatic, renal, and hepatic ducts[221]. Following administration of tamoxifen, which binds to the fused estrogen receptor, Cre recombinase can

access the nuclear compartment of cells to facilitate excision of the loxP-flanked STOP cassette flanking the Gt(ROSA)26SOR locus[221,222]. This permits robust tdTomato fluorescence in cells that express CK19, permanently labeling these cells[222]. This allows for fate-mapping of CK19-expressing cells through hMSC CM-induced islet regeneration to investigate their contribution to the new β-cell population.

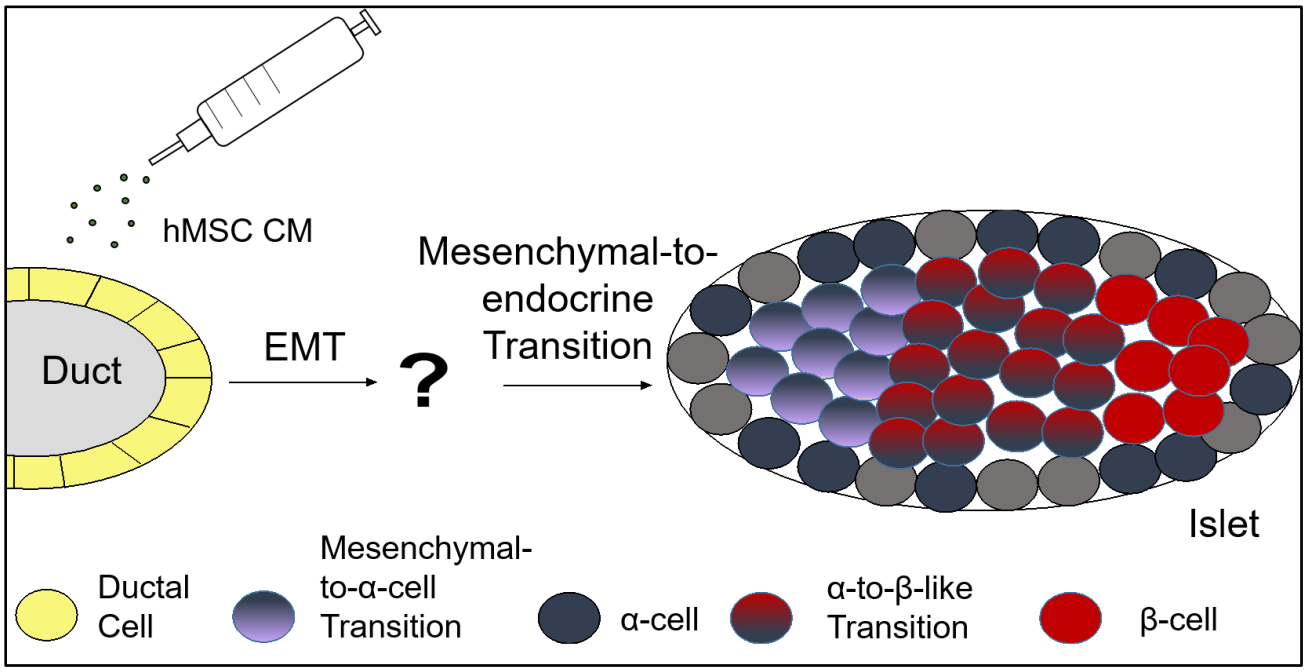

Figure 1.2 Proposed mechanism for islet cell regeneration in hyperglycemic mice following Wnt+ hMSC CM iPan injection. We hypothesize iPan injection of Wnt+ hMSC CM will stimulate β-cell regeneration from ductal derived facultative precursors following EMT in hyperglycemic mice.

1.5 Hypothesis and Objectives

The overall objective of my thesis was to develop and characterize a model for assessing the contribution of CK19-expressing pancreatic duct cells in hMSC Wnt+ CM induced islet regeneration.

Based on the recent recognition of islet cell plasticity, we hypothesized Wnt+ hMSC CM would stimulate β-cell regeneration from ductal-derived precursor cells after direct injection into the pancreas of hyperglycemic mice.

To address this, the following aims were proposed:

(1) To compare the regenerative functions of hMSC CM on isolated CK19-expressing ductal cells *in vitro*.

(2) To characterize a lineage tracing model to assess the contribution of CK19+ ductal cells in islet regenerative mechanisms induced by hMSC CM.

2.0 Cytokeratin 19-expressing cells as a potential target for islet regeneration

2.1 Introduction

Allogeneic bone marrow transplantation is used to treat hematological cancers, including acute myeloid leukemia, to replace unhealthy, cancerous stem cells with healthy ones that regenerate the blood system[223]. The human bone marrow also hMSC, commonly referred to as mesenchymal stem/progenitor cells, that serve as long-term precursors for bone, cartilage, fat, and muscle cells[224]. Aside from the support of the self-renewing properties of hematopoietic progenitor cells in the bone marrow, MSC also secrete immunomodulatory, anti-apoptotic, pro-angiogenic, proliferative, and growth factors[187,190–192]. The pioneering work by Hess *et al.*[198] has shown that transplantation of bone marrow-derived progenitor cells of hematopoietic and mesenchymal lineages improved serum insulin levels and reduced hyperglycemia via paracrine mechanisms in STZ-treated mice[199,200,207,225,226]. Follow-up studies have supported the regenerative paracrine properties of bone marrow-derived hematopoietic and mesenchymal progenitor cell subtypes that stimulate β-cell proliferation or neoislet formation, respectively[199,200]. Circumventing the complications of cellular transplantation, intrapancreatic injection of human bone marrow-derived MSC CM has also shown the potential to stimulate islet regeneration and rescue hyperglycemia in STZ-treated mice[207].

Diabetes, which is associated with autoimmune β-cell attack (T1D) or insulin resistance resulting in β-cell dysfunction (T2D), results in β-cell destruction leaving patients unable to control blood glucose levels. With the prevalence of diabetes steadily rising[48], and the occurrence of severe cardiovascular comorbidities associated with hyperglycemia, investigation into novel curative therapies to rescue β-cell mass in patients with T1D and late-stage T2D is highly sought. Currently, reduced serum insulin and hyperglycemia are treated with exogenous insulin administration and other pharmacological agents to improve glycemic control[103]. However, these treatments do not recapitulate the fine-tuned physiological responses set in motion following nutrient intake and patients remain at risk for extreme peaks and troughs in blood glucose levels. Consequently, comorbidities are highly prevalent in patients with T2D (>95%), the most common of which are severe cardiovascular complications including hypertension, critical limb ischemia, heart attack, and stroke[227]. While islet replacement strategies via the Edmonton Protocol have shown promise in helping patients control blood glucose[113], shortages of donor tissue[117–119], the necessity for lifelong immunosuppressive drugs[117–121], and compromised long-term success islet survival and

sustaining insulin secretion[118,120] remain major for islet transplantation. However, β-cell mass expansion during pregnancy and obesity suggests β-cells can either proliferate *in situ* or differentiate from progenitor cells upon the generation of a regenerative microenvironment[228,229]. Identification of pathways that regulate β-cell proliferation and/or neogenesis is highly sought in regenerating β-cell mass. While β-cell proliferation is the primary driver of neonatal β-cell expansion, the proliferative capacity of adult β-cells sharply declines with age[141]. Although targeting pathways that mediate this decline have been of high interest, clinically applicable stimulation of β-cell proliferation using biological or pharmacological stimuli has been difficult to achieve[136,148]. Thus, investigation into the regeneration of β-cells from non-β-cell sources remains highly relevant. Endocrine cell plasticity has been reported through lineage tracing studies in mice whereby non-β-cells, including α-cells or ductal cells, have demonstrated the capacity to transition towards the β-cell lineage[16,18,19,154,156,157,159,161,230]. Because endocrine cells arise from bipotent endocrine/ductal trunk cells during embryonic development, it has been hypothesized that facultative progenitors reside in the ductal epithelium[4,6,7]. Thus, a clinically applicable stimulator(s) of this dormant β-cell regenerative remains an elusive target in the search for a curative therapy for diabetes.

The regenerative secretome of bone marrow-derived hMSC represent a promising, readily available biotherapeutic agent to mediate β-cell mass rescue. hMSC can be rapidly expanded *ex vivo*, and the secretome containing regenerative and immunomodulatory stimuli can be concentrated to generate cell-free CM. Although the islet regenerative capacity of hMSC is donor dependent after transplantation and diminishes with prolonged culture[199,200,207,208], the activity of the canonical Wnt/β-catenin signaling pathway has been identified as a key regulator of islet regenerative capacity[207,208]. Small molecule stimulation of the Wnt pathway using the GSK3 inhibitor CHIR99021 with low-passage hMSC *in vitro* generated CM that reliably rescued glycemia and β-cell mass in hyperglycemic mice. Although increased survival and proliferation of human β-cells was observed[207,208], neoislets and insulin+ cell clusters were highly localized adjacent to ductule regions, and glucagon+ cells within islets co-localized with β-cell markers Nkx6.1, MafA, and insulin[198–200,207]. Thus, harnessing pancreatic plasticity using cell-free hMSC CM represents an attractive approach to modulate β-cell mass. While iPan-injection of Wnt+

hMSC CM reliably rescues hyperglycemia and β-cell mass, the identity of 'signal-receiving cells' within the pancreas that mediate islet regeneration remains unknown.

To investigate the identity of the 'signal-receiving' cell within the pancreas during hMSC CM induced islet regeneration, we developed a model to focus on CK19-expressing ductal cells. We hypothesized that hMSC CM supplementation *in vitro* would increase proliferation of murine CK19+ pancreas cells and stimulate proliferation. Additionally, we hypothesized that CK19-CreERT;Ai9(RCL-tdT) mice would reliably label CK19+ cells within the pancreas following tamoxifen administration and become hyperglycemic following STZ treatment. CK19-expressing cells cultured with hMSC CM exhibited increased proliferation *in vitro*. However, neither epithelial-to-mesenchymal transition nor transition towards an endocrine phenotype were observed *in vitro* following hMSC CM supplementation. Additionally, we characterized a lineage tracing mouse model [CK19-CreERT;Ai9(RCL-tdT)] that reliably labelled CK19-expressing cells within the pancreas. This model also exhibited hyperglycemia, impaired glucose tolerance, and reduced β-cell mass following STZ treatment (60 mg/kg/day x 5 days). These data showcase the preparation and optimization of a model that can be confidently used in subsequent experiments to assess the contributions of CK19-expressing cells during hMSC CM induced islet regeneration.

2.2 Methods

2.2.1 Assessing pancreatic phenotypic changes in STZ-treated Non-Obese Diabetic/Severe Combined Immunodeficient (NOD/SCID) mice

Mice (8-10 weeks old) were administered 35 mg/kg/day STZ by intraperitoneal (i.p.) injection for 5 consecutive days. STZ was solubilized in sodium citrate buffer at pH 4.5 and injected into mice within 15 min of preparing the mixture. Mice were monitored for non-fasting blood glucose and body weight at Days 0, 1, 5, and 10. At each timepoint, pancreata were dissected from euthanized mice and digested using collagenase V and trypsin-EDTA. Cells were fixed and permeabilized using 10% formalin and 1% Triton X-100. Single cell suspensions were assessed for DBA lectin (Vector Laboratories, Burlington, ON) uptake, CK19 (Abcam, Cambridge, UK), CD45 (BioLegend, San Diego, CA), and F4/80 (BioLegend) expression by flow cytometry on an LSRII flow cytometry machine (BD Biosciences, Mississauga, ON). Flow cytometry data were analyzed using FlowJo software (Treestar, Ashland, OR, USA).

2.2.2 Validating the effects of CHIR99021 and IWR-1 on intracellular β-catenin in hMSC

Human bone marrow was obtained with informed consent from healthy donors at the London Health Sciences Centre (London, ON, Canada). hMSC were purified using density gradient centrifugation and cultured in supplemented Amniomax^{TM} media (Invitrogen, Carlsbad, CA) for expansion[199,200]. Low passage (P3-P4), 80% confluent hMSC cultures were washed with phosphate-buffered saline (PBS) to remove serum and growth factors, then cultured in serum-free basal Amniomax^{TM} media supplemented with increasing concentrations of CHIR99021 (0 µM, 5 µM, 10 µM, 15 µM, 20 µM; AbMole Bioscience, Houston, TX) or IWR-1 (0 µM, 10 µM, 20 µM, 30 µM, 50 µM, Sigma-Aldrich, St. Louis, MO). In cell cultures without CHIR99021 or IWR-1, dimethyl sulfoxide (DMSO) was added as a vehicle control. Cells were fixed in 10% formalin and permeabilized using 1% Triton X-100. hMSC were assessed for survival [(7-Aminoactinomycin D, 7-AAD (BioLegend)], apoptosis [(Annexin V (BD Biosciences)], and β-catenin (Invitrogen) expression by flow cytometry at the London Regional Flow Cytometry Facility and analyses were performed using Flowjo software.

2.2.3 Generating hMSC CM

Low passage (P4), 80% confluent hMSC were washed with PBS to remove serum and growth factors and cultured in serum-free basal Amniomax^{TM} media supplemented with either DMSO (vehicle control), 10 µM CHIR99021, or 20 µM IWR-1 for 24h to generate Untreated, Wnt+, and Wnt- CM, respectively. CM was collected and concentrated (≈ 40-fold) by centrifugation at 4,100 g for 75 minutes using 3 kDa filter spin columns. Secreted contents >3 kDa separated by the filter were collected and the CM protein concentration was quantified using a NanoDrop analyzer.

2.2.4 Murine ductal cell culture and hMSC CM supplementation

Pancreata from healthy or STZ-treated adult mice (8-10 weeks old) were purified using fluorescence activated cell sorting (FACS) at the London Regional Flow Cytometry Facility (London, ON) to obtain 7AAD-/Dolichos Bifluorus Agglutinin (DBA) lectin+ cells following collagenase V and trypsin EDTA-mediated tissue digestion according to the protocol previously outlined by Reichart *et al*[231] (**Fig. 2.1**). 7-AAD marks dead cells with compromised membrane integrity by intercalating double-stranded DNA[232]. DBA lectin has carbohydrate specificity toward α-linked N-acetylgalactosamine common on ductal epithelial cells[233]. DBA lectin+ cell cultures were first established in complete pancreatic ductal cell (PDC) media [Dulbecco-s Modified Eagle Medium/Ham's F-12 (DMEM/F-12) + 5% Nu Serum, 25 µg/ml bovine pituitary extract, 0.5% ITS+ (insulin, human transferrin, selenous acid) Premix, 20 ng/ml epidermal growth factor, 1µM dexamethasone, 5 mg/ml glucose, 1.22 mg/ml nicotinamide] for 24 hours before replacing media with either complete PDC media, basal DMEM/F-12, or DMEM/F-12 supplemented with Untreated, Wnt+, or Wnt- hMSC CM (protein dose of 8µg/ well for approximately 8,000 cells) for 2 or 5 days at 37°C + 5% CO_2. Cell cultures were assessed for proliferative response using ethynyldeoxyuridine (EdU) incorporation following 24h pulse label at 50 µM, and phenotype transition (vimentin, insulin, glucagon expression) was assessed by immunofluorescence. Ductal cell phenotype was verified using CK19 labeling.

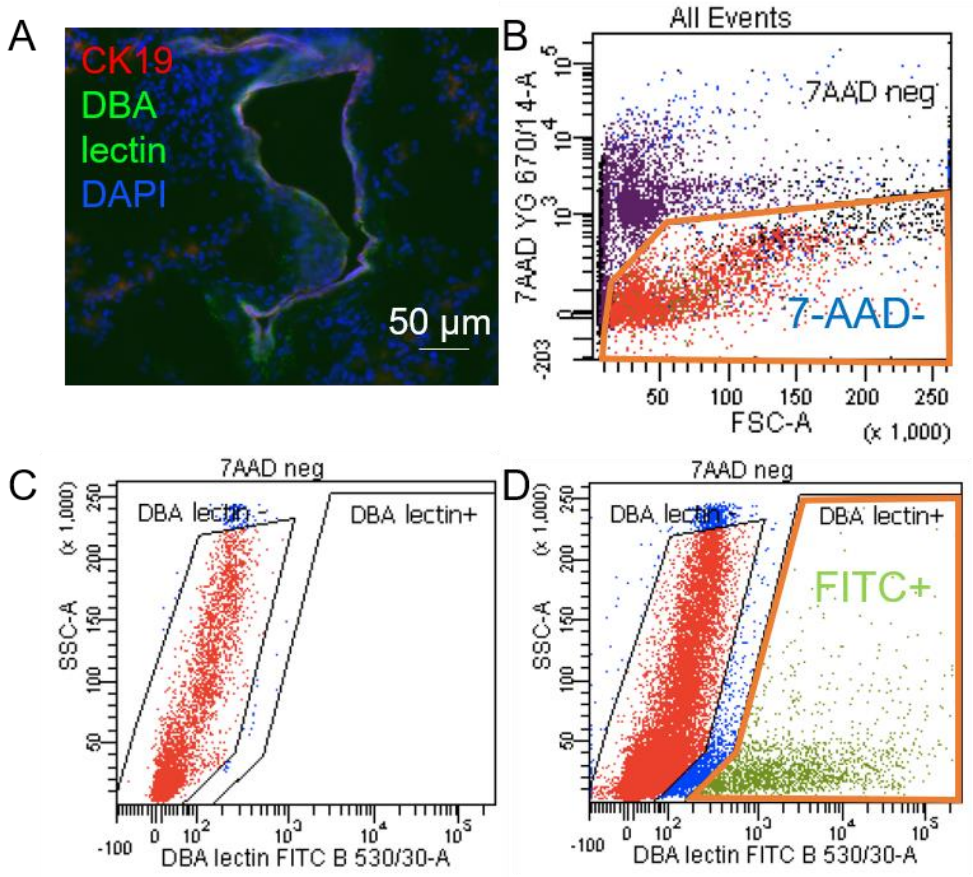

Figure 2.1 Fluorescence-activated cell sorting (FACS) strategy to isolate murine 7-AAD-/DBA lectin+ cells. (A) Representative photomicrograph of a mouse pancreas section for DBA lectin showed cellular co-localization with CK19. Pancreata from mice (8-10 weeks old) were digested and single cell suspension was purified by FACS with a strategy for (**B**) live (7-AAD-) cells, (**C**) setting a gate for DBA lectin using unstained samples, and (**D**) sorting for DBA lectin+ cells.

2.2.5 Optimization of STZ treatment in CK19-CreERT;Ai9(RCL-tdT) mice

CK19-CreERT;Ai9(RCL-tdT) mice (8-12 weeks old) [breeding CK19-CreERT mice (Jackson Labs, Bar Harbor, Maine, USA) with Ai9(RCL-tdT) mice (Jackson Labs, Bar Harbor, Maine, USA)] were treated with increasing concentrations of STZ (40 mg/kg/day, 50 mg/kg/day, 60 mg/kg/day, or 65 mg/kg/day) dissolved in citric acid buffer (CAB) for 5 consecutive days by i.p. injection and assessed for non-fasting blood glucose and body weight at Days 0, 7, 10, and 14.

2.2.6 Islet size, number, and β-cell mass quantification

Pancreata from STZ-treated CK19-CreERT;Ai9(RCL-tdT) mice sacrificed at Day 14 were frozen in optimal cutting temperature media and sectioned (12 μm) so each of the 3 sections per slide were >150 μm apart. Sections were fixed in formalin, blocked with peroxidase block and horse serum, and stained for insulin using a mouse insulin primary antibody (Sigma) and detected using a peroxidase anti-mouse secondary antibody (Vector Laboratories). *ImmPACT*™ DAB (Vector Laboratories) staining was performed to detect antibody binding, followed by hematoxylin counterstain and mounting in Vectamount (Vector Laboratories). A minimum of 10 clustered insulin+ cells was required to be classified as an islet. Islet number and size were quantified using light microscopy and ImageScope x64 software, counting all islets within 3 sections per mouse. β-cell mass was calculated by:

$$\beta \text{ cell mass} = \frac{\beta \ cell \ area}{Total \ pancreas \ section \ area} x \ Pancreas \ weight$$

2.2.7 Glucose tolerance test

CK19-CreERT;Ai9(RCL-tdT) mice treated with 60 mg/kg/day of STZ (Days 1-5) and CAB control mice were fasted for 3 hours on Day 14 before receiving bolus glucose (2 mg/kg) by i.p. injection. Blood glucose was assessed at 0, 5, 10, 15, 30, 45, 60, 90, and 120 minutes.

2.2.8 Assessing pancreatic phenotypic changes in STZ-treated CK19-CreERT;Ai9(RCL-tdT) mice

Mice (8-10 weeks old) were administered 6 mg tamoxifen dissolved in corn oil by oral gavage. After 7 days of rest, mice were treated with 60 mg/kg/day STZ by i.p. injection for 5 consecutive days. Mice were monitored for non-fasting blood glucose and body weight at Days 0, 1, 7, and 14. At each timepoint, pancreata were dissected and digested using collagenase V and TrypLE (Thermo Fisher). Cells were fixed and permeabilized using 10% formalin and 1% Triton X-100. Single cell suspensions were assessed for tdTomato, CK19 (Abcam), insulin (BD Biosciences), and CD45 (BioLegend) expression by flow cytometry. Data were analyzed using FlowJo software.

2.2.8 Statistical Analysis

All data was expressed as mean ± standard deviation (SD) unless otherwise stated. Analysis was performed by a two-way analysis of variance (ANOVA) for blood glucose curves, and by one-way ANOVA followed by Tukey's multiple comparison test for all other analyses, unless otherwise stated.

2.3 Results

2.3.1 STZ treatment induced systemic hyperglycemia and increased the frequency of DBA lectin+ cells within the pancreas

To investigate the effects of STZ on mouse CK19, CD45 (pan-leukocyte marker), DBA lectin (binds to the α-linked N-acetylgalactosamine carbohydrate moiety), and F4/80 (mouse macrophage marker) expression, NOD/SCID mice were injected with 35 mg/kg/day of STZ for 5 consecutive days and mouse pancreata were harvested and assessed for the frequency of CD45+, CK19+, and DBA lectin+ expression at Days 0, 1, 5, and 10 (Figure 2.2D-I). Mice demonstrated increased non-fasting blood glucose levels at Day 10 compared to Days 0, 1, and 5 (Figure 2.2A). Additionally, the proportion of insulin+ cells was significantly decreased at Days 1 and 10, while the proportion of glucagon+ cells did not change across time (Figure 2B,C). While the proportion of CD45+ and CK19+ within the pancreas did not change over time, the proportion of DBA lectin+ cells was significantly increased at Day 10 compared to Day 0 (Figure 2.2J and K). While CK19 expression is commonly used as a pancreatic ductal marker, it requires cell fixation and permeabilization for detection[234]. However, to purify viable ductal cells for subsequent culture, identification of a live cell marker was required. Various studies have cited DBA lectin as a ductal epithelial marker within the pancreas[231,233,235–240]. However, DBA lectin can also bind non-specifically to some hematopoietic cells including macrophages[241–244]. Within the DBA lectin+ cell population, the proportion of CK19+ cells was enriched two-fold compared to ungated cells (≈ 40% vs. ≈ 20%, respectively)(Figure 2.2 H). In contrast, the proportion of CD45+ cells within DBA lectin+ cells did not change compared to ungated cells. Although the DBA lectin+ cell population was comprised of 20% hematopoietic cells, isolation of live DBA lectin+ cells by FACS followed by 24-hour culture in complete PDC media resulted in 83% CK19+ cell purity (CK19+/DAPI+ cells). Therefore, isolation of pancreatic DBA lectin+ cells followed by culture in complete PDC media represents a purification strategy for murine CK19+ ductal epithelial cells.

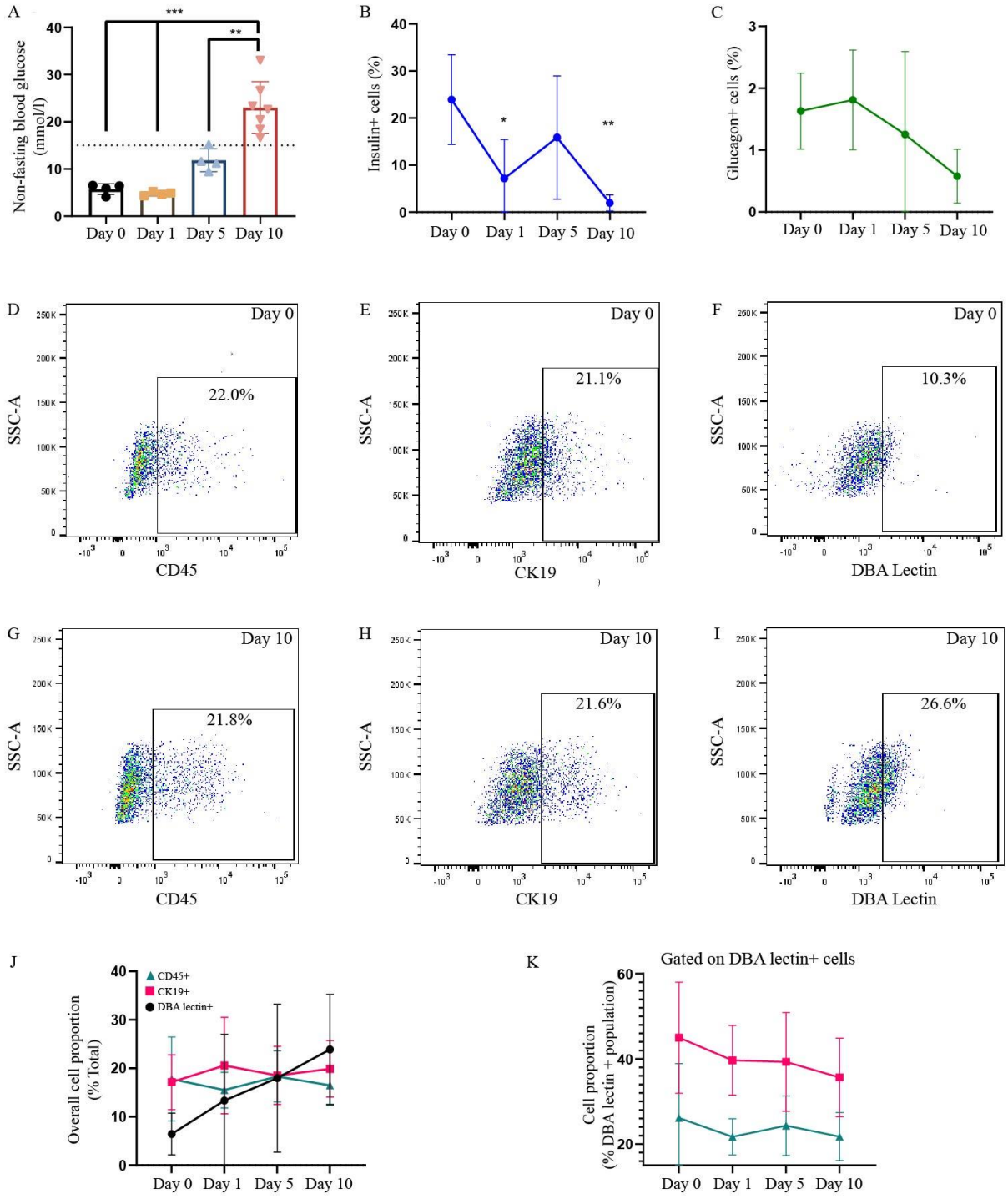
A
Non-fasting blood glucose (mmol/l)
***
**
Day 0 Day 1 Day 5 Day 10
B
Insulin+ cells (%)
*
**
Day 0 Day 1 Day 5 Day 10
C
Glucagon+ cells (%)
Day 0 Day 1 Day 5 Day 10
D
Day 0
22.0%
SSC-A
CD45
E
Day 0
21.1%
SSC-A
CK19
F
Day 0
10.3%
SSC-A
DBA Lectin
G
Day 10
21.8%
SSC-A
CD45
H
Day 10
21.6%
SSC-A
CK19
I
Day 10
26.6%
SSC-A
DBA Lectin
J
CD45+
CK19+
DBA lectin+
Overall cell proportion (% Total)
Day 0 Day 1 Day 5 Day 10
K
Gated on DBA lectin+ cells
Cell proportion (% DBA lectin + population)
Day 0 Day 1 Day 5 Day 10

Figure 2.2 STZ treatment induced systemic hyperglycemia and increased the proportion of DBA lectin+ cells within the pancreas. NOD/SCID mice (8-10 weeks old) were treated with 35 mg/kg/day STZ for 5 days (Days 1-5). At Day 0 (n=3-4), Day 1 (n=4), Day 5 (n=4), and Day 10 (n=7) mouse pancreata were assessed for insulin+, glucagon+, DBA lectin+, CK19+, and CD45+ cell frequencies by flow cytometry. **(A)** At Day 10 mice demonstrated significantly increased non-fasting blood glucose levels compared to all other timepoints. **(B)** The proportion of insulin+ β-cells was significantly decreased at Days 1 and 10 compared to Day 0. **(C)** The proportion of glucagon+ α-cells did not change across time. Representative plots for DBA lectin+, CK19+, and CD45+ cells are shown at **(D-F)** Day 0 and **(G-I)** Day 10. **(J)** The proportion of DBA lectin+ cells was significantly increased at Day 10 compared to Day 0 (*$p<0.05$). The proportions of CK19+ and CD45+ cells showed no change with time. **(I)** Within the DBA lectin+ cell population, the proportion of CK19+ cells was enriched two-fold compared to ungated cells. In contrast, the proportion of CD45+ cells within DBA lectin+ cells did not change compared to ungated cells. Data represent mean ± SD compared using a one-way ANOVA followed by Tukey's multiple comparison test. (**$p<0.01$, ***$p<0.001$)

2.3.2 STZ treatment increased the proportion of F4/80+ cells within CD45+ and CK19+ cells within the pancreas

To assess potential macrophage infiltration in response to STZ treatment, mouse pancreata were assessed for F4/80+ expression, a widely used mouse macrophage marker[245–247] (Figure 2.3 A-D). At Day 10, increased hematopoietic macrophage infiltration was observed, as there was an increase in the proportion of F4/80+ cells within the pancreas and within the CD45+ cell compartment compared to Day 0 (Figure 2.3E,F). Within the CK19+ cell population, the proportion of F4/80+ cells was increased at Day 5 compared to Day 1 (Figure 2.3G). Within DBA lectin+ cells, the proportion of F4/80+ cells remained unchanged with time (Figure 2.3H). Collectively, these data suggest that macrophage infiltration was observed following STZ treatment, which may play a role in islet destruction.

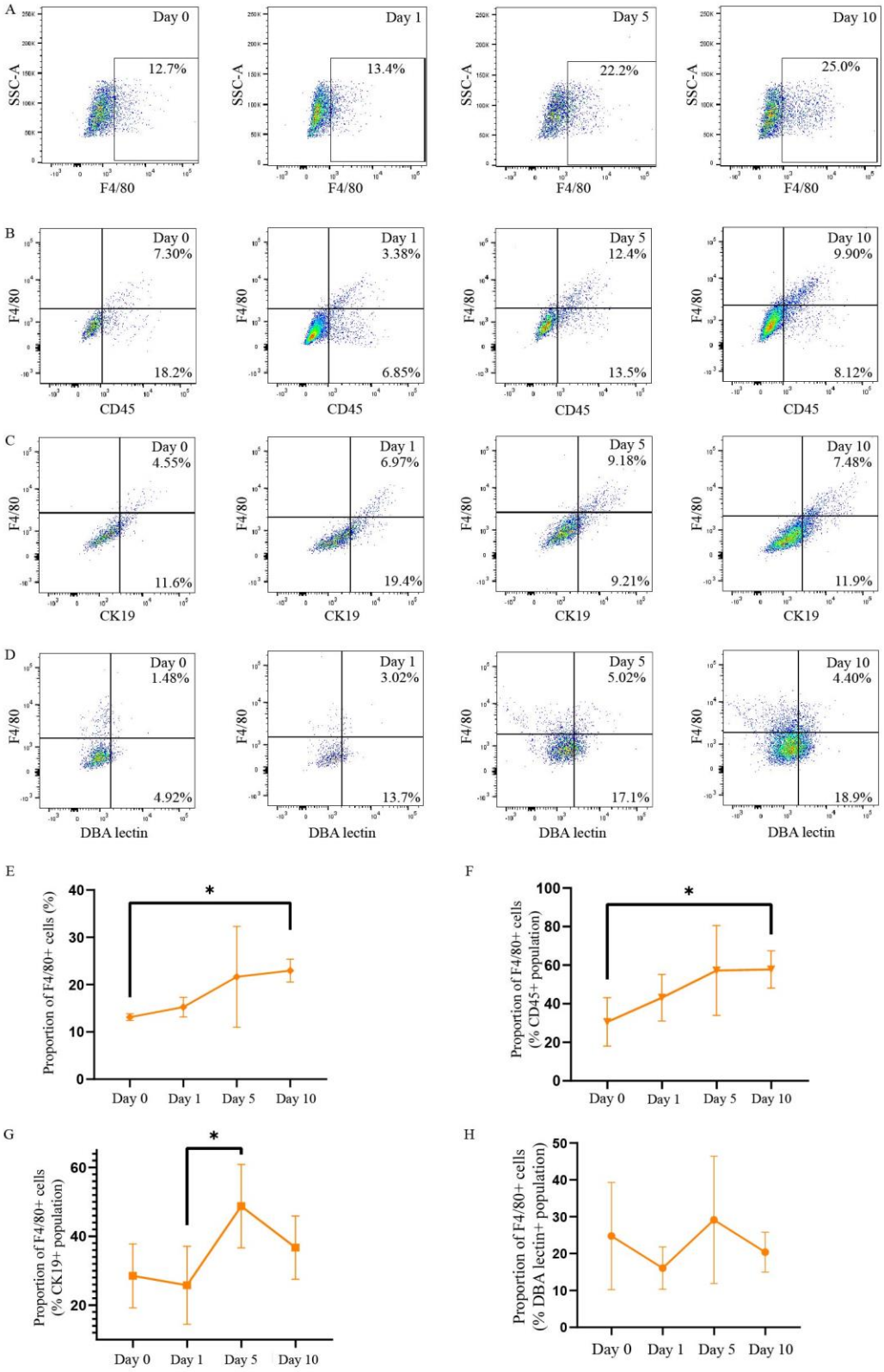
A
Day 0
12.7%
Day 1
13.4%
Day 5
22.2%
Day 10
25.0%
SSC-A
F4/80
B
Day 0
7.30%
18.2%
Day 1
3.38%
6.85%
Day 5
12.4%
13.5%
Day 10
9.90%
8.12%
F4/80
CD45
C
Day 0
4.55%
11.6%
Day 1
6.97%
19.4%
Day 5
9.18%
9.21%
Day 10
7.48%
11.9%
F4/80
CK19
D
Day 0
1.48%
4.92%
Day 1
3.02%
13.7%
Day 5
5.02%
17.1%
Day 10
4.40%
18.9%
F4/80
DBA lectin
E
Proportion of F4/80+ cells (%)
Day 0
Day 1
Day 5
Day 10
F
Proportion of F4/80+ cells (% CD45+ population)
G
Proportion of F4/80+ cells (% CK19+ population)
H
Proportion of F4/80+ cells (% DBA lectin+ population)

Figure 2.3 STZ treatment increased the proportion of F4/80+ macrophages within CD45+ and CK19+ cell populations within the pancreas. NOD/SCID mice (8-10 weeks old) were treated with 35 mg/kg/day STZ for 5 days (Days 1-5). At Day 0 (n=3-4), Day 1 (n=4), Day 5 (n=4), and Day 10 (n=7), mouse pancreata were assessed for DBA lectin+, CK19+, CD45+, and F4/80+ cell frequencies by flow cytometry. **(A)** Representative dot plots showing the overall proportion of F4/80+ macrophages in the pancreas at each timepoint are shown. **(B)** Representative dot plots showing the proportion of F4/80+ cells within CD45+ leukocytes at each timepoint are shown. **(C)** Representative dot plots showing the proportion of F4/80+ macrophages within CK19+ ductal cells at each timepoint. **(D)** Representative dot plots showing the proportion of F4/80+ cells within DBA lectin+ cells at each timepoint. **(E)** The proportion of F4/80+ macrophages in the pancreas was significantly increased at Day 10 compared to Day 0. **(F)** The proportion of F4/80+ macrophages within CD45+ leukocytes was significantly increased at Day 10 compared to Day 0. **(G)** The proportion of F4/80+ macrophages within the CK19+ ductal cell population was significantly increased at Day 5 compared to Day 1. **(H)** The proportion of F4/80+ macrophages remained unchanged within the DBA lectin+ cell population over the 10-day time course. Data represent mean ± SD compared using a one-way ANOVA followed by Tukey's multiple comparison test (*$p<0.05$).

2.3.3 Treatment of hMSC with CHIR99021 increased intracellular β-catenin and did not affect cell survival

As the GSK3 inhibitor CHIR99021 promotes destabilization of the β-catenin destruction complex, increasing intracellular stores of β-catenin which affects transcription of factors implicated in cell growth, proliferation, and differentiation[208]. Therefore, we sought to titrate CHIR99021 treatment concentration to optimally stimulate the Wnt pathway in cultured hMSC, measured by intracellular β-catenin levels[208,248,249]. Following 24-hour treatment, hMSC treated with 10 μM, 15 μM, or 20 μM CHIR99021 in serum-free basal Amniomax^{TM} media showed significantly increased mean fluorescence intensity (M.F.I.) of intracellular β-catenin by flow cytometry compared to the DMSO control (0 μM) and 5 μM treatment (***$p<0.001$)(Figure 2.4). Treatment with 5 μM showed no difference in β-catenin M.F.I. compared to the DMSO control. There were no significant differences in the frequency of dead cells (7AAD+/Annexin V+) or apoptotic cells (7AAD-/Annexin V+) between any of the treatment conditions (Figure 2.5). Thus, 10 μM CHIR99021 was chosen to optimally stimulate the canonical Wnt/β-catenin pathway in hMSC.

2.3.4 Treatment of hMSC with IWR-1 did not affect intracellular β-catenin or cell survival

In contrast, IWR-1 stabilizes Axin, and by extension promotes the intracellular destruction of β-catenin resulting in the blockade of canonical Wnt/β-catenin signaling. Next, we sought to titrate the optimal IWR-1 treatment concentration to inhibit the Wnt-pathway in cultured hMSC, as measured by intracellular β-catenin levels[208,214,249]. Following 24-hour treatment, hMSC treated with 10 μM, 20 μM, 30 μM, or 50 μM IWR-1 in basal Amniomax^{TM} media surprisingly showed no significant difference in intracellular β-catenin M.F.I. by flow cytometry compared to the DMSO control (0 μM) (Figure 2.6). In addition, here were also no significant differences in the frequency of dead cells (7AAD+/Annexin V+) or apoptotic cells (7AAD-/Annexin V+) between the treatment conditions (Figure 2.7). These results contradict previous findings which identified 20 μM IWR-1 treatment to optimally inhibit the Wnt/β-catenin pathway[207,208].

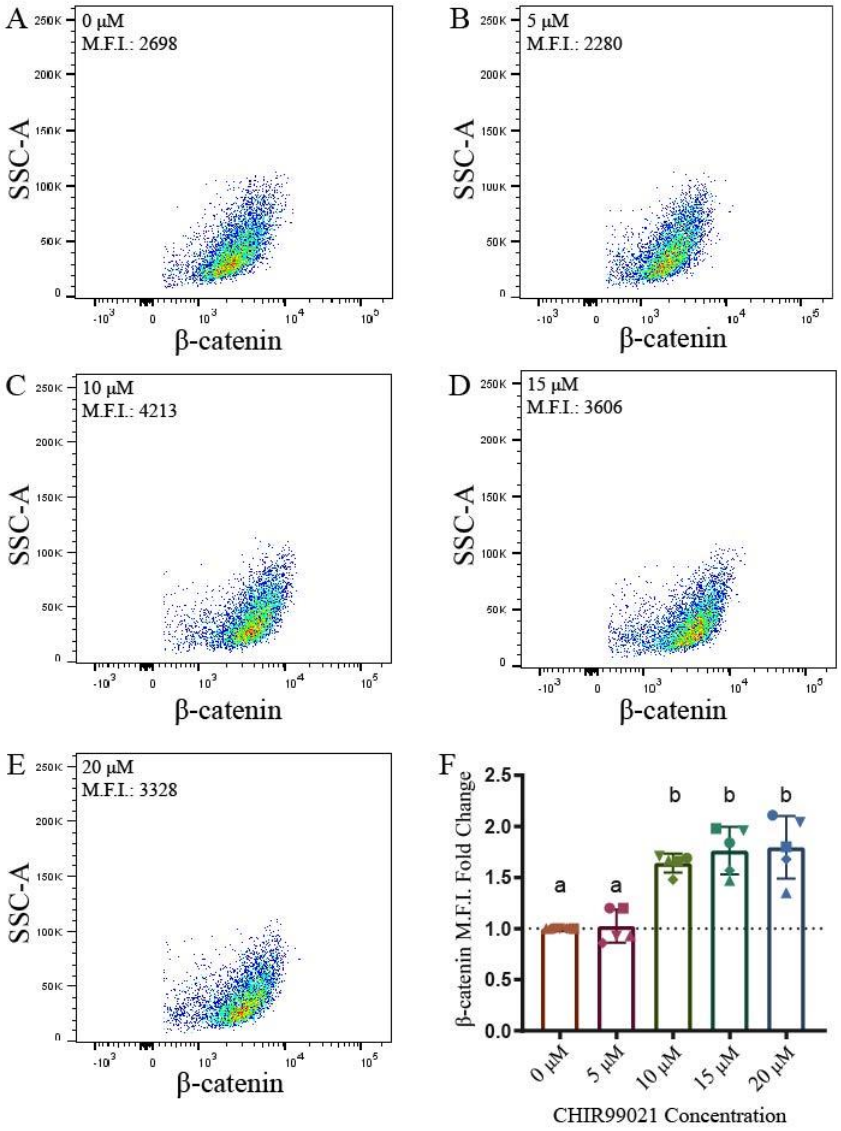

Figure 2.4 Treatment of hMSC with CHIR99021 increased intracellular β-catenin. Low passage (P3-P4), 80% confluent hMSC (N=5) were treated with 5 µM, 10 µM, 15 µM, or 20 µM of CHIR99021 or DMSO (0 µM) for 24 hours in basal Amniomax™ media and assessed for intracellular β-catenin M.F.I. by flow cytometry. **(A-E)** Representative β-catenin vs. SSC-A dot plots for 0 µM, 5 µM, 10 µM, 15 µM, and 20 µM treatments with CHIR99021 are shown. **(F)** Treatment with 10 µM, 15 µM, and 20 µM of CHIR90021 significantly increased β-catenin M.F.I. compared to the DMSO control (***$p<0.001$). Data represent mean fold change ± SD compared using a one-way ANOVA followed by Tukey's multiple comparison test. Means with different letters represent significantly different values.

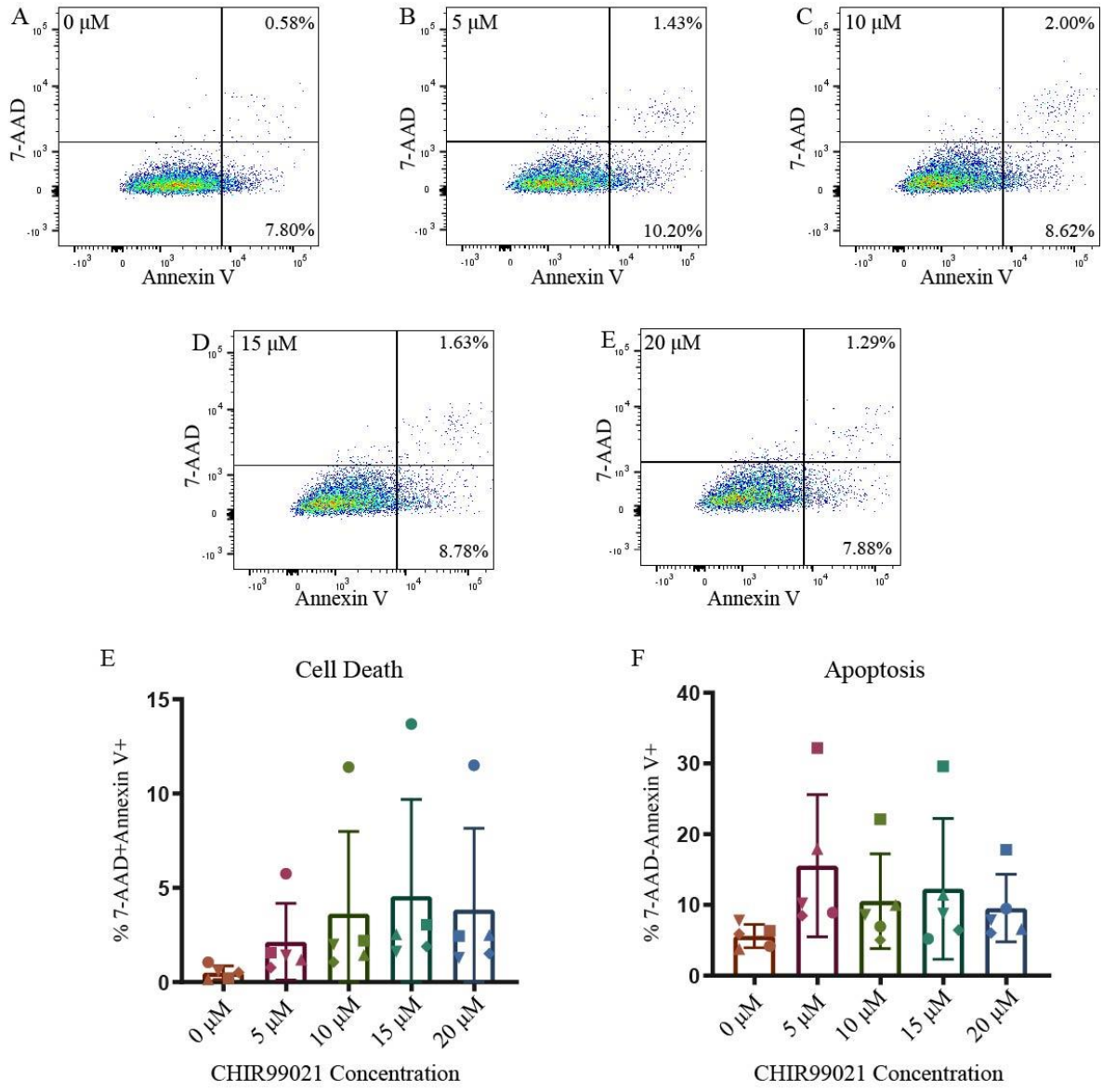

Figure 2.5 Treatment with CHIR99021 did not affect hMSC survival or apoptosis. Low passage (P3-P4), 80% confluent hMSC (N=5) were treated with 5 µM, 10 µM, 15 µM, or 20 µM of CHIR99021 or DMSO (0 µM) for 24 hours in basal Amniomax™ media and assessed for cell death (7-AAD+) and apoptosis (Annexin V+) by flow cytometry. **(A-E)** Representative dot plots for 7-AAD and Annexin V for 0 µM, 5 µM, 10 µM, 15 µM, and 20 µM treatment with CHIR99021 are shown. Treatment with CHIR99021 did not alter **(F)** cell death (proportion of 7-AAD+/Annexin V+ cells) or **(G)** apoptosis (7-AAD-/Annexin V+ cells). Data represents mean ± SD compared using a one-way ANOVA.

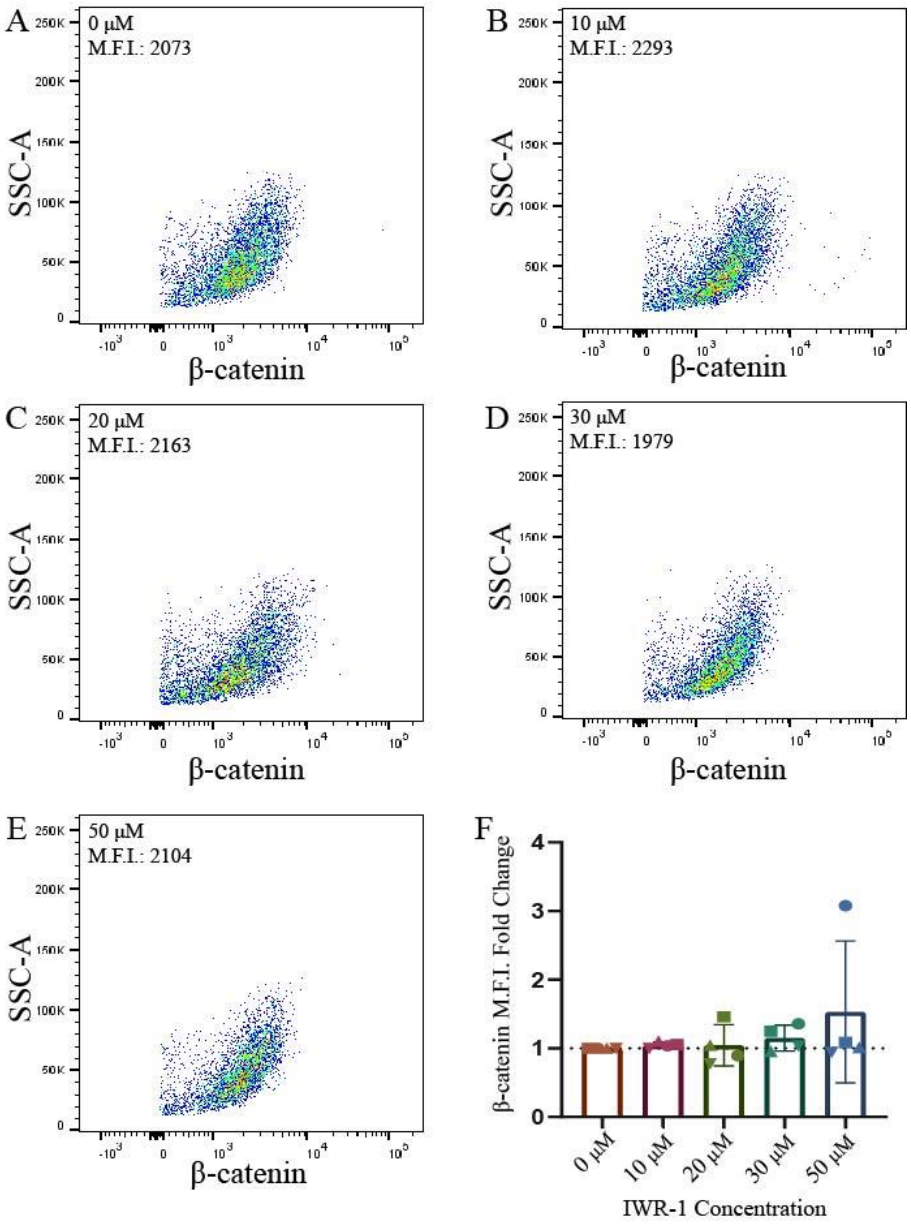

Figure 2.6 Treatment of hMSC with IWR-1 did not affect intracellular β-catenin levels. Low passage (P3-P4), 80% confluent hMSC (N=4) were treated with 10 µM, 20 µM, 30 µM, or 50 µM of IWR-1 or DMSO (0 µM) for 24 hours in basal Amniomax™ media and assessed for intracellar β-catenin M.F.I. by flow cytometry. **(A-E)** Representative β-catenin vs. SSC-A dot plots for 0 µM, 10 µM, 20 µM, 30 µM, and 50 µM IWR-1 are shown. **(F)** Treatment with IWR-1 did not alter β-catenin M.F.I. compared to DMSO (0 µM) control. Data represent mean fold change ± SD compared using a one-way ANOVA.

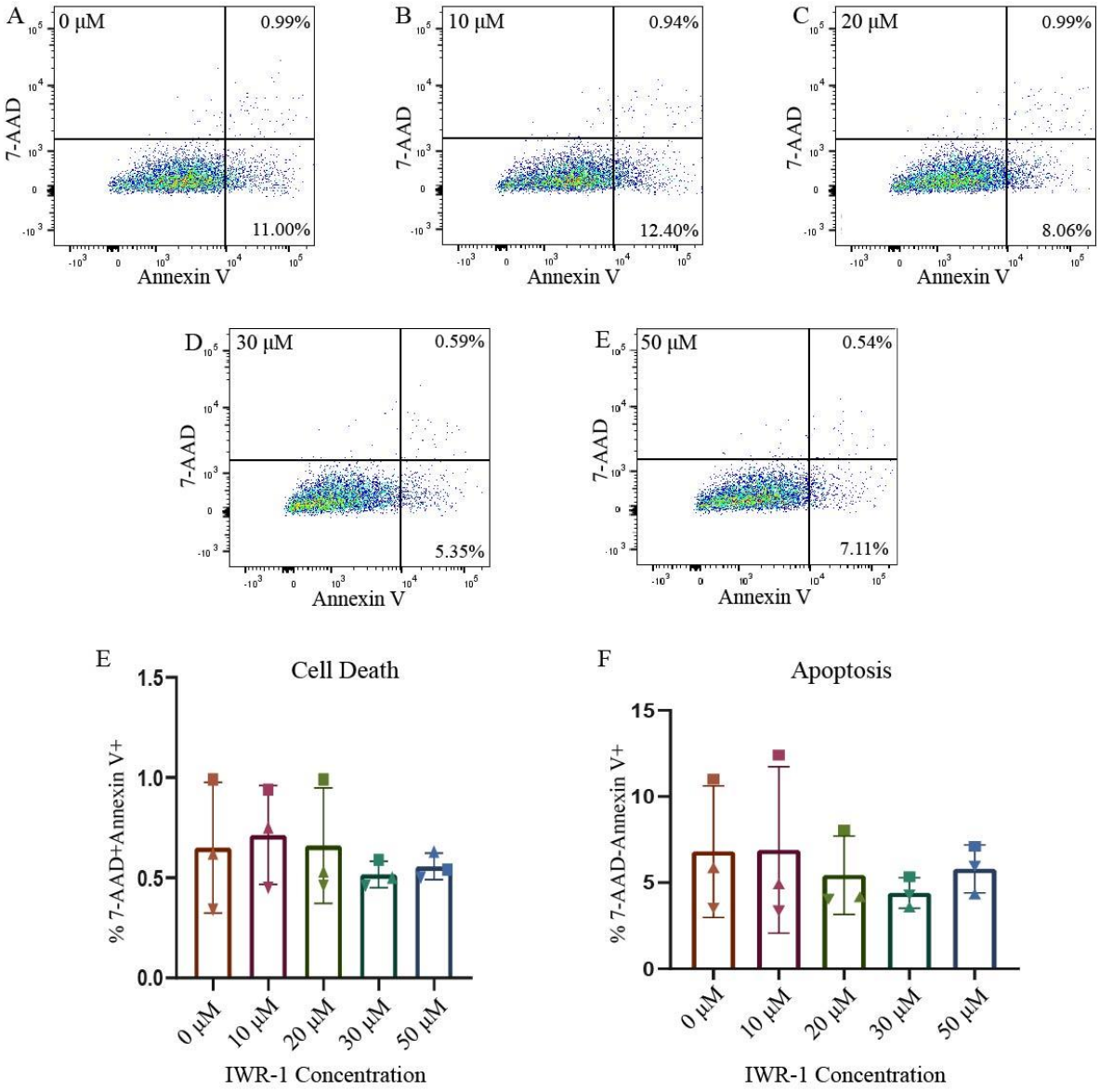

Figure 2.7 Treatment with IWR-1 did not affect hMSC survival or apoptosis. Low passage (P3-P4), 80% confluent hMSC (N=3) were treated with 10 µM, 20 µM, 30 µM, or 50 µM of IWR-1 or DMSO for 24 hours in basal Amniomax™ media and assessed for cell death (7-AAD+) and apoptosis (Annexin V+) by flow cytometry. **(A-E)** Representative dot plots for 7-AAD and Annexin V are shown for 0 µM, 10 µM, 20 µM, 30 µM, and 50 µM IWR-1. Treatment with IWR-1 did not alter the proportion of **(F)** dead cells (7-AAD+/Annexin V+) or **(G)** apoptotic cells (7-AAD-/Annexin V+) compared to DMSO (0 µM). Data represents mean ± SD compared using a one-way ANOVA.

2.3.5 hMSC CM stimulated proliferation of CK19+ cells *in vitro*

To investigate the effects of hMSC CM supplementation on cultured CK19-expressing cells, FACS isolated 7-AAD-/DBA lectin+ cells from healthy or STZ-treated (35 mg/kg/day) NOD/SCID mice (8-10 weeks old) were cultured in complete PDC media for 24 hours to facilitate cell adhesion. Cell media was then replaced either with complete PDC media, basal DMEM/F-12, or DMEM/F-12 supplemented with Untreated, Wnt+, or Wnt- hMSC CM. After 2 or 5 days, CK19+ cells were assessed for proliferation (24-hour EdU pulse label). After 2 days in culture, DBA lectin+ cells isolated from healthy mice supplemented with Untreated, Wnt+, or Wnt- CM showed significantly increased frequencies of proliferating CK19+ cells compared to basal DMEM/F-12 (Figure 2.8F). Ductal cell cultures with bovine serum albumin (BSA) showed no significant change in proliferation frequency, indicating that hMSC CM benefits were not a result of generic protein supplementation in culture. After 5 days culture, there was no significant difference in the frequencies of proliferating CK19+ cells between hMSC CM supplemented and basal DMEM/F-12 conditions. DBA lectin+ cells isolated from STZ-treated mice showed no difference in the frequency of proliferating CK19+ cells after 2 or 5 days in culture (Figure 2.8G). Additionally, DBA lectin+ cells purified from STZ-treated mice exhibited decreased frequencies of EdU+/CK19+ cells compared to cells isolated from healthy mice after 2 days culture (Figure 2.9).

2.3.6 Epithelial-to-mesenchymal transition and endocrine phenotype acquisition were not observed in DBA lectin+ cells exposed to hMSC CM *in vitro*

While hMSC CM supplementation increased CK19-expressing cell proliferation *in vitro*, the next point of interest was whether hMSC CM affected cell phenotype and differentiation. FACS purified 7AAD-/DBA lectin+ cells from healthy or STZ-treated mice cultured in complete PDC media, basal DMEM/F-12, or DMEM/F-12 supplemented with Untreated, Wnt+, or Wnt- hMSC CM for 2, 4, or 7 days did not show colocalization of vimentin and CK19, suggesting no EMT was observed *in vitro*. Similarly, endocrine phenotype transition was not observed, as colocalization of glucagon or insulin with CK19 was not identified at each of these timepoints (Figure 2.10). Thus, mesenchymal or endocrine phenotype transition were not observed under these culture conditions, future studies can look at earlier markers of mesenchymal or endocrine phenotype, including mRNA or transcription factor changes.

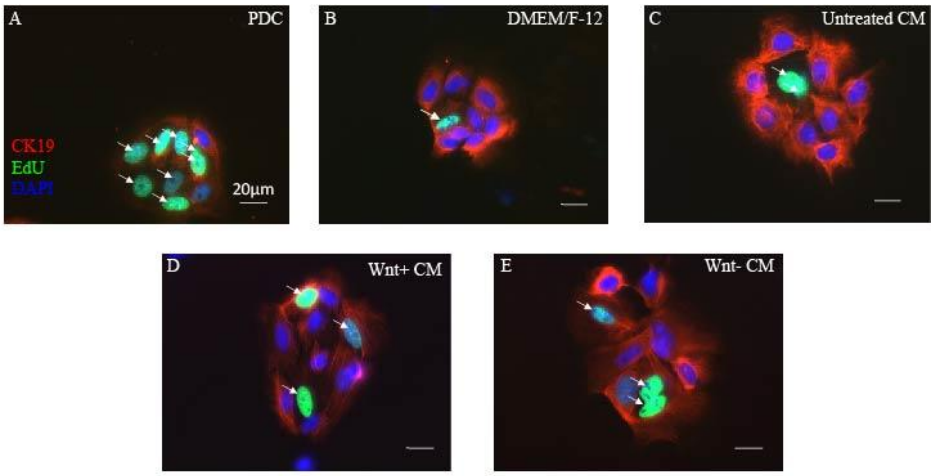
A
PDC
CK19
EdU
DAPI
20μm
B
DMEM/F-12
C
Untreated CM
D
Wnt+ CM
E
Wnt- CM

F

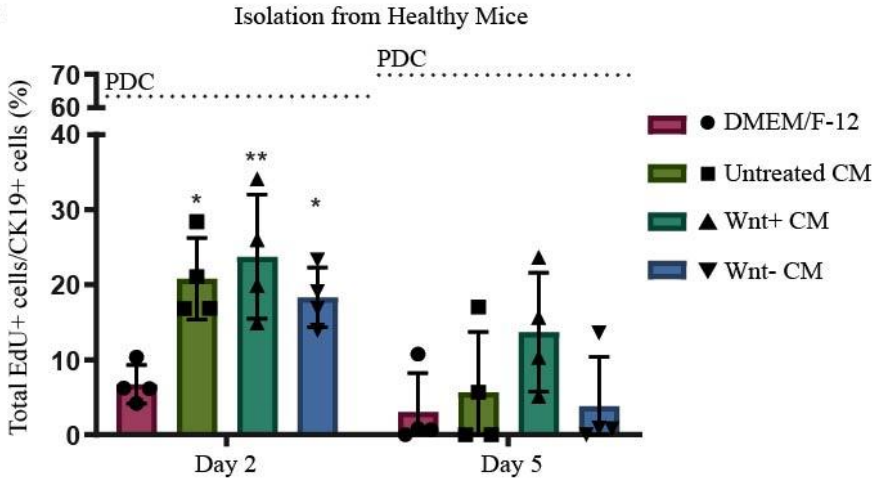
Isolation from Healthy Mice
PDC
PDC
Total EdU+ cells/CK19+ cells (%)
70
60
40
30
20
10
0
*
**
*
Day 2
Day 5
DMEM/F-12
Untreated CM
Wnt+ CM
Wnt- CM

G

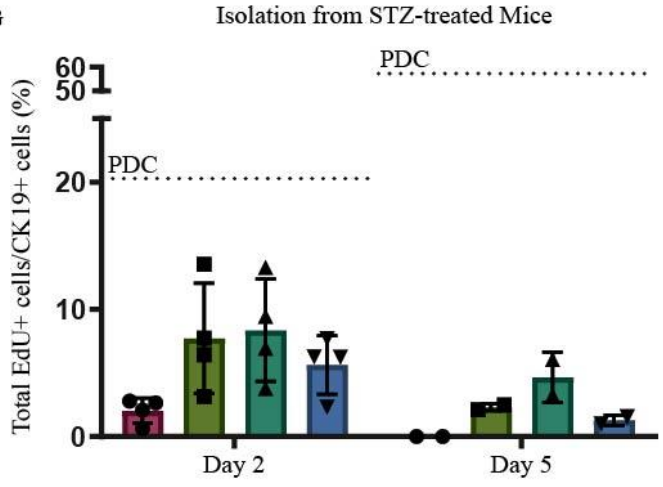
Isolation from STZ-treated Mice
PDC
PDC
Total EdU+ cells/CK19+ cells (%)
60
50
20
10
0
Day 2
Day 5

Figure 2.8 Treatment with hMSC CM increased the frequency of proliferating CK19+ cells *in vitro*. FACS isolated 7-AAD-/DBA lectin + cells from healthy or STZ-treated 8-10 week-old mice were cultured in **(A)** complete PDC media, **(B)** basal DMEM/F-12, or DMEM/F-12 supplemented with **(C)** Untreated, **(D)** Wnt+, or **(E)** Wnt- hMSC CM (N=4). After 2 or 5 days, CK19+ cells were assessed for proliferation [EdU incorporation following 24h pulse label (50 μM)]. Arrows indicate DAPI+/CK19+/EdU+ cells. **(F)** DBA lectin+ cells from healthy mice cultured in DMEM/F-12 supplemented with Untreated, Wnt+, or Wnt- hMSC CM showed significantly increased frequencies of EdU+/CK19+ cells after 2 days of culture compared to DBA lectin+ cells cultured in basal DMEM/F-12. After 5 days culture, there was no significant difference in the frequency of EdU+/CK19+ cells between CM supplemented cultures and culture in basal DMEM/F-12. **(G)** DBA lectin+ cells isolated from STZ-treated mice showed no significant difference in the frequency of proliferating CK19+ cells after 2 or 5 days in culture. Data represent mean ± SD compared using a one-way ANOVA followed by Tukey's multiple comparison test comparing back to DMEM/F-12 for each timepoint (*$p<0.05$, **$p<0.01$).

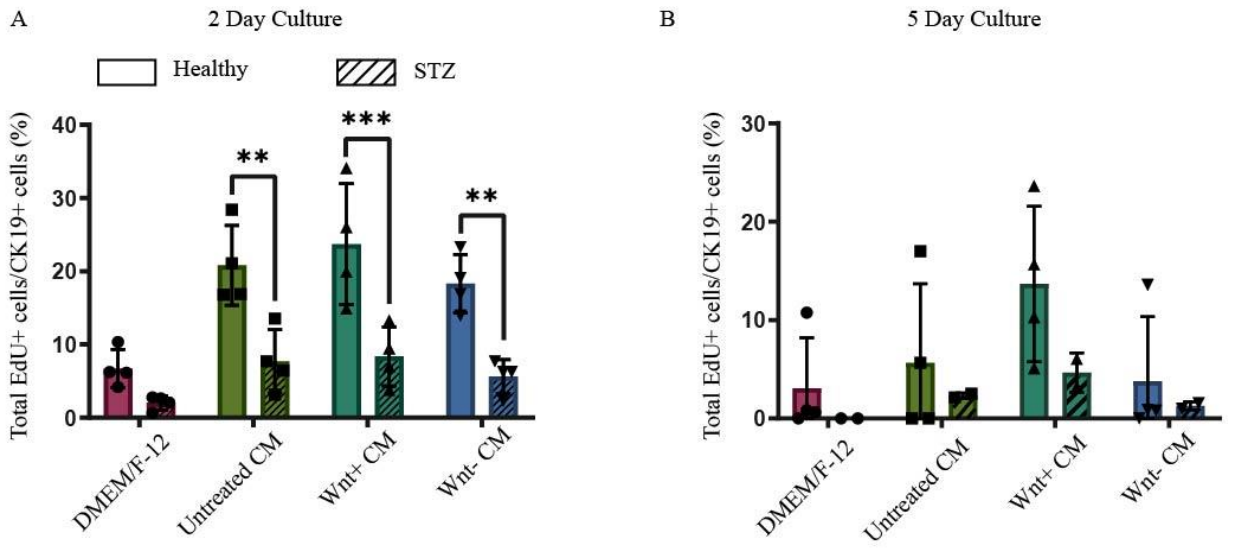

Figure 2.9 STZ treatment decreased DBA lectin+ pancreatic cell proliferation *in vitro*. FACS purified 7-AAD-/DBA lectin+ pancreatic cells from 8-10 week-old healthy or STZ-treated mice were cultured in complete PDC media, basal DMEM/F-12 media , or DMEM/F-12 supplemented with Untreated, Wnt+, or Wnt- hMSC CM for 2 or 5 days. DBA lectin+ cells purified from STZ-treated mice exhibited decreased frequencies of EdU+/CK19+ cells compared to cells isolated from healthy mice at **(A)** 2 days or **(B)** 5 days of culture (N=2-4). Data represent mean ± SD compared using a two-way ANOVA followed by Tukey's multiple comparison test (**$p<0.01$, ***$p<0.001$).

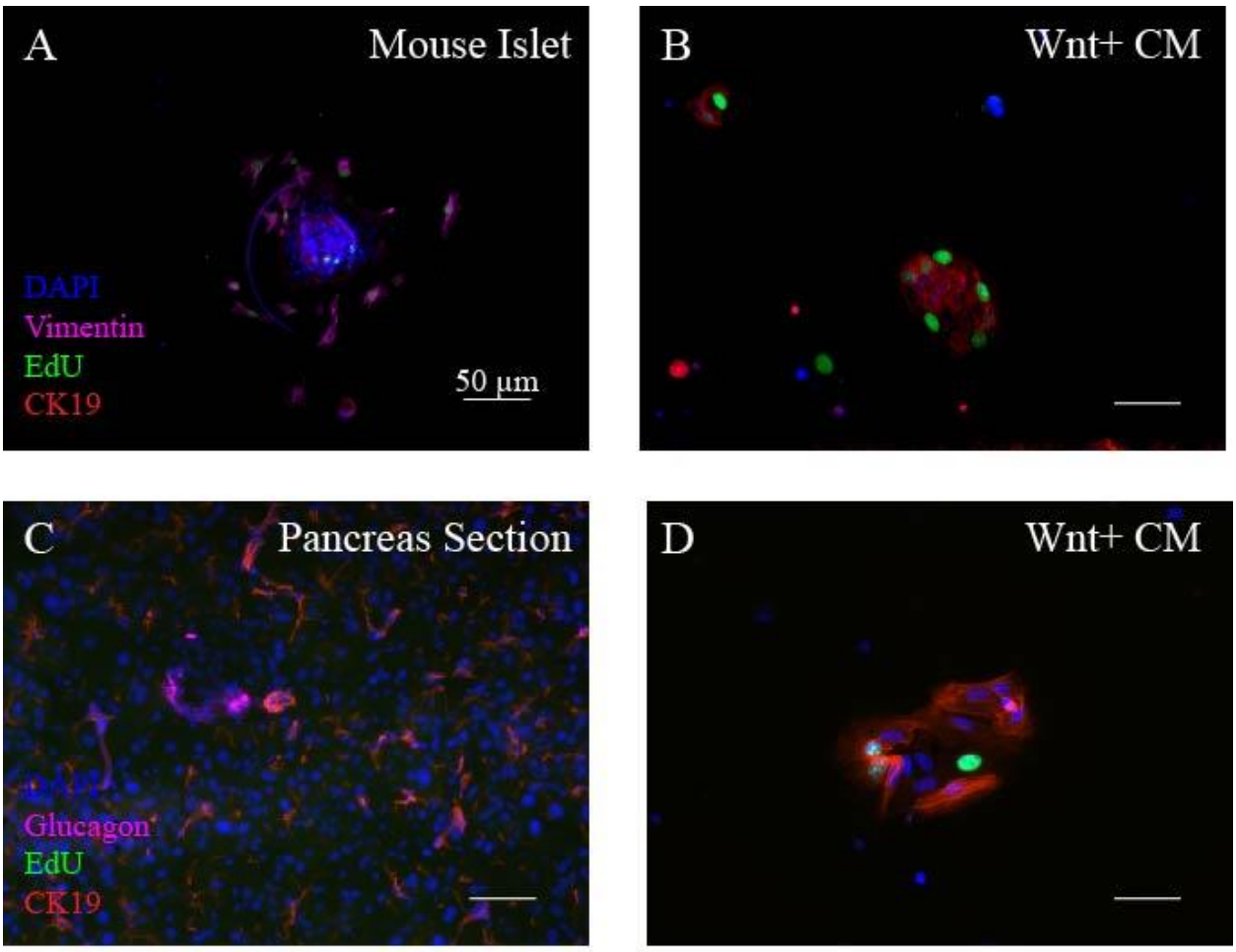

Figure 2.10 Epithelial-to-mesenchymal transition and endocrine phenotype acquisition were not observed in DBA lectin+ cells exposed to hMSC CM *in vitro*. FACS purified 7-AAD-/DBA lectin+ cells from healthy or STZ-treated mice were cultured in complete PDC media, basal DMEM/F-12 media, or DMEM/F-12 supplemented with Untreated, Wnt+, or Wnt- hMSC CM in DMEM/F-12 for 2, 4, or 7 days. Representative photomicrographs of **(A)** mouse islets and **(B)** DBA lectin+ cells (cultured in DMEM/F-12 supplemented with Wnt+ CM) stained for vimentin and CK19. No co-localization of vimentin and CK19 was observed. Representative photomicrographs of **(C)** a mouse pancreas section and **(D)** DBA lectin+ cells (cultured in DMEM/F-12 supplemented with Wnt+ hMSC CM) showed no co-localization of glucagon or insulin (not shown) with CK19.

2.3.7 STZ Treatment (60 mg/kg/day x 5 days) induced hyperglycemia in CK19-CreERT;Ai9(RCL-tdT) mice

To assess the optimal STZ dose to induce hyperglycemia and reduce β-cell mass, CK19-CreERT;Ai9(RCL-tdT) mice (8-12 weeks old) were treated with 40, 50, 60, or 65 mg/kg/day STZ for 5 consecutive days (Days 1-5). On Days 0, 7, 10 and 14, mice were assessed for non-fasting blood glucose and body weight. Treatment with 60 mg/kg/day of STZ resulted in significantly increased non-fasting blood glucose levels at Day 14 compared to Day 0 and Day 7 (Figure 2.11A). Treatment with 40, 50, or 65 mg/kg/day showed no differences in non-fasting blood glucoses over time. There were no significant differences in the area under the curve (A.U.C.) for blood glucose between Days 0 and 14 for STZ-treated mice compared to CAB control mice (Figure 2.11B). Assessing differences between the effects of STZ administration in males vs. females on blood glucose, male mice administered 60 mg/kg/day exhibited significantly increased non-fasting blood glucose levels at Day 14 compared to Day 7 (Figure 2.11C). No differences over time were observed in other male/female groups administered STZ. There were no significant differences in A.U.C. for blood glucose between males/females administered STZ compared to CAB control mice (Figure 2.11D). Mice treated with 50, 60, or 65 mg/kg/day of STZ demonstrated weight loss (D14/D0) compared to CAB control mice, which should be monitored upon further experimentation and extension of the model (Figure 2.11E). Among STZ-treated mice, those administered 60 mg/kg/day produced the highest proportion (30%) of mice with non-fasting blood glucose levels ≥15 mmol/l at Day 14 (Figure 2.11F). Mice deemed hyperglycemic and suitable for hMSC CM transplantation should have non-fasting blood glucose between 15 and 25 mmol/l[199,200,207,225,226].

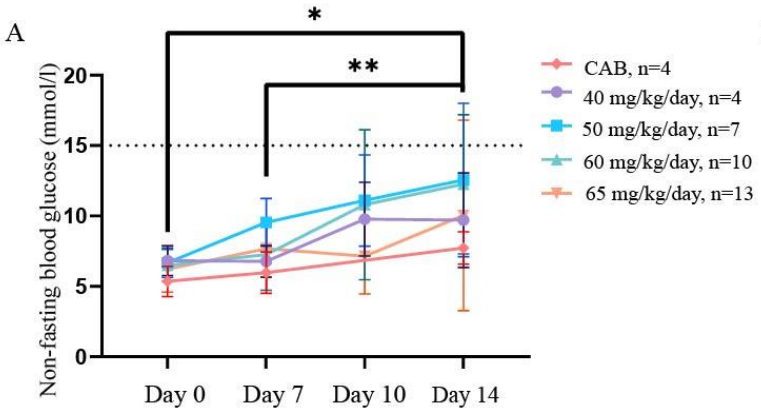
A
*
**
Non-fasting blood glucose (mmol/l)
20
15
10
5
0
Day 0
Day 7
Day 10
Day 14
CAB, n=4
40 mg/kg/day, n=4
50 mg/kg/day, n=7
60 mg/kg/day, n=10
65 mg/kg/day, n=13

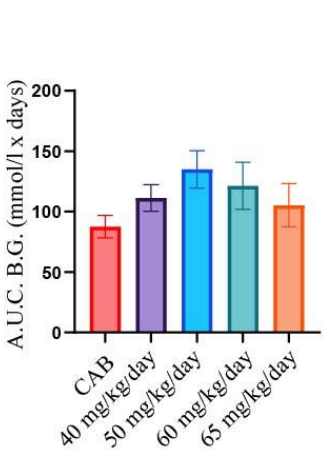
B
A.U.C. B.G. (mmol/l x days)
200
150
100
50
0
CAB
40 mg/kg/day
50 mg/kg/day
60 mg/kg/day
65 mg/kg/day

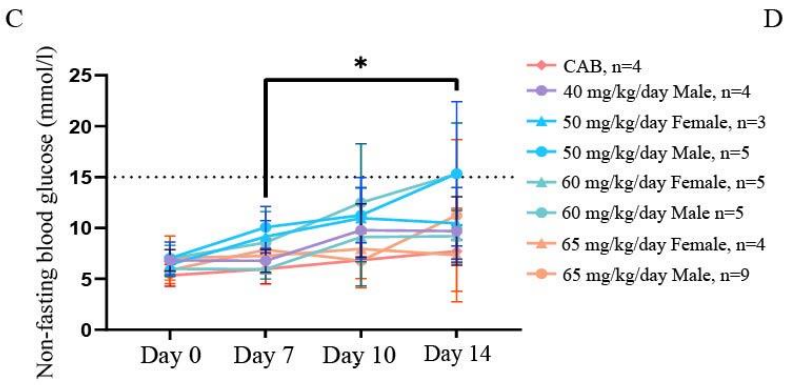
C
*
Non-fasting blood glucose (mmol/l)
25
20
15
10
5
0
Day 0
Day 7
Day 10
Day 14
CAB, n=4
40 mg/kg/day Male, n=4
50 mg/kg/day Female, n=3
50 mg/kg/day Male, n=5
60 mg/kg/day Female, n=5
60 mg/kg/day Male n=5
65 mg/kg/day Female, n=4
65 mg/kg/day Male, n=9

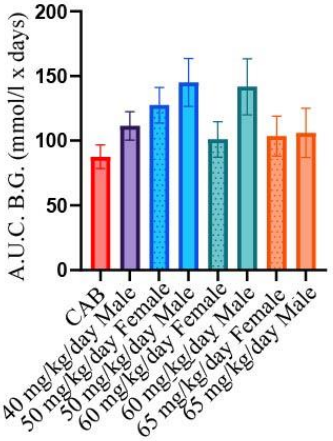
D
A.U.C. B.G. (mmol/l x days)
200
150
100
50
0
CAB
40 mg/kg/day Male
50 mg/kg/day Female
50 mg/kg/day Male
60 mg/kg/day Female
60 mg/kg/day Male
65 mg/kg/day Female
65 mg/kg/day Male

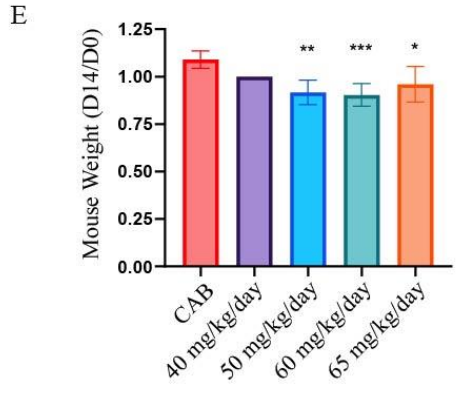
E
Mouse Weight (D14/D0)
1.25
1.00
0.75
0.50
0.25
0.00
**
***
*
CAB
40 mg/kg/day
50 mg/kg/day
60 mg/kg/day
65 mg/kg/day

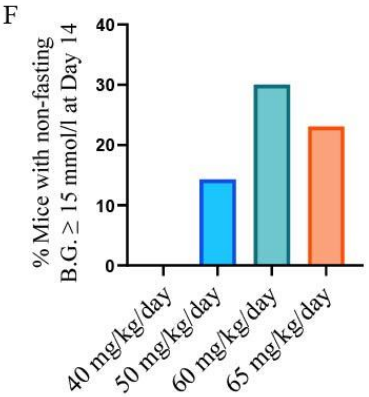
F
% Mice with non-fasting B.G. ≥ 15 mmol/l at Day 14
40
30
20
10
0
40 mg/kg/day
50 mg/kg/day
60 mg/kg/day
65 mg/kg/day

Figure 2.11 STZ treatment (60 mg/kg/day x 5 days) of CK19-CreERT;Ai9(RCL-tdT) mice resulted in elevated glycemia (≥ 15 mmol/l) at Day 14. CK19-CreERT;Ai9(RCL-tdT) mice (8-12 weeks old) administered 40, 50, 60, or 65 mg/kg/day STZ for 5 consecutive days were assessed for non-fasting blood glucose and body weight at Days 0, 7, 10, and 14. **(A)** Treatment with 60 mg/kg/day of STZ (n=10) resulted in significantly increased non-fasting blood glucose levels at Day 14 compared to Day 0 and 7 values (*$p<0.05$ and **$p<0.01$, respectively). Treatment with 40 (n=4), 50 (n=7), or 65 mg/kg/day of STZ (n=13) showed no difference in non-fasting blood glucoses levels over time. **(B)** There were no significant differences in the areas under the curve between different concentrations of STZ administered compared to the CAB control. **(C)** Male mice administered 60 mg/kg/day STZ (n=5) had significantly increased non-fasting blood glucose levels at Day 14 compared to Day 7 (*$p<0.05$). There were no differences in non-fasting glucose levels for 40 mg/kg/day Males (n=4), 50 mg/kg/day Females (n=4), 50 mg/kg/day Males (n=3), 60 mg/kg/day Females (n=5), 65 mg/kg/day Females (n=4), and 65 mg/kg/day Males (n=9) over time. **(D)** There were no significant differences in the areas under the curve between each of the treatment concentrations (categorized by sex) compared to the CAB control. **(E)** Mice treated with 50 mg/kg/day, 60 mg/kg/day, or 65 mg/kg/day STZ exhibited weight loss (D14/D0) compared to CAB control mice. **(F)** Treatment with 60 mg/kg/day of STZ resulted in the highest proportion (30%) of mice with non-fasting blood glucose ≥ 15 mmol/l at Day 14. Data represent mean ± standard error of the mean (SEM) for A.U.C. graphs and mean ± SD for all remaining data. Non-fasting blood glucose curves were compared using a repeated measures two-way ANOVA followed by Tukey's multiple comparison test. Areas under blood glucose curves and changes in body weight were compared using a one-way ANOVA followed by Tukey's multiple comparison test (*$p<0.05$, **$p<0.01$, ***$p<0.001$).

2.3.8 STZ treatment reduced β-cell mass and islet number in CK19-CreERT;Ai9(RCL-tdT) mice

While STZ treatment seemed to modestly induce hyperglycemia in CK19-CreERT;Ai9(RCL-tdT) mice, histological analysis of the pancreas gives a better indication of β-cell death. CK19-CreERT;Ai9(RCL-tdT) mice treated with 40, 50, 60, or 65 mg/kg/day (Days 1-5) of STZ exhibited decreased β-cell mass and islet number (per mm^2) at Day 14 compared to mice that did not receive STZ (Figure 2.12 F, G). Additionally, treatment with 60 mg/kg/day of STZ resulted in significantly fewer islets per mm^2 compared to treatment with 50 mg/kg/day. STZ treatment did not affect islet circumference compared to control mice (Figure 2.12 H). Based on the effects of 60 mg/kg/day STZ treatment on non-fasting blood glucose and β-cell mass, we decided this dose would be optimal for administration in CK19-CreERT;Ai9(RCL-tdT) mice prior to hMSC CM iPan injection.

2.3.9 Glucose tolerance was impaired in STZ-treated CK19-CreERT;Ai9(RCL-tdT) mice

Based on the collective effects of STZ treatment on non-fasting blood glucose, β-cell mass, and islet density, we chose 60 mg/kg/day as our optimal dose. A glucose tolerance test gives a better indication of real-time β-cell function in controlling blood glucose. CK19-CreERT;Ai9(RCL-tdT) mice treated with 60 mg/kg/day of STZ (Days 1-5) and CAB control mice were fasted for 3 hours on Day 14 before receiving bolus glucose (2 mg/kg) by i.p. injection. Blood glucose was assessed at 0, 5, 10, 15, 30, 45, 60, 90, and 120 minutes. STZ-treated mice demonstrated significantly increased blood glucose levels 120 minutes after bolus injection compared to CAB control mice (Figure 2.13A). STZ treated mice had significantly increased A.U.C. for blood glucose compared to CAB control mice, indicating impaired glucose tolerance (Figure 2.13B).

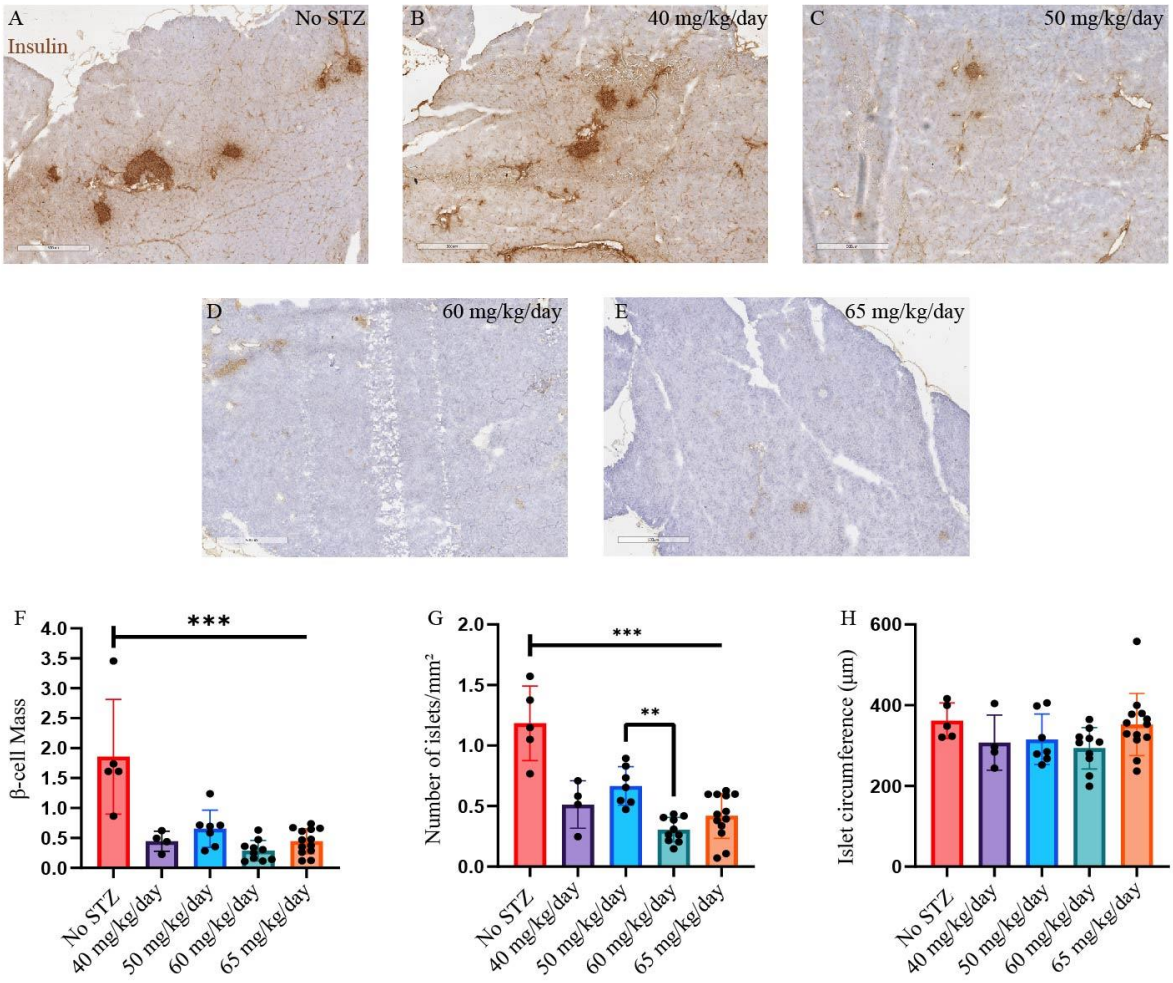

Figure 2.12 STZ treatment in CK19-CreERT;Ai9(RCL-tdT) mice decreased β-cell mass and islet number. CK19-CreERT;Ai9(RCL-tdT) mice (8-12 weeks old) were treated with 40 (n=4), 50 (n=7), 60 (n=10), or 65 (n=13) mg/kg/day of STZ by i.p. injection (Days 1-5). **(A-E)** Representative photomicrographs of frozen pancreas sections at Day 14 are shown. STZ treatment resulted in significantly decreased **(F)** β-cell mass and **(G)** number of islets per mm^2 compared to no STZ control mice. Treatment with 60 mg/kg/day resulted in significantly fewer islets per mm^2 compared to treatment with 50 mg/kg/day. **(H)** STZ treatment did not affect islet circumference compared to no STZ control mice. Data represent mean ± SD compared using a one-way ANOVA followed by Tukey's multiple comparison test (**p<0.01, ***p<0.001).

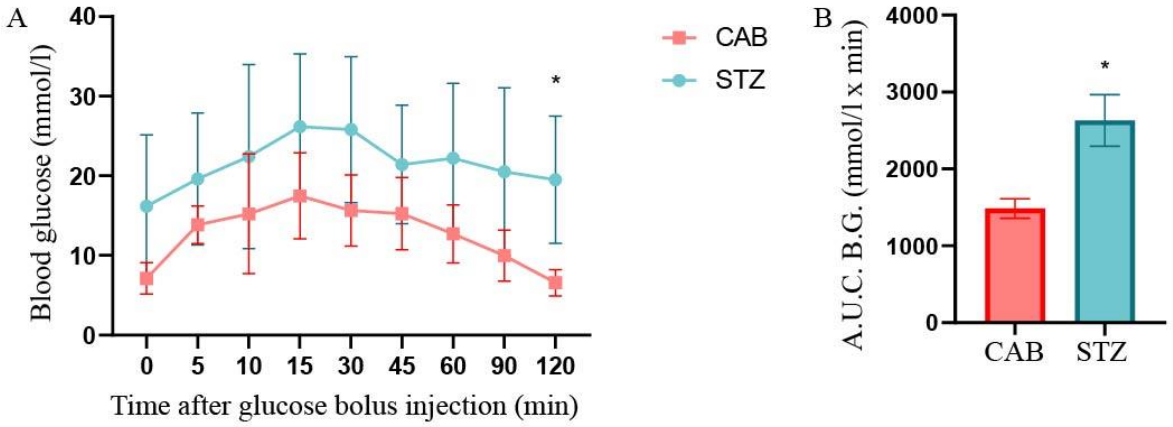

Figure 2.13 Glucose tolerance was impaired in STZ-treated CK19-CreERT;Ai9(RCL-tdT) mice. CK19-CreERT;Ai9(RCL-tdT) (8-12 weeks old) were treated with 60 mg/kg/day of STZ (n=7) or CAB (n=4) for 5 consecutive days. On Day 14, mice were fasted for 3 hours before receiving bolus glucose (2 mg/kg) by i.p. injection and blood glucose was assessed at 0, 5, 10, 15, 30, 45, 60, 90, and 120 minutes. **(A)** STZ-treated mice had significantly increase blood glucose levels 120 minutes after bolus injection compared to mice injected with CAB. **(B)** STZ-treated mice demonstrated impaired glucose tolerance compared to mice injected with CAB. Data represent mean ± SD compared using a two-way ANOVA followed by Tukey's multiple comparison test for the glucose tolerance time course. A.U.C. data represents mean ± SEM compared using a student's t-test to compare area under the curve (*$p<0.05$).

2.3.10 tdTomato labels CK19-expressing cells in the pancreas of CK19-CreERT;Ai9(RCL-tdT) mice following tamoxifen administration

To assess whether this model specifically labels CK19+ cells and quantify labeling efficiency, CK19-CreERT;Ai9(RCL-tdT) mice were administered 6 mg tamoxifen by oral gavage 7 days before 60 mg/kg/day STZ treatment by i.p. injection for 5 consecutive days. Mouse pancreata were harvested at Days 0, 1, 7, and 14 and assessed for tdTomato and CK19 expression by flow cytometry and fluorescent microscopy. Mice treated with CAB (vehicle control) were euthanized on Day 14. Gated based on F.M.O. samples, live tdTomato+ cells labelled CK19-expressing pancreas cells at all timepoints in STZ-treated and CAB-treated mice (Figure 2.14A-D). To assess tdTomato labelling efficiency within the CK19+ population, live CK19+ cells were assessed for tdTomato expression based on the tdTomato FMO. tdTomao expression was observed in approximately 20% of CK19-expressing cells at each timepoint (Figure 2.14E-H). Future studies to optimize tamoxifen administration may improve CK19+ cell labeling efficiency, as the administered dose and repeated injection frequency may increase the efficiency of Cre recombinase activation in CK19-expressing cells[250]. tdTomato expression was not detected (<0.001%) when mice were administered corn oil without tamoxifen.

2.3.11 Pancreatic insulin expression diminished following STZ treatment in CK19-CreERT;Ai9(RCL-tdT) mice

While CK19-CreERT;Ai9(RCL-tdT) mice exhibited decreased β-cell mass and impaired glucose tolerance following STZ treatment, the proportion of insulin+ cells during STZ treatment is an important indicator of the effectiveness of STZ treatment. Mice were treated with 6 mg Tamoxifen followed by 7 days of rest. Mice were subsequently treated with 60 mg/kg/day of STZ (Days 1-5). At Days 0, 1, 7, and 14, pancreatic insulin expression was assessed by flow cytometry. Non-fasting blood glucose at Day 14 was not significantly increased compared to Day 0 (Figure 2.15C). The total proportion of insulin-expressing cells within the pancreas was significantly decreased at Days 7 and 14 compared to Day 0 (Figure 2.14A, D). Insulin expression within tdTomato+ cells was significantly reduced at Day 14 compared to Days 0 and 1 (Figure 2.15B,E).

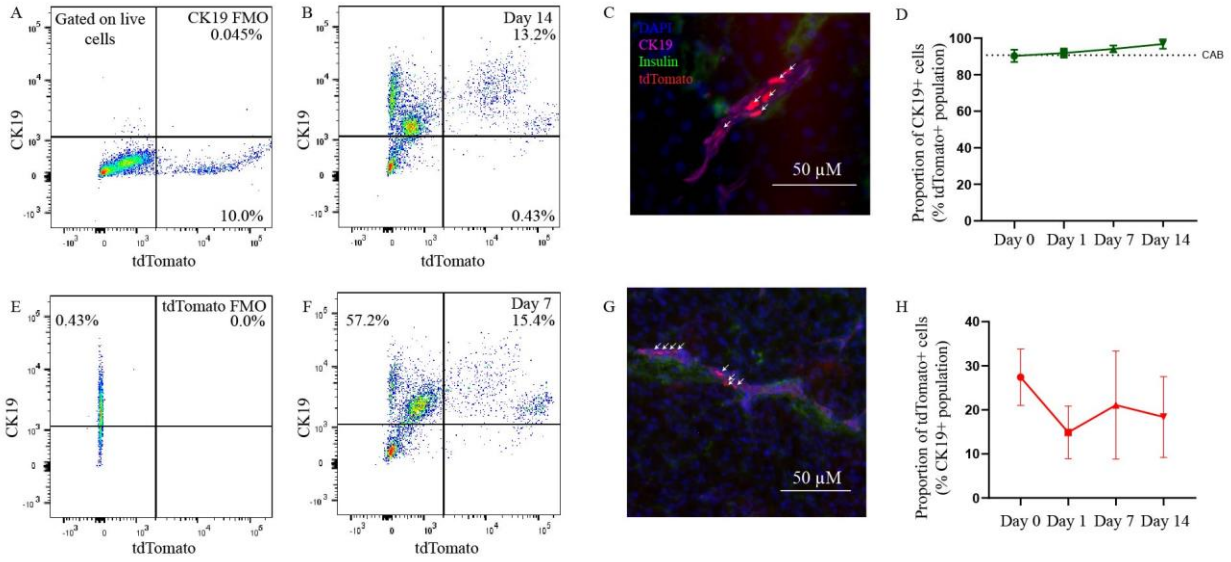

Figure 2.14 tdTomato labeled CK19-expressing cells in the pancreas following tamoxifen treatment in CK19-CreERT;Ai9(RCL-tdT) mice. CK19-CreERT;Ai9(RCL-tdT) mice were treated with 6 mg Tamoxifen by oral gavage. After 7 days rest, mice were administered 60 mg/kg/day STZ by i.p. injection for 5 consecutive days. Mouse pancreata were harvested at Days 0, 1, 7, and 14 and assessed for tdTomato and CK19 expression by flow cytometry (n=4-7) and fluorescent microscopy. Mice treated with CAB (vehicle control) instead of STZ were sacrificed 14 days after the first day of treatment (n=4). **(A)** Live (Zombie-) tdTomato+ cells were assessed for CK19 expression based on the CK19 F.M.O samples. **(B)** Representative dot plot of CK19 expression vs. SSC-A (gated on live tdTomato+ cells). **(C)** Representative photomicrograph of tdTomato and CK19 expression. **(D)** tdTomato labelled CK19-expressing pancreatic ductal cells at all timepoints in STZ-treated and CAB mice. To assess tdTomato labelling efficiency within the CK19+ ductal population, live CK19+ cells were assessed for tdTomato expression based on the **(E)** tdTomato FMO. **(F)** Representative dot plot showing tdTomato expression in live CK19+ cells. **(G)** Representative photomicrograph showing CK19 and tdTomato expression in a duct. **(H)** tdTomato expression was observed in approximately 20% of CK19+ ductal cells at each timepoint.

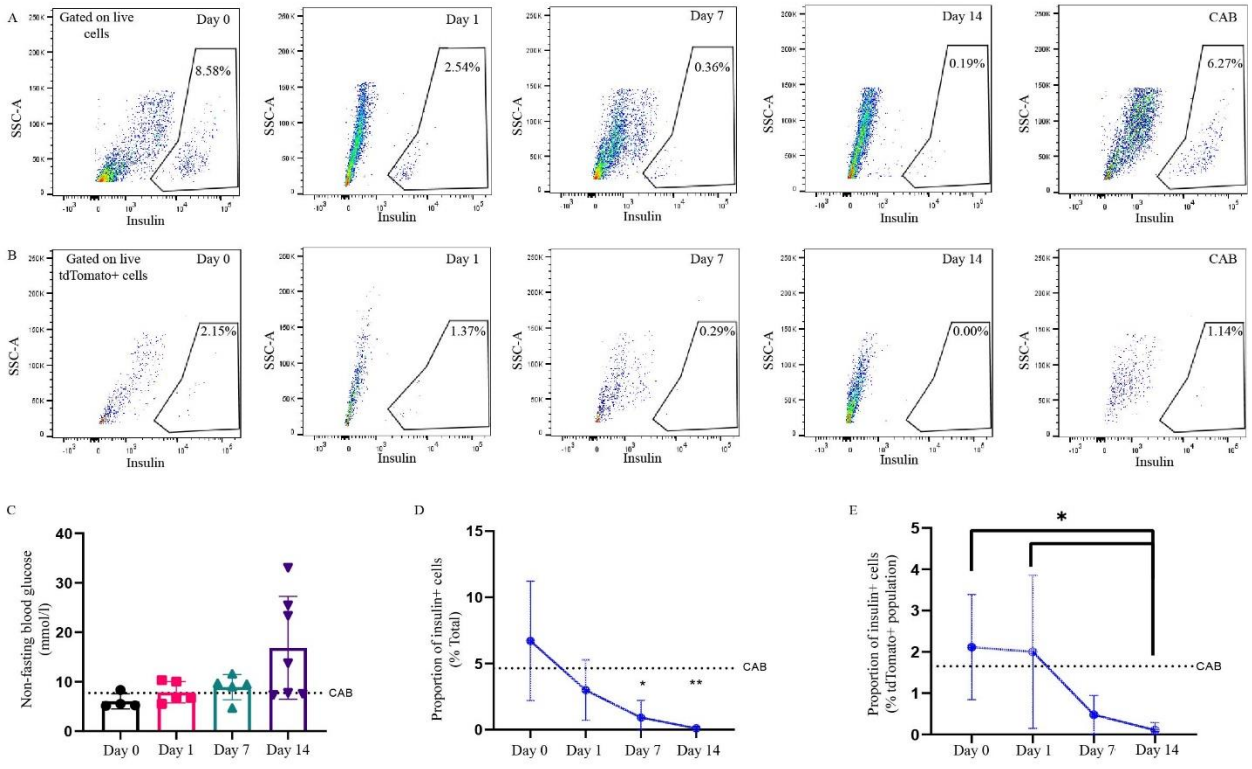

Figure 2.15 STZ treatment in CK19-CreERT;Ai9(RCL-tdT) mice decreased the proportion of insulin-expressing cells within the pancreas. CK19-CreERT;Ai9(RCL-tdT) mice were treated with 6 mg Tamoxifen by oral gavage. After 7 days rest, mice were treated with 60 mg/kg/day STZ by i.p. injection for 5 consecutive days. At Days 0, 1, 7, and 14, pancreatic insulin expression was assessed by flow cytometry (n=4-7). **(A)** Representative dot plots for insulin vs. SSC-A (gated on live cells) at each timepoint and CAB control mice are shown. **(B)** Representative dot plots for insulin vs. SSC-A (gated on live tdTomato+ cells) at each timepoint and CAB control mice are shown. **(C)** Non-fasting blood glucose at Day 14 was not significantly different compared to Day 0. **(D)** Insulin-expressing β-cells at Days 7 and 14 were significantly decreased compared to Day 0. **(E)** Within tdTomato+ cells, the proportion of insulin+ β-cells was significantly decreased at Day 14 compared to Days 0 and 1. Data represent mean ± SD compared using a one-way ANOVA followed by Tukey's multiple comparison test (*$p<0.05$, **$p<0.01$).

2.3.12 STZ treatment increased the proportion of infiltrating CD45+ cells in the pancreas of CK19-CreERT;Ai9(RCL-tdT) mice

To further investigate whether leukocyte infiltration plays a role in STZ-mediated injury, pancreata from CK19-CreERT;Ai9(RCL-tdT) mice treated with Tamoxifen 7 days before STZ treatment (Days 1-5) were assessed for CD45 expression, a pan-leukocyte marker[251,252], by flow cytometry. The proportion of CD45+ cells in the pancreas was significantly increased at Days 1 and 7 compared to Day 0 (Figure 2.16A,D). Within CK19+ cells, the proportion of CD45+ cells was significantly increased at Day 7 compared to Days 0 and 14 (Figure 2.15B,E). Within the tdTomato+ cell population, the proportion of CD45+ cells was significantly increased at Day 7 compared to Day 0 (Figure 2.16C,F).

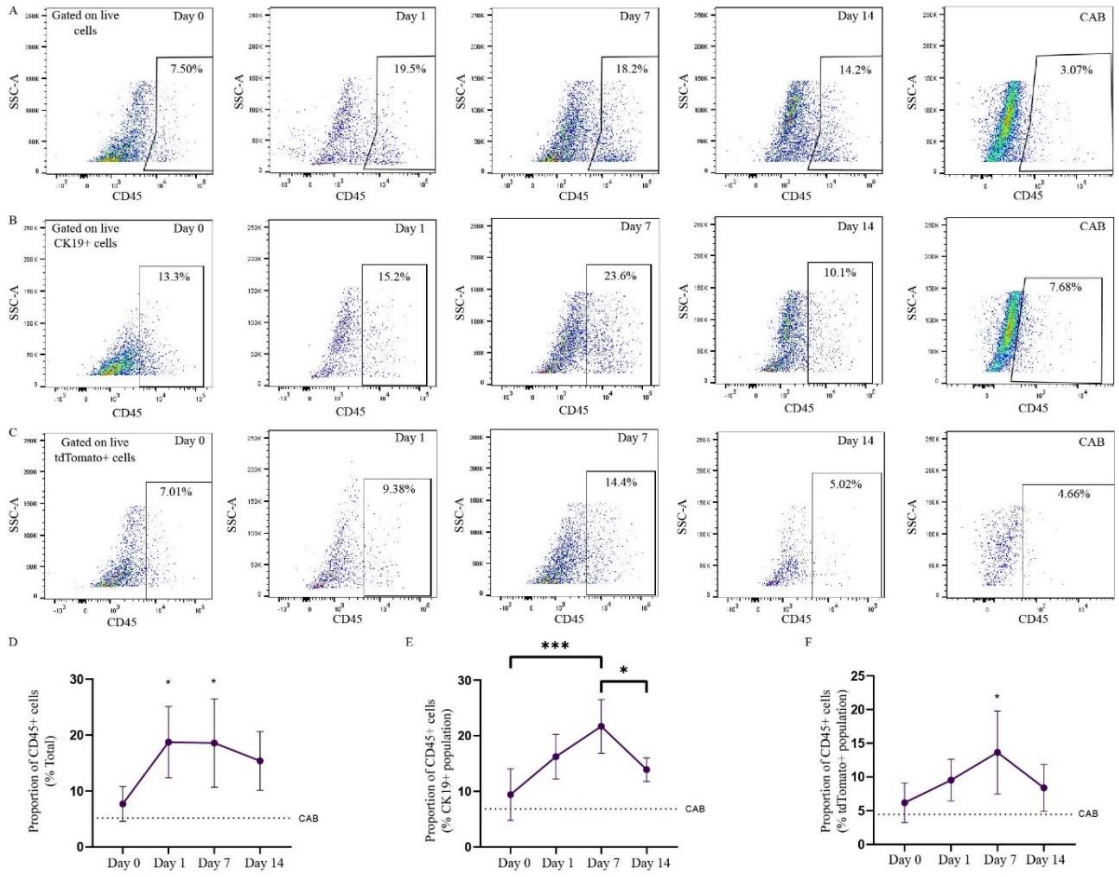

Figure 2.16 STZ treatment in CK19-CreERT;Ai9(RCL-tdT) mice increased the proportion of CD45+ cells in the pancreas. CK19-CreERT;Ai9(RCL-tdT) mice were treated with 6 mg Tamoxifen by oral gavage. After 7 days rest, mice were treated with 60 mg/kg/day STZ for 5 days. At 0, 1, 7, and 14 after STZ treatment, pancreatic CD45 expression was assessed by flow cytometry (n=4-7). **(A)** Representative dot plots for CD45 vs. SSC-A (gated on live cells) at each timepoint and for CAB control mice are shown. **(B)** Representative dot plots for CD45 vs SSC-A (gated on live CK19+ cells) at each timepoint and for CAB control mice are shown. **(C)** Representative dot plots for CD45 vs. SSC-A (gated on live tdTomato+ cells) at each time point and for CAB control mice are shown. **(D)** CD45+ leukocytes within the pancreas were significantly increased at Days 1 and 7 compared to Day 0. **(E)** Within CK19+ ductal cells, the proportion of CD45+ leukocytes was significantly increased at Day 7 compared to Days 0 and 14. **(F)** Within tdTomato+ cells, the proportion of CD45+ cells was significantly increased at Day 7 compared to Day 0. Data represent mean ± SD compared using a one-way ANOVA followed by Tukey's multiple comparison test (*$p<0.05$, ***$p<0.001$).

2.4 Discussion

These studies demonstrated that hMSC CM increased CK19+ cell proliferation *in vitro* and characterized a lineage tracing mouse model to follow CK19+ cell fate following STZ-induced β-cell ablation followed by hMSC CM intrapancreatic injection in hyperglycemic mice. We utilized DBA lectin expression followed by serum supplemented culture as methodology to purify and culture viable cells enriched for CK19 expression[231]. hMSC CM supplementation increased proliferation rates of CK19-expressing cells *in vitro*, although indication of mesenchymal or endocrine phenotype transition were not observed. We also characterized a lineage tracing mouse model that labels CK19-expressing cells in the pancreas following tamoxifen administration. Low-dose STZ treatment for 5 days induced hyperglycemia and diminished the insulin+ population within the pancreas. Collectively, these data suggest that hMSC CM positively impacts the growth kinetics of CK19-expressing cells *in vitro* and that CK19-CreERT;Ai9(RCL-tdT) mice may be used in future experiments to assess the contribution of CK19-expressing cells during islet regeneration following hMSC CM intrapancreatic injection in hyperglycemic mice.

While DBA lectin+ cells exhibited ~40% CK19 expression as assessed by flow cytometry, subsequent culture in complete PDC media further enriched for CK19 expression within this population (≈ 83% purity). Thus, this purification and culture process represents a reliable methodology to culture viable mouse pancreatic cells enriched for CK19 expression. hMSC CM supplementation into the culture media of DBA lectin+ cells isolated from healthy mice increased their proliferative response at 2 days, but no difference was observed at 5 days. This increase in proliferation was not observed in cell cultures from STZ-treated mice. The MSC secretome, comprised of soluble factors and extracellular vesicles, contains immunomodulatory, anti-apoptotic, pro-angiogenic, proliferative, and growth factors that facilitate tissue repair[187,190–192]. hMSC CM has previously been shown to improve viability and migratory capacity of a human proximal tubular epithelial cell line following toxic chemical exposure, showcasing its protective effects on cells exposed to harsh environments including chemical treatment and cell culture assays[253]. Protective effects of hMSC CM, including enhanced survival, proliferation, or immunodulatory effects, has also been observed in endothelial cell, synovial explant, and microglia cultures[254–256]. Interestingly, cultured CK19+ cells isolated from healthy mice exhibited higher rates of proliferation compared to cells isolated from STZ-treated mice. While the effects

of STZ treatment on pancreatic β-cells have been well characterized, phenotypic and functional changes in non-endocrine pancreatic cells, including the duct and acinar cells, and the ability of STZ to indirectly impact islet regeneration following β-cell destruction has not been reported. Further characterization of these phenotypic changes on non-endocrine cell populations, such as the expression of cell cycle regulators or EMT markers, could reveal additional cellular targets that contribute to pancreatic repair in hyperglycemic mice.

Mesenchymal or endocrine phenotype transition was not observed in cultures of DBA lectin+ cells from healthy or STZ-treated mice after 2, 4, or 7 days of cultured with hMSC CM. Further evaluation of phenotypic changes should be conducted in a 3-dimensional culture environment (e.g. cells suspended in collagen spheres) and transcriptome analysis of cell cycle, mesenchymal, and endocrine cell regulators should be investigated. Evidence for MSC CM modulation of differentiation following culture supplementation has been reported. hMSC CM has previously been shown to enhance chondrogenic, osteogenic, and hematopoietic differentiation in hESC cultures[257,258]. Culture supplementation with MSC CM also upregulated expression of cardiomyocyte-related genes in cardiac progenitor cells[259].

To evaluate the contribution of CK19-expressing cells in hMSC CM induced islet regeneration, we first aimed to develop and characterize a model to follow the fate of CK19-expressing cells within the pancreas. We used CK19-CreERT;Ai9(RCL-tdT) mice, which utilize tamoxifen pulse-chase labelling of CK19+ cells[221,222]. A single tamoxifen treatment (6 mg) was sufficient to induce specific labelling of CK19-expressing cells in the pancreas one-week post-administration. Absence of tdTomato detection following corn oil vehicle control administration indicated that the CK19-CreERT promoter was not leaky. tdTomato labelling efficiency of CK19+ cells was approximately 20% across time. Further optimization of tamoxifen dosage (e.g. multiple administrations) may increase labeling efficiency. tdTomato labelling and promoter leakiness should also be assessed over a long-term period (e.g. 42 days) when characterizing hMSC CM-induced islet regeneration in these mice.

As CK19-CreERT;Ai9(RCL-tdT) mice possess active DNA-dependent protein kinase (DNA-PK), a DNA repair enzyme which is truncated and inactive in NOD/SCID mice[260,261], we hypothesized that a higher STZ dose would be required to induce hyperglycemia and loss of β-cell mass compared to the 35 mg/kg/day administered to NOD/SCID mice, as greater STZ sensitivity has been reported in NOD/SCID mice which lack functional T-cells[262]. Consistent induction of severe hyperglycemia was difficult to achieve in CK19-CreERT;Ai9(RCL-tdT) mice. Treatment with 60 mg/kg/day for 5 consecutive days caused the greatest proportion of mice to become hyperglycemic (≥15 mmol/l non-fasting blood glucose) by Day 14. These mice exhibited decreased β-cell mass and islet density with no change in islet circumference, compared to control mice, and demonstrated impaired glucose tolerance following glucose bolus injection. Similarly, pancreatic biopsies from patients with T1D exhibit decreased islet density, while islet size was maintained compared to healthy subjects[263]. While there were some mice who did not become hyperglycemic, those considered suitable for hMSC CM injection will have non-fasting blood glucose levels between 15 and 25 mmol/l at Day 14.

Along with pancreatic β-cell loss, insulin+ cells within the pancreas were significantly decreased at Days 7 and 14. Similarly, within the tdTomato+ cell population, the frequency of insulin+ cells was diminished over time and were rare at Day 14 (<0.5%). This indicates that STZ treatment was successful in mediating β-cell destruction, and that emergence of insulin-expressing tdTomato+ cells following hMSC CM iPan injection, if absent in vehicle control mice, could truly be attributed to the regenerative microenvironment of the hMSC secretome in future experiments.

Additionally, STZ treatment induced leukocyte infiltration in mice. While NOD/SCID mice treated with 35 mg/kg/day STZ demonstrated a stable proportion of CD45+ cells within the pancreas, F4/80 upregulation at Day 10 indicated macrophage differentiation in response to increased β-cell apoptosis. Within CK19+ cells, an increase in F4/80+ cells on the last day of STZ treatment (Day 5) may indicate macrophage infiltration in response to pancreatic injury. Treatment of CK19-CreERT;Ai9(RCL-tdT) mice with 60 mg/kg/day of STZ induced pancreatic infiltration of CD45+ cells at Days 1 and 7. Within CK19+ and tdTomato+ cells, CD45+ leukocyte infiltration at Day 7 was observed, indicating possible interactions between leukocytes and pancreatic epithelial cells in response to STZ treatment. Future studies investigating leukocyte subpopulation breakdowns (e.g. macrophages, T-cells) during STZ-induced CD45+ cell infiltration will provide

insight into cellular phenotypes mediating the immune response. Macrophage and T-cell islet infiltration and subsequent release of inflammatory cytokines, including IL-1β, IFN-γ, and TNF-α, mark key steps in diabetes pathogenesis resulting in β-cell destruction[22,56–61]. Macrophages play a crucial role in tissue repair in response to injury or stress. During inflammation, macrophages secrete chemotactic factors to recruit immune cells and clear cellular debris from apoptotic cells via phagocytosis[264]. Evidence for pancreatic macrophage infiltration following STZ treatment has been reported[265–267]. While macrophages normally play an anti-inflammatory role in tissue repair, phagocytosis of apoptotic β-cells and elevated blood glucose levels promote a proinflammatory macrophage phenotype, potentially tipping the balance to favour β-cell destruction over regeneration[268,269]. T-cell dependent Class II MHC antigen expression and subsequent pancreatic T-cell infiltration has been demonstrated in mice following multiple low dose STZ treatment[270,271]. Infiltrating T-cells increase INF-γ release, further mediating inflammation and destruction within the pancreas[271]. Thus, macrophages and T-cells represent key targets in attenuating inflammation and destruction in response to β-cell injury, and their regulation may play an important role in developing a regenerative microenvironment to promote islet regeneration.

In summary, these studies show increased proliferation of hMSC CM supplemented murine ductal cells *in vitro* and provide proof-of-concept characterization of CK19-CreERT;Ai9(RCL-tdT) mice during STZ treatment *in vivo*. The CK19-CreERT;Ai9(RCL-tdT) mouse model represents a valuable tool that required characterization prior to use in future studies to follow the fate of CK19-expressing cells during hMSC CM induced islet regeneration. Future studies, including optimization of tamoxifen treatment and in-depth characterization of pancreatic leukocyte infiltration in response to STZ treatment, will further solidify CK19-CreERT;Ai9(RCL-tdT) mice as a sound model for CK19+ cell lineage tracing and identify additional potential cellular targets to maximize islet regeneration, respectively. These studies ultimately aid in developing a cell-free regenerative therapy to stimulate islet regeneration to treat patients with diabetes.

3.0 Discussion

3.1 Summary

The primary objective of this research was to determine the effects of hMSC CM on murine ductal cells *in vitro* and to characterize a lineage tracing mouse model for the future assessment of CK19-expressing cell contribution to hMSC CM stimulated islet regeneration *in vivo*. We have previously shown that iPan injection of Wnt+ hMSC CM reliably reduces systemic blood glucose and rescues β-cell mass in hyperglycemic mice by stimulating the formation of small ductal-associated islet clusters via paracrine signals in mice with STZ-mediated β-cell ablation[198–200,207]. Bone marrow-derived hMSC (P4, 80% confluent) were cultured in serum-free media for 24h to generate Untreated, Wnt+, or Wnt- CM using pharmacological small molecule treatment. CK19+ cells from mouse pancreata, purified by DBA lectin+ FACS were cultured in basal DMEM/F-12 media supplemented with hMSC CM. CK19+ cells from healthy mice exhibited increased proliferation at 2 days in culture with either Untreated, Wnt+, or Wnt- hMSC CM compared to basal media alone. Although proliferation was diminished at 5 days after hMSC CM supplementation, we found that hMSC CM, irrespective of Wnt-pathway stimulation, secreted regenerative stimuli that support short-term proliferation of CK19+ cells *in vitro*. Notably, CK19+ cells isolated from STZ-treated mice did not exhibit increased proliferation compared to basal DMEM/F-12 at 2 or 5 days of culture. Indeed, CK19+ cells isolated from STZ-treated mouse pancreata exhibited less proliferation in culture compared to cells from healthy mice, suggesting STZ treatment changes CK19+ cell growth rates in subsequent culture. Finally, evidence of epithelial-to-mesenchymal transition and endocrine phenotype acquisition were not observed in hMSC CM supplemented cultures with or without STZ treatment.

Next, characterization of CK19-CreERT;Ai9(RCL-tdT) lineage tracing mice was conducted. A single dose of tamoxifen (6 mg) induced specific labeling (tdTomato+) of CK19+ cells within the pancreas. The labelling efficiency of CK19+ cells with tdTomato was approximately 20%. Low dose STZ treatment (60 mg/kg/day) for 5 consecutive days induced hyperglycemia by Day 14 and insulin+ cells within the pancreas were also diminished at Day 14, with a corresponding decrease in β-cell mass. Reduced islet density was observed, while average islet circumference remained unchanged after STZ treatment. STZ treatment also stimulated pancreatic infiltration of leukocytes, which was also reflected within the CK19+ and tdTomato+ cell populations as there was a higher proportion of CD45+ cells. This may indicate immune cell

targeting of these populations as an indirect consequence of STZ treatment. Similarly, treatment of NOD/SCID mice with low dose STZ (35 mg/kg/day for 5 consecutive days) also resulted in macrophage (F4/80+) infiltration into the pancreas. Collectively, these findings suggest that CK19-CreERT;Ai9(RCL-tdT) mice represent a suitable model to characterize CK19+ cell contribution to islet regeneration following iPan injection of hMSC CM in STZ-treated mice.

3.2 hMSC CM improved proliferation of murine CK19+ cell *in vitro,* irrespective of Wnt-pathway stimulation or inhibition

As observed by Kuljanin *et al.*[208], treatment of hMSC with CHIR99021 (≥ 10 μM) increased intracellular β-catenin levels without impacting hMSC viability, indicating Wnt-pathway stimulation was achieved. However, hMSC treatment with IWR-1 did not reduce intracellular β-catenin levels, contrary to previous observations using exclusively regenerative hMSC samples[208]. Low baseline levels of β-catenin/Wnt-pathway signaling in these non-regenerative hMSC samples may possibly contribute to this lack of observed downregulation and suggests that the Wnt-pathway was not active in all cultured hMSC samples.

Isolation of DBA lectin+ cells from mouse pancreata, followed by culture in complete PDC media proved effective in purifying viable CK19+ cells (~83% CK19+/DAPI+). As CK19 is an intracellular marker requiring antibody labeling, cells must be fixed and permeabilized to visualize or isolate CK19+ cells. As a surrogate marker for viable CK19+ ductal epithelial cells[240,272], DBA lectin, which specifically labels the α-linked N-acetylgalactosamine carbohydrate moiety, enriched 2-fold for viable CK19+ cells[233]. Further purification was achieved by culturing DBA lectin+ cells in complete PDC media as outlined by Reichert *et al*[231]. While supplementation of DBA lectin+ cells with hMSC CM, irrespective of Wnt-pathway stimulation or inhibition, improved proliferation of CK19+ cells at Day 2 compared to basal DMEM/F-12, this proliferative effect was diminished at Day 5. hMSC CM supplementation of DBA lectin+ cells isolated from STZ treated mice did not significantly change CK19+ cell proliferative frequencies. hMSC CM contains a combination of secreted factors and extracellular vesicles that commonly exhibit proliferative, pro-survival, and immunomodulatory effects to facilitate tissue repair[187,190–192]. Previous studies have shown that the hMSC secreted factors, such as PDGF-β, IL-6, Erk1/2 pathway activators, VEGF,

and monocyte chemotactic protein 1, can contribute to enhanced proliferation in co-culture with multiple cell types[273–275]. hMSC CM supplementation can increase survival and proliferation in endothelial cell, synovial explant, and microglia cell cultures[254–256]. hMSC CM supplementation has also been reported to improve culture efficiency of epithelial cells from the human proximal tubule and increased cell viability and migratory capacity following toxic chemical exposure[253]. Interestingly, pancreatic ductal cell proliferation rate is increased in obese individuals and in patients with T2D 10-fold and 4-fold, respectively[276]. Based on our previous observations of increased islet/ductal association after intrapancreatic hMSC CM injection[207], this compensatory proliferative mechanism, stimulated by the presence of regenerative effectors, may contribute to murine islet regeneration *in situ*. Interestingly, CK19+ cells isolated from STZ-treated mouse pancreata exhibited less proliferation compared to cells from healthy mice across conditions. While the effects of STZ treatment on pancreatic β-cells have been well characterized, phenotypic and functional changes in nearby pancreatic cells, including the duct and acinar cells, and the ability of STZ to indirectly impact islet regeneration following β-cell destruction has not been reported. Further characterization of these phenotypic changes on non-endocrine cell populations, such as the expression of cell cycle regulators or EMT markers, could reveal additional cellular targets that contribute to pancreatic repair in hyperglycemic mice.

Studies conducted by the Collombat and Bonner-Weir groups suggest that islet regeneration involves EMT of duct-associated facultative progenitors followed by α- then β-cell endocrine transition[18,19,148,153,154,156,160,277,278]. To investigate whether hMSC CM could stimulate phenotype transition of murine CK19+ cells *in vitro*, we looked for evidence of vimentin or glucagon/insulin expression during short-term cell culture. CK19 and vimentin co-localization was not observed 2, 4, or 7 days after hMSC CM supplementation. Additionally, CK19+ cells with glucagon or insulin co-localization was also not observed at each timepoint. Further evaluation of phenotypic changes should be conducted in a 3-dimensional culture environment (e.g. cells suspended in collagen spheres), which more closely mimics native tissue metabolic responses[279]. Transcriptome analyses of cell cycle, mesenchymal, and endocrine cell regulators should also be investigated in future studies. Evidence of hMSC CM-directed differentiation has been previously observed. hMSC CM has been shown to enhance differentiation of undifferentiated hESC into chondrogenic, osteogenic, and hematopoietic lineages[257,258]. Evidence of enhanced cardiac

progenitor cell differentiation into cardiomyocytes based on upregulation of lineage-specific genes has also been reported[259]. Additionally, further investigation into hMSC-mediated improvement of functional outcomes in models of central nervous system injury through trophic effects revealed that hMSC culture supplementation selectively promoted neuronal stem cell differentiation into neurons and oligodendrocytes[280]. Thus, enhanced differentiation of a putative, pancreas-derived, facultative stem cell population *in vivo* following tissue injury seems plausible given regenerative signals provided by hMSC CM. While we have previously shown that Wnt+ hMSC CM reliably rescues hyperglycemia and β-cell mass following STZ-mediated ablation, the contribution of β-cell proliferation alone could not explain this robust improvement, while neoislet budding from pancreatic ducts seemed common[207]. Given this evidence, it is plausible that hMSC CM may stimulate differentiation of facultative progenitors within the pancreas, and cells within the ducts (CK19+) represent a strong candidate. While differentiation of CK19+ cells into endocrine cells was not observed *in vitro* following hMSC CM supplementation, evaluation of their contribution to islet regeneration in their native tissue environment *in vivo* will provide deeper insight into whether this population represents a cell responsive to hMSC secreted signals.

3.3 CK19-CreERT;Ai9(RCL-tdT) mice represent a strong model to characterize CK19+ cell contribution to islet regeneration

Lineage tracing mouse models which use lineage-specific promoters can label and permit long-term fate tracking even if phenotype transition or differentiation occurs. We used the CK19-CreERT;Ai9(RCL-tdT) mouse model to label CK19-expressing cells following tamoxifen administration. First described by Means *et al.*, the tamoxifen-inducible Cre-ERT was knocked into the CK19 locus[221]. Tamoxifen administration in postnatal mice induced labeling in a wide array of epithelial populations, including pancreatic ducts, hepatic ducts, stomach, and intestinal cells[221]. The reporter Ai9(RCL-tdT) mouse line has shown strong native fluorescence when crossed with different Cre lines[222]. Thus, we bred CK19-CreERT mice with Ai9(RCL-tdT) reporter mice to generate a mouse line that would label CK19+ cells with bright tdTomato fluorescence following tamoxifen administration. Single dose (6 mg p.o.) tamoxifen treatment induced labeling in CK19+ cells within the pancreas at one-week post-administration. Of the tdTomato+ cells, >90% were CK19+ by flow cytometry, indicating strong CK19-labeling

specificity. Administration of corn oil vehicle control (no tamoxifen) resulted in < 0.001% tdTomato+ cell detection, indicating that this Cre recombinase system was not leaky. Of the CK19+ cells detected, only 20% were tdTomato+ after a single injection of tamoxifen. Future studies to optimize tamoxifen administration may improve CK19+ cell labeling efficiency, as the administered dose and repeated injection frequency may increase the efficiency of Cre recombinase activation in CK19-expressing cells[250]. Higher tamoxifen dose, or multiple low doses, should maximize labeling in future studies and should permit localization of labelled cells during hMSC CM neoislet formation[281,282]. Whether the CK19+ cell population directly contributes to neoislet formation or indirectly facilitates neoislet budding from an alternative lineage, labeling studies using this mouse model should be performed to determine the origins of islet regeneration. However, tamoxifen toxicity represents a challenge in lineage tracing models. High doses of tamoxifen have been shown to cause gastric epithelium and liver damage[283,284]. Thus, the optimal tamoxifen dose should be that which induces maximal Cre activation without injury to the mice. Future studies are underway to determine this optimal dose. Additionally, as single-cell transcriptome analysis has suggested heterogeneity within the pancreatic ductal cell population, further investigation into differential expression of ductal cell markers, including CK19, within the tamoxifen labeled population would clarify the presence of a potential progenitor population[149].

Another aspect of the model we needed to assess prior to inducing hMSC CM mediated islet regeneration was hyperglycemia induction after STZ treatment. Previously, we have shown that administration of low dose STZ (35 mg/kg/day) for 5 consecutive days results in hyperglycemia (non-fasting blood glucose 15-25 mmol/l) and impaired glucose tolerance at Day 10 in NOD/SCID mice[198–200,207,225,226]. Thus, we used a similar strategy administering STZ to C57BL/6 CK19-CreERT;Ai9(RCL-tdT) mice. Because CK19-CreERT;Ai9(RCL-tdT) mice are immunocompetent and contain intact of DNA-PK, a DNA repair enzyme that confers the SCID phenotype when inactivated[260,261], we hypothesized that a higher STZ dose would be required to induce hyperglycemia, as greater STZ sensitivity has been reported in NOD/SCID mice[262]. We found that 60 mg/kg/day STZ treatment for 5 days induced hyperglycemia and impaired glucose tolerance in 1/3 to 1/2 of the mice at Day 14. CAB control mice exhibited normoglycemia and normal glucose tolerance at Day 14. While not all the mice were hyperglycemic at Day 14, only mice that have non-fasting blood glucose values between 15 and 25 mmol/l will be used for hMSC

CM transplantation studies. Mice that received STZ treatment had decreased β-cell mass and islet density, while islet circumference remained unchanged.

Following with the trends seen in decreasing β-cell mass, the proportion of insulin+ cells in the pancreas decreased with time during the STZ treatment protocol. At Days 7 and 14 following the start of STZ treatment, the proportion of insulin+ cells within the pancreas had significantly decreased, indicating that the STZ treatment protocol was effective in achieving β-cell ablation. Additionally, insulin+ cells within the tdTomato+ cell population decreased with time following STZ treatment. Very low detection levels of insulin+ cells at Day 14 means that any observed tdTomato+/insulin+ cells following hMSC CM iPan injection, pending emergence of this population is not seen in PBS control mice, could be attributed to the islet regenerative effects of the hMSC secretome. Based on studies including those from the Collombat and Bonner-Weir groups, there has been growing support that ductal cells, or subpopulations within the ductal lineage, may serve as a facultative progenitor population to compensate for pancreatic injury or disease[44,154,156]. In order to investigate whether hMSC CM stimulates this reprogramming, lineage tracing models, like the CK19-CreERT;Ai9(RCL-tdT) mice described in this study, will need to be utilized to assess the relative contributions of various pancreatic cell populations to islet regeneration. This study lays the groundwork to identify key pancreatic target populations to increase islet regenerative efficiency.

3.4 Leukocyte infiltration plays a role in STZ-mediated pancreatic injury

Apoptosis of β-cells in diabetes pathogenesis results from T-cell and macrophage islet infiltration and subsequent release of inflammatory cytokines, including IL-1β, IFN-γ, and TNF-α which activate signalling pathways that mediate cell death[22,56–61]. Macrophage and T-cell pancreatic infiltration has also been reported following STZ treatment[265–267,270,271]. Treatment of NOD/SCID mice with low dose STZ resulted in increased F4/80+ macrophage specification within pancreatic CD45+ leukocytes. Additionally, treatment of immunocompetent CK19-CreERT;Ai9(RCL-tdT) mice with low dose STZ (60 mg/kg/day x 5 days) resulted in increased CD45+ leukocyte pancreatic infiltration. Macrophages play a crucial role in mediating tissue repair in response to injury or stress. While macrophages normally play an anti-inflammatory role to facilitate tissue repair following tissue insult, STZ treatment stimulates phagocytosis of apoptotic

β-cells, which polarizes macrophages towards a pro-inflammatory phenotype[268,269]. Similarly, STZ stimulates T-cell pancreatic infiltration in immunocompetent mice and inflammatory cytokine release[271]. Chronic inflammation is associated with the onset of diabetes and its complications[83,285,286]. Upregulation of inflammatory cytokines, including IFN-γ, TNF-α, and IL-1β are associated with increased reactive oxidative species production that play a significant role in β-cell apoptosis[286]. STZ treatment also increased CD45+ cell co-localization with CK19 and tdTomato, indicating that these cells may also be affected by the STZ-mediated inflammatory response. Further investigation into the specific leukocyte lineages that drive this observed infiltration will provide insight into the inflammatory mechanism at play and identify potential targets to prevent the progression of diabetic complications. Trials aimed at attenuating pro-inflammatory immunity, including anti-CD20 antibody[287,288], inflammatory cytokine antagonist[289,290], and anti-inflammatory pharmacological agent[291–295] administration have shown some success in attenuating β-cell apoptosis and symptoms. Thus, dampening the pro-inflammatory immune response mediated by macrophages and T-cells may represent a promising approach to slow disease progression in diabetes pathogenesis, reduce complications, and create a regenerative microenvironment to facilitate tissue repair.

It is well-established that the hMSC secretome exhibits immunomodulatory properties which have shown some success in treating immune disorders, including graft versus host disease[296–298] and models of multiple sclerosis[299–302]. Immunomodulatory functions of MSC include promotion of as anti-inflammatory macrophage phenotype, macrophage homing to the site of injury, limiting mast cell degranulation, inhibition of lymphocyte proliferation, decreasing lymphocyte pro-inflammatory cytokine synthesis, and increasing lymphocyte anti-inflammatory cytokine synthesis[180]. While we've previously shown that Wnt+ hMSC CM injection provides a regenerative microenvironment that stimulates islet regeneration in the NOD/SCID mouse, it is possible that the immunomodulatory properties secreted by Wnt+ hMSC may also play a role in promoting tissue repair over progressive destruction. Further investigation into the hMSC secreted contents that mediate immune modulation may provide insight into strategies to prevent disease progression following early diagnosis.

3.5 Clinical Implications

Our data characterizes an immunocompetent lineage tracing mouse model that can be used to determine the contribution of CK19+ ductal cells to hMSC CM stimulated islet regeneration. hMSC are readily available and can be expanded efficiently in culture. For hMSC CM to be used in a clinical setting, production and expansion of hMSC may need to be scaled up to generate an appropriate dose. hMSC CM generated in serum-free culture conditions represents a cell-free mixture in which individual factors that are essential for islet regeneration can be identified to produce a therapy without the need for cellular purification and expansion. As Wnt-stimulation of hMSC in culture generates CM that consistently induces reduced hyperglycemia and β-cell rescue, we can circumvent the donor-dependent regenerative variability previously observed by pharmacological stimulation of the Wnt-pathway. However, since the hMSC secretome contains such a wide variety of factors that may be implicated in islet regeneration and immunomodulation, identification of individual essential components may prove to be challenging and labour intensive. While a single injection into hyperglycemic mice early in disease progression provides long term therapeutic effects, translation to a clinical setting may require multiple treatments. Additionally, characterization of β-cell regenerative ability in aged mice (>10 months) will provide further insight into hMSC CM clinical potential for older patients with diabetes.

The CK19-CreERT;Ai9(RCL-tdT) mouse model described in these studies comes from a C57BL/6 background strain. Previously, we have demonstrated islet regeneration in NOD/SCID mice, which lack functional T- and B-cells, exhibit low natural killer cell activity, and have reduced antigen-presenting cell function[303]. While NOD/SCID mice previously allowed us to transplant cells without immune rejection, now that we are using a cell-free agent, we can use an immunocompetent mouse model which is more applicable to the clinical setting. The progression of both T1D and T2D involves aberrant immune system activation or inflammation, so an immunocompetent model to characterize treatment with hMSC CM alongside the associated innate and adaptive immune responses is essential if we are looking towards clinical application. Apoptosis of β-cells is mediated by islet infiltration by pro-inflammatory macrophages, as well as T-cells in the case of T1D, resulting in cytokine release and phagocytosis[22,56–61,304,305]. Nonetheless, characterizing islet regeneration in CK19-CreERT;Ai9(RCL-tdT) mice will provide further insight into response to hMSC CM treatment in the presence of functioning immune cells.

Characterization of CK19-CreERT;Ai9(RCL-tdT) mice as a lineage tracing model to determine the contribution of CK19+ cells to islet regeneration following hMSC CM injection will aid in elucidating the cellular cascade leading to β-cell mass rescue. RNA-seq of human pancreata has revealed heterogeneity and intermediate stages within endocrine cell populations, which could indicate potential plasticity within the human pancreas[149–152]. One hypothesis that has gained considerable traction in recent years is the presence of a facultative progenitor cell population which resides in the ductal tree[44,118,153,154,156]. Following *Pax4*-mediated α- to β-cell transition, *Hnf1β*$^{+}$ duct-lining cells demonstrated transient activation of *Neurogenin 3*, an endocrine progenitor marker, before adopting an α- then β-cell phenotype and function[19,154,156]. Misexpression of Ngn3 in *Hnf1β*$^{+}$ cells stimulated reactivation of the endocrine lineage specification pathway, resulting in their transition into functional β-like cells in mice[154]. Lending support to duct cell plasticity, 15% of insulin-expression β-cells, which were not associated with other islet cells, have been found in or budding from ductules, paralleling β-cell lineage specification processes in the developing pancreas[162]. Thus, characterization of CK19-CreERT;Ai9(RCL-tdT) mice, which represents a feasible model to study hMSC CM mediated islet regeneration, is a considerable step forward in testing this hypothesis and finding the 'signal-receiving cell'.

Our study has some limitations that need to be addressed as we plan for clinical translation[22,62–66]. Firstly, pathophysiology of T1D involves autoantibodies and autoimmune destruction of β-cells. However, our model involves chemical ablation of β-cells to induce hyperglycemia. Thus, our model does not address the autoimmune aspects of T1D that may actively delete regenerating β-cells. Additionally, this model does not address the obesity-induced insulin resistance characteristic of T2D, meaning obesity specific inflammatory cytokines and metabolites will not be present throughout our proposed studies. STZ treatment of CK19-CreERT;Ai9(RCL-tdT) mice results in weight loss compared to control mice, which must be monitored closely as hyperglycemia progresses. Additionally, while lineage tracing provides us with direct fate-mapping of CK19+ cells with negligible leakiness, increasing labeling efficiency to maximize the probability of observing duct-to-β-cell transition requires administration higher dosages of tamoxifen, which has the potential to cause gastric and liver complications[283,284].

3.6 Future Directions

This study showed that tamoxifen administration to CK19-CreERT;Ai9(RCL-tdT) mice specifically labeled CK19+ cells and that low dose STZ treatment can result in hyperglycemia, impaired glucose tolerance, and reduced β-cell mass. Our next steps in this investigation are to investigate whether hMSC CM can induce islet regeneration in an immunocompetent host to determine the contribution of CK19+ cells to neoislets. This protocol will require treatment with tamoxifen followed by a rest period, STZ injection (60 mg/kg/day for 5 days), hMSC CM iPan injection, blood glucose monitoring, and histological and flow cytometric analysis according to the proposed model and timelines outlined in Figure 3.1. Analysis of tdTomato+ cells by histology and flow cytometry during the islet regenerative process will be conducted to determine whether they have acquired endocrine phenotype and will provide definitive evidence of any possible CK19+ cell contribution to neoislets. Co-localization of tdTomato with β-cell markers including insulin, MafA, and Nkx6.1 on a single cell level by flow cytometry and confirmation by confocal microscopy would provide strong evidence if this event occurred. tdTomato co-localization with other pancreatic cell markers, including those for other endocrine cell types (α-cells, somatostatin cells, and PP cells), mesenchymal cells (e.g. vimentin), and acinar cells (e.g. elastase) should also be assessed to investigate other avenues of pancreatic plasticity.

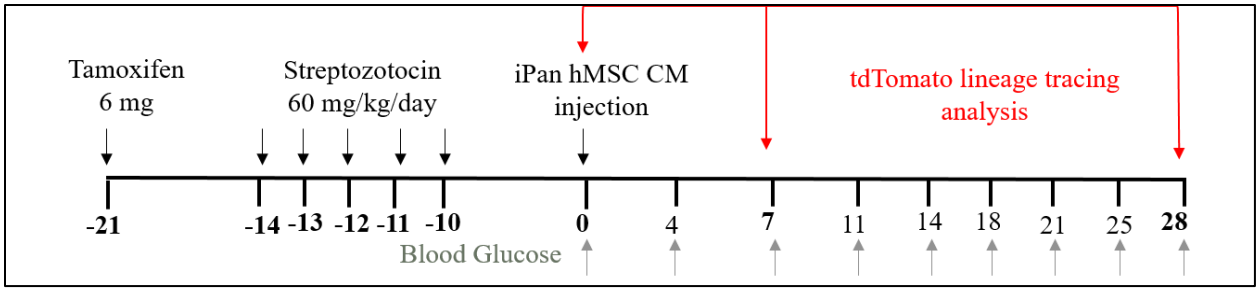

Figure 3.1 Proposed experimental strategy for assessing ductal cell contribution to β-cell regeneration in CK19-CreERT;Ai9(RCL-tdT) mice. CK19-CreERT;Ai9(RCL-tdT) mice will be used to fate map ductal cells following tamoxifen administration (6 mg per os, Day -21). To induce hyperglycemia, mice will be treated with STZ (60 mg/kg/day i.p. injection, Days -14 to -10), and subsequently receive hMSC CM iPan injection (Untreated, Wnt+, or Wnt-) on Day 0. Mice will be monitored twice weekly for non-fasted blood glucose concentrations and euthanized at Days 0, 7, and 28 (n=6-8) to assess tdTomato+ cell contribution to β-cell regeneration by immunohistochemistry on frozen pancreas sections and flow cytometry on dissociated, fixed, and permeabilized pancreatic tissue. EdU will be injected i.p. (200 µg/100 µl) 24h prior to euthanasia to assess replication of ductal, α-, or β-cells with or without tdTomato labeling.

Whether CK19+ cells contribute to islet regeneration or not, we will subsequently assess the contribution of other pancreatic cell types. Based on the hypothesis of ductal-to-α-to-β-cell transition[18,19,44,154,156], we plan to also use the Glucagon-CreERT2 mouse line crossed with Ai9(RCL-tdT) reporter mice to map the fate of α-cells during hMSC CM induced β-cell regeneration[306]. The experimental strategy and timeline will mirror that presented for CK19-CreERT;Ai9(RCL-tdT) mice.

While hMSC CM is a more clinically applicable therapeutic option compared to cellular therapies, identification of the specific components of the hMSC secretome that mediate islet regeneration would provide further translational ability. Identification and optimization of these factors and their relative doses will help ensure uniformity and reproducibility as a treatment option to improve outcomes for patients with diabetes. To do this, proteomic analysis and RNA sequencing can be used to identify key differences between regenerative and non-regenerative hMSC CM and these factors can be modulated to determine whether they are essential to stimulate islet regeneration. Further understanding of the islet regenerative cascade leading to β-cell mass rescue and the key CM components that mediate this process can be used to generate a cell-free therapy, in combination with treatments to combat ongoing autoimmunity in the case of T1D or harmful metabolites in the case of T2D, to improve outcomes and β-cell functionality in patients with diabetes.

4.0 References

1. Ballian, N. & Brunicardi, F. C. Islet vasculature as a regulator of endocrine pancreas function. *World J. Surg.* **31**, 705–714 (2007).
2. Polak, M., Bouchareb-Banaei, L., Scharfmann, R. & Czernichow, P. Early pattern of differentiation in the human pancreas. *Diabetes* **49**, 225–232 (2000).
3. Jeon, J., Correa-Medina, M., Ricordi, C., Edlund, H. & Diez, J. A. Endocrine cell clustering during human pancreas development. *J. Histochem. Cytochem.* **57**, 811–824 (2009).
4. Pan, F. C. & Brissova, M. Pancreas development in humans. *Curr. Opin. Endocrinol. Diabetes. Obes.* **21**, 77–82 (2014).
5. Burlison, J. S., Long, Q., Fujitani, Y., Wright, C. V. E. & Magnuson, M. A. Pdx-1 and Ptf1a concurrently determine fate specification of pancreatic multipotent progenitor cells. *Dev. Biol.* **316**, 74–86 (2008).
6. Solar, M. *et al.* Pancreatic exocrine duct cells give rise to insulin-producing beta cells during embryogenesis but not after birth. *Dev. Cell* **17**, 849–860 (2009).
7. Zhou, Q. *et al.* A multipotent progenitor domain guides pancreatic organogenesis. *Dev. Cell* **13**, 103–114 (2007).
8. Bastidas-Ponce, A., Scheibner, K., Lickert, H. & Bakhti, M. Cellular and molecular mechanisms coordinating pancreas development. *Development* **144**, 2873–2888 (2017).
9. Rahier, J., Wallon, J. & Henquin, J. C. Cell populations in the endocrine pancreas of human neonates and infants. *Diabetologia* **20**, 540–546 (1981).
10. Gradwohl, G., Dierich, A., LeMeur, M. & Guillemot, F. neurogenin3 is required for the development of the four endocrine cell lineages of the pancreas. *Proc. Natl. Acad. Sci. U. S. A.* **97**, 1607–1611 (2000).
11. Stefan, Y. *et al.* Quantitation of endocrine cell content in the pancreas of nondiabetic and diabetic humans. *Diabetes* **31**, 694–700 (1982).
12. Rahier, J., Goebbels, R. M. & Henquin, J. C. Cellular composition of the human diabetic pancreas. *Diabetologia* **24**, 366–371 (1983).
13. Clark, A. *et al.* Islet amyloid, increased A-cells, reduced B-cells and exocrine fibrosis: quantitative changes in the pancreas in type 2 diabetes. *Diabetes Res.* **9**, 151–159 (1988).
14. Roder, P. V, Wu, B., Liu, Y. & Han, W. Pancreatic regulation of glucose homeostasis. *Exp. Mol. Med.* **48**, e219 (2016).
15. Riedel, M. J. *et al.* Immunohistochemical characterisation of cells co-producing insulin and glucagon in the developing human pancreas. *Diabetologia* **55**, 372–381 (2012).
16. Collombat, P. *et al.* Embryonic endocrine pancreas and mature beta cells acquire alpha and PP cell phenotypes upon Arx misexpression. *J. Clin. Invest.* **117**, 961–970 (2007).
17. Collombat, P. *et al.* Opposing actions of Arx and Pax4 in endocrine pancreas development. *Genes Dev.* **17**, 2591–2603 (2003).
18. Courtney, M. *et al.* The inactivation of Arx in pancreatic alpha-cells triggers their neogenesis and conversion into functional beta-like cells. *PLoS Genet.* **9**, e1003934 (2013).
19. Collombat, P. *et al.* The ectopic expression of Pax4 in the mouse pancreas converts progenitor cells into alpha and subsequently beta cells. *Cell* **138**, 449–462 (2009).
20. Unger, R. H., Dobbs, R. E. & Orci, L. Insulin, glucagon, and somatostatin secretion in the regulation of metabolism. *Annu. Rev. Physiol.* **40**, 307–343 (1978).
21. Thorens, B. GLUT2, glucose sensing and glucose homeostasis. *Diabetologia* **58**, 221–232 (2015).

22. Fu, Z., Gilbert, E. R. & Liu, D. Regulation of insulin synthesis and secretion and pancreatic Beta-cell dysfunction in diabetes. *Curr. Diabetes Rev.* **9**, 25–53 (2013).
23. Rorsman, P. & Braun, M. Regulation of insulin secretion in human pancreatic islets. *Annu. Rev. Physiol.* **75**, 155–179 (2013).
24. Khan, A. H. & Pessin, J. E. Insulin regulation of glucose uptake: a complex interplay of intracellular signalling pathways. *Diabetologia* **45**, 1475–1483 (2002).
25. Kohn, A. D., Summers, S. A., Birnbaum, M. J. & Roth, R. A. Expression of a constitutively active Akt Ser/Thr kinase in 3T3-L1 adipocytes stimulates glucose uptake and glucose transporter 4 translocation. *J. Biol. Chem.* **271**, 31372–31378 (1996).
26. Zisman, A. *et al.* Targeted disruption of the glucose transporter 4 selectively in muscle causes insulin resistance and glucose intolerance. *Nat. Med.* **6**, 924–928 (2000).
27. Seino, Y., Fukushima, M. & Yabe, D. GIP and GLP-1, the two incretin hormones: Similarities and differences. *J. Diabetes Investig.* **1**, 8–23 (2010).
28. Reimann, F. *et al.* Glucose sensing in L cells: a primary cell study. *Cell Metab.* **8**, 532–539 (2008).
29. Parker, H. E., Habib, A. M., Rogers, G. J., Gribble, F. M. & Reimann, F. Nutrient-dependent secretion of glucose-dependent insulinotropic polypeptide from primary murine K cells. *Diabetologia* **52**, 289–298 (2009).
30. Elliott, R. M. *et al.* Glucagon-like peptide-1 (7-36)amide and glucose-dependent insulinotropic polypeptide secretion in response to nutrient ingestion in man: acute post-prandial and 24-h secretion patterns. *J. Endocrinol.* **138**, 159–166 (1993).
31. Kuhre, R. E. *et al.* Fructose stimulates GLP-1 but not GIP secretion in mice, rats, and humans. *Am. J. Physiol. Gastrointest. Liver Physiol.* **306**, G622-30 (2014).
32. Reimann, F., Williams, L., da Silva Xavier, G., Rutter, G. A. & Gribble, F. M. Glutamine potently stimulates glucagon-like peptide-1 secretion from GLUTag cells. *Diabetologia* **47**, 1592–1601 (2004).
33. Tolhurst, G. *et al.* Short-chain fatty acids stimulate glucagon-like peptide-1 secretion via the G-protein-coupled receptor FFAR2. *Diabetes* **61**, 364–371 (2012).
34. Vander Mierde, D. *et al.* Glucose activates a protein phosphatase-1-mediated signaling pathway to enhance overall translation in pancreatic beta-cells. *Endocrinology* **148**, 609–617 (2007).
35. Harding, H. P. *et al.* Regulated translation initiation controls stress-induced gene expression in mammalian cells. *Mol. Cell* **6**, 1099–1108 (2000).
36. Shi, Y. *et al.* Identification and characterization of pancreatic eukaryotic initiation factor 2 alpha-subunit kinase, PEK, involved in translational control. *Mol. Cell. Biol.* **18**, 7499–7509 (1998).
37. Ximenes, H. M. A., Hirata, A. E., Rocha, M. S., Curi, R. & Carpinelli, A. R. Propionate inhibits glucose-induced insulin secretion in isolated rat pancreatic islets. *Cell Biochem. Funct.* **25**, 173–178 (2007).
38. Porte, D. J. & Williams, R. H. Inhibition of insulin release by norepinephrine in man. *Science* **152**, 1248–1250 (1966).
39. Peterhoff, M. *et al.* Inhibition of insulin secretion via distinct signaling pathways in alpha2-adrenoceptor knockout mice. *Eur. J. Endocrinol.* **149**, 343–350 (2003).
40. Porte, D. J. A receptor mechanism for the inhibition of insulin release by epinephrine in man. *J. Clin. Invest.* **46**, 86–94 (1967).
41. Bonner-Weir, S. Islet growth and development in the adult. *J. Mol. Endocrinol.* **24**, 297–

302 (2000).
42. Montanya, E., Nacher, V., Biarnes, M. & Soler, J. Linear correlation between beta-cell mass and body weight throughout the lifespan in Lewis rats: role of beta-cell hyperplasia and hypertrophy. *Diabetes* **49**, 1341–1346 (2000).
43. Yoon, K. H. *et al.* Selective beta-cell loss and alpha-cell expansion in patients with type 2 diabetes mellitus in Korea. *J. Clin. Endocrinol. Metab.* **88**, 2300–2308 (2003).
44. Bonner-Weir, S. *et al.* The pancreatic ductal epithelium serves as a potential pool of progenitor cells. *Pediatr. Diabetes* **5 Suppl 2**, 16–22 (2004).
45. Bhaskar, M. E. *et al.* Presenting features of diabetes mellitus. *Indian J. Community Med.* **35**, 523–525 (2010).
46. Ahmed, A. M. History of diabetes mellitus. *Saudi Med. J.* **23**, 373–378 (2002).
47. Wilkin, T. J. The accelerator hypothesis: weight gain as the missing link between Type I and Type II diabetes. *Diabetologia* **44**, 914–922 (2001).
48. Saeedi, P. *et al.* Global and regional diabetes prevalence estimates for 2019 and projections for 2030 and 2045: Results from the International Diabetes Federation Diabetes Atlas, 9(th) edition. *Diabetes Res. Clin. Pract.* **157**, 107843 (2019).
49. Collaboration, N. R. F. Worldwide trends in diabetes since 1980: a pooled analysis of 751 population-based studies with 4.4 million participants. *Lancet (London, England)* **387**, 1513–1530 (2016).
50. Notkins, A. L. & Lernmark, A. Autoimmune type 1 diabetes: resolved and unresolved issues. *J. Clin. Invest.* **108**, 1247–1252 (2001).
51. Chen, C., Cohrs, C. M., Stertmann, J., Bozsak, R. & Speier, S. Human beta cell mass and function in diabetes: Recent advances in knowledge and technologies to understand disease pathogenesis. *Mol. Metab.* **6**, 943–957 (2017).
52. Leete, P. *et al.* Differential Insulitic Profiles Determine the Extent of beta-Cell Destruction and the Age at Onset of Type 1 Diabetes. *Diabetes* **65**, 1362–1369 (2016).
53. Barker, A. *et al.* Age-dependent decline of beta-cell function in type 1 diabetes after diagnosis: a multi-centre longitudinal study. *Diabetes. Obes. Metab.* **16**, 262–267 (2014).
54. Klinke, D. J. 2nd. Extent of beta cell destruction is important but insufficient to predict the onset of type 1 diabetes mellitus. *PLoS One* **3**, e1374 (2008).
55. Forouhi, N. G. & Wareham, N. J. Epidemiology of diabetes. *Medicine (Baltimore).* **47**, 22–27 (2019).
56. Rabinovitch, A. & Suarez-Pinzon, W. L. Cytokines and their roles in pancreatic islet beta-cell destruction and insulin-dependent diabetes mellitus. *Biochem. Pharmacol.* **55**, 1139–1149 (1998).
57. Thomas, H. E., Darwiche, R., Corbett, J. A. & Kay, T. W. H. Interleukin-1 plus gamma-interferon-induced pancreatic beta-cell dysfunction is mediated by beta-cell nitric oxide production. *Diabetes* **51**, 311–316 (2002).
58. Corbett, J. A. & McDaniel, M. L. Intraislet release of interleukin 1 inhibits beta cell function by inducing beta cell expression of inducible nitric oxide synthase. *J. Exp. Med.* **181**, 559–568 (1995).
59. Campbell, I. L., Kay, T. W., Oxbrow, L. & Harrison, L. C. Essential role for interferon-gamma and interleukin-6 in autoimmune insulin-dependent diabetes in NOD/Wehi mice. *J. Clin. Invest.* **87**, 739–742 (1991).
60. Rabinovitch, A., Suarez-Pinzon, W. L., Shi, Y., Morgan, A. R. & Bleackley, R. C. DNA fragmentation is an early event in cytokine-induced islet beta-cell destruction.

Diabetologia **37**, 733–738 (1994).
61. Suarez-Pinzon, W. *et al.* Beta-cell destruction in NOD mice correlates with Fas (CD95) expression on beta-cells and proinflammatory cytokine expression in islets. *Diabetes* **48**, 21–28 (1999).
62. Pilstrom, B., Bjork, L. & Bohme, J. Monokine-producing cells predominate in the recruitment phase of NOD insulitis while cells producing Th1-type cytokines characterize the effector phase. *J. Autoimmun.* **10**, 147–155 (1997).
63. Faust, A., Rothe, H., Schade, U., Lampeter, E. & Kolb, H. Primary nonfunction of islet grafts in autoimmune diabetic nonobese diabetic mice is prevented by treatment with interleukin-4 and interleukin-10. *Transplantation* **62**, 648–652 (1996).
64. Thivolet, C., Bendelac, A., Bedossa, P., Bach, J. F. & Carnaud, C. CD8+ T cell homing to the pancreas in the nonobese diabetic mouse is CD4+ T cell-dependent. *J. Immunol.* **146**, 85–88 (1991).
65. Parsa, R. *et al.* Adoptive transfer of immunomodulatory M2 macrophages prevents type 1 diabetes in NOD mice. *Diabetes* **61**, 2881–2892 (2012).
66. Marino, E., Silveira, P. A., Stolp, J. & Grey, S. T. B cell-directed therapies in type 1 diabetes. *Trends Immunol.* **32**, 287–294 (2011).
67. McKenzie, M. D. *et al.* Perforin and Fas induced by IFNgamma and TNFalpha mediate beta cell death by OT-I CTL. *Int. Immunol.* **18**, 837–846 (2006).
68. Noble, J. A. & Valdes, A. M. Genetics of the HLA region in the prediction of type 1 diabetes. *Curr. Diab. Rep.* **11**, 533–542 (2011).
69. van Lummel, M. *et al.* Posttranslational modification of HLA-DQ binding islet autoantigens in type 1 diabetes. *Diabetes* **63**, 237–247 (2014).
70. Tait, B. D. *et al.* HLA genes associated with autoimmunity and progression to disease in type 1 diabetes. *Tissue Antigens* **61**, 146–153 (2003).
71. Esposito, S. *et al.* Environmental Factors Associated With Type 1 Diabetes. *Front. Endocrinol. (Lausanne).* **10**, 592 (2019).
72. Fagherazzi, G. & Ravaud, P. Digital diabetes: Perspectives for diabetes prevention, management and research. *Diabetes Metab.* **45**, 322–329 (2019).
73. Daaboul, J. & Schatz, D. Overview of prevention and intervention trials for type 1 diabetes. *Rev. Endocr. Metab. Disord.* **4**, 317–323 (2003).
74. Willcox, A. & Gillespie, K. M. Histology of Type 1 Diabetes Pancreas. *Methods Mol. Biol.* **1433**, 105–117 (2016).
75. Cersosimo, E., Triplitt, C., Solis-Herrera, C., Mandarino, L. J. & DeFronzo, R. A. Pathogenesis of Type 2 Diabetes Mellitus. in (eds. Feingold, K. R. et al.) (2000).
76. Weyer, C., Bogardus, C., Mott, D. M. & Pratley, R. E. The natural history of insulin secretory dysfunction and insulin resistance in the pathogenesis of type 2 diabetes mellitus. *J. Clin. Invest.* **104**, 787–794 (1999).
77. Zaccardi, F., Webb, D. R., Yates, T. & Davies, M. J. Pathophysiology of type 1 and type 2 diabetes mellitus: a 90-year perspective. *Postgrad. Med. J.* **92**, 63–69 (2016).
78. Arner, P., Pollare, T., Lithell, H. & Livingston, J. N. Defective insulin receptor tyrosine kinase in human skeletal muscle in obesity and type 2 (non-insulin-dependent) diabetes mellitus. *Diabetologia* **30**, 437–440 (1987).
79. Griffin, M. E. *et al.* Free fatty acid-induced insulin resistance is associated with activation of protein kinase C theta and alterations in the insulin signaling cascade. *Diabetes* **48**, 1270–1274 (1999).

80. Rhodes, C. J. Type 2 diabetes-a matter of beta-cell life and death? *Science* **307**, 380–384 (2005).
81. Stolar, M. Glycemic control and complications in type 2 diabetes mellitus. *Am. J. Med.* **123**, S3-11 (2010).
82. Crook, M. A., Tutt, P., Simpson, H. & Pickup, J. C. Serum sialic acid and acute phase proteins in type 1 and type 2 diabetes mellitus. *Clin. Chim. Acta.* **219**, 131–138 (1993).
83. Pickup, J. C. Inflammation and activated innate immunity in the pathogenesis of type 2 diabetes. *Diabetes Care* **27**, 813–823 (2004).
84. Grant, R. W., Moore, A. F. & Florez, J. C. Genetic architecture of type 2 diabetes: recent progress and clinical implications. *Diabetes Care* **32**, 1107–1114 (2009).
85. Ling, C. & Groop, L. Epigenetics: a molecular link between environmental factors and type 2 diabetes. *Diabetes* **58**, 2718–2725 (2009).
86. Murea, M., Ma, L. & Freedman, B. I. Genetic and environmental factors associated with type 2 diabetes and diabetic vascular complications. *Rev. Diabet. Stud.* **9**, 6–22 (2012).
87. Sobngwi, E. *et al.* Effect of a diabetic environment in utero on predisposition to type 2 diabetes. *Lancet (London, England)* **361**, 1861–1865 (2003).
88. Li, R. *et al.* Medical costs associated with type 2 diabetes complications and comorbidities. *Am. J. Manag. Care* **19**, 421–430 (2013).
89. Chatzigeorgiou, A., Halapas, A., Kalafatakis, K. & Kamper, E. The use of animal models in the study of diabetes mellitus. *In Vivo* **23**, 245–258 (2009).
90. Bortell, R. & Yang, C. The BB rat as a model of human type 1 diabetes. *Methods Mol. Biol.* **933**, 31–44 (2012).
91. Mordes, J. P., Bortell, R., Blankenhorn, E. P., Rossini, A. A. & Greiner, D. L. Rat models of type 1 diabetes: genetics, environment, and autoimmunity. *ILAR J.* **45**, 278–291 (2004).
92. Baxter, A. G. & Duckworth, R. C. Models of type 1 (autoimmune) diabetes. *Drug Discov. Today Dis. Model.* **1**, 451–455 (2004).
93. Rees, D. A. & Alcolado, J. C. Animal models of diabetes mellitus. *Diabet. Med.* **22**, 359–370 (2005).
94. Lenzen, S. The mechanisms of alloxan- and streptozotocin-induced diabetes. *Diabetologia* **51**, 216–226 (2008).
95. King, A. J. F. The use of animal models in diabetes research. *Br. J. Pharmacol.* **166**, 877–894 (2012).
96. Kobayashi, K. *et al.* The db/db mouse, a model for diabetic dyslipidemia: molecular characterization and effects of Western diet feeding. *Metabolism.* **49**, 22–31 (2000).
97. Kitada, M., Ogura, Y. & Koya, D. Rodent models of diabetic nephropathy: their utility and limitations. *Int. J. Nephrol. Renovasc. Dis.* **9**, 279–290 (2016).
98. Sone, H. & Kagawa, Y. Pancreatic beta cell senescence contributes to the pathogenesis of type 2 diabetes in high-fat diet-induced diabetic mice. *Diabetologia* **48**, 58–67 (2005).
99. Heydemann, A. An Overview of Murine High Fat Diet as a Model for Type 2 Diabetes Mellitus. *J. Diabetes Res.* **2016**, 2902351 (2016).
100. Deji, N. *et al.* Structural and functional changes in the kidneys of high-fat diet-induced obese mice. *Am. J. Physiol. Renal Physiol.* **296**, F118-26 (2009).
101. Mazur, A. Why were 'starvation diets' promoted for diabetes in the pre-insulin period? *Nutr. J.* **10**, 23 (2011).
102. Quianzon, C. C. & Cheikh, I. History of insulin. *J. community Hosp. Intern. Med. Perspect.* **2**, (2012).

103. Tan, S. Y. *et al.* Type 1 and 2 diabetes mellitus: A review on current treatment approach and gene therapy as potential intervention. *Diabetes Metab. Syndr.* **13**, 364–372 (2019).
104. He, L. *et al.* Metformin and insulin suppress hepatic gluconeogenesis through phosphorylation of CREB binding protein. *Cell* **137**, 635–646 (2009).
105. Lin, S. H. *et al.* Effect of metformin monotherapy on serum lipid profile in statin-naive individuals with newly diagnosed type 2 diabetes mellitus: a cohort study. *PeerJ* **6**, e4578 (2018).
106. Proks, P., Reimann, F., Green, N., Gribble, F. & Ashcroft, F. Sulfonylurea stimulation of insulin secretion. *Diabetes* **51 Suppl 3**, S368-76 (2002).
107. Davies, M. J. *et al.* Real-world factors affecting adherence to insulin therapy in patients with Type 1 or Type 2 diabetes mellitus: a systematic review. *Diabet. Med.* **30**, 512–524 (2013).
108. French, M. B. *et al.* Transgenic expression of mouse proinsulin II prevents diabetes in nonobese diabetic mice. *Diabetes* **46**, 34–39 (1997).
109. Ferber, S. *et al.* Pancreatic and duodenal homeobox gene 1 induces expression of insulin genes in liver and ameliorates streptozotocin-induced hyperglycemia. *Nat. Med.* **6**, 568–572 (2000).
110. Wang, H. *et al.* Pdx1 level defines pancreatic gene expression pattern and cell lineage differentiation. *J. Biol. Chem.* **276**, 25279–25286 (2001).
111. Zhou, Q., Brown, J., Kanarek, A., Rajagopal, J. & Melton, D. A. In vivo reprogramming of adult pancreatic exocrine cells to beta-cells. *Nature* **455**, 627–632 (2008).
112. Xiao, X. *et al.* Endogenous Reprogramming of Alpha Cells into Beta Cells, Induced by Viral Gene Therapy, Reverses Autoimmune Diabetes. *Cell Stem Cell* **22**, 78-90.e4 (2018).
113. Shapiro, A. M. *et al.* Islet transplantation in seven patients with type 1 diabetes mellitus using a glucocorticoid-free immunosuppressive regimen. *N. Engl. J. Med.* **343**, 230–238 (2000).
114. Senior, P. A., Kin, T., Shapiro, J. & Koh, A. Islet Transplantation at the University of Alberta: Status Update and Review of Progress over the Last Decade. *Can. J. Diabetes* **36**, 32–37 (2012).
115. Shapiro, A. M. J. Islet transplantation in type 1 diabetes: ongoing challenges, refined procedures, and long-term outcome. *Rev. Diabet. Stud.* **9**, 385–406 (2012).
116. Castro-Gutierrez, R., Michels, A. W. & Russ, H. A. beta Cell replacement: improving on the design. *Curr. Opin. Endocrinol. Diabetes. Obes.* **25**, 251–257 (2018).
117. Zhou, Q. & Melton, D. A. Pancreas regeneration. *Nature* **557**, 351–358 (2018).
118. Aguayo-Mazzucato, C. & Bonner-Weir, S. Pancreatic beta Cell Regeneration as a Possible Therapy for Diabetes. *Cell Metab.* **27**, 57–67 (2018).
119. Ryan, E. A. *et al.* Five-year follow-up after clinical islet transplantation. *Diabetes* **54**, 2060–2069 (2005).
120. Welsch, C. A., Rust, W. L. & Csete, M. Concise Review: Lessons Learned from Islet Transplant Clinical Trials in Developing Stem Cell Therapies for Type 1 Diabetes. *Stem Cells Transl. Med.* **8**, 209–214 (2019).
121. Senior, P. A., AlMehthel, M., Miller, A. & Paty, B. W. Diabetes and Transplantation. *Can. J. diabetes* **42 Suppl 1**, S145–S149 (2018).
122. Thomson, J. A. *et al.* Embryonic stem cell lines derived from human blastocysts. *Science* **282**, 1145–1147 (1998).

123. Takahashi, K. & Yamanaka, S. Induction of pluripotent stem cells from mouse embryonic and adult fibroblast cultures by defined factors. *Cell* **126**, 663–676 (2006).
124. Rezania, A. *et al.* Reversal of diabetes with insulin-producing cells derived in vitro from human pluripotent stem cells. *Nat. Biotechnol.* **32**, 1121–1133 (2014).
125. Pagliuca, F. W. *et al.* Generation of functional human pancreatic beta cells in vitro. *Cell* **159**, 428–439 (2014).
126. Russ, H. A. *et al.* Controlled induction of human pancreatic progenitors produces functional beta-like cells in vitro. *EMBO J.* **34**, 1759–1772 (2015).
127. Saxena, P. *et al.* A programmable synthetic lineage-control network that differentiates human IPSCs into glucose-sensitive insulin-secreting beta-like cells. *Nat. Commun.* **7**, 11247 (2016).
128. Rajaei, B., Massumi, M. & Wheeler, M. Glucose-Responsiveness of Pancreatic beta-Like (GRP beta-L) Cells Generated from Human Pluripotent Stem Cells. *Curr. Protoc. Hum. Genet.* **100**, e71 (2019).
129. Weir, G. C. Islet encapsulation: advances and obstacles. *Diabetologia* **56**, 1458–1461 (2013).
130. Sneddon, J. B. *et al.* Stem Cell Therapies for Treating Diabetes: Progress and Remaining Challenges. *Cell Stem Cell* **22**, 810–823 (2018).
131. Farina, M., Alexander, J. F., Thekkedath, U., Ferrari, M. & Grattoni, A. Cell encapsulation: Overcoming barriers in cell transplantation in diabetes and beyond. *Adv. Drug Deliv. Rev.* (2018) doi:10.1016/j.addr.2018.04.018.
132. Korsgren, O. Islet Encapsulation: Physiological Possibilities and Limitations. *Diabetes* **66**, 1748–1754 (2017).
133. Pullen, L. C. Stem Cell-Derived Pancreatic Progenitor Cells Have Now Been Transplanted into Patients: Report from IPITA 2018. *American journal of transplantation : official journal of the American Society of Transplantation and the American Society of Transplant Surgeons* vol. 18 1581–1582 (2018).
134. Afelik, S. & Rovira, M. Pancreatic beta-cell regeneration: Facultative or dedicated progenitors? *Mol. Cell. Endocrinol.* **445**, 85–94 (2017).
135. Bouwens, L. & Rooman, I. Regulation of pancreatic beta-cell mass. *Physiol. Rev.* **85**, 1255–1270 (2005).
136. Wang, P. *et al.* Diabetes mellitus--advances and challenges in human beta-cell proliferation. *Nat. Rev. Endocrinol.* **11**, 201–212 (2015).
137. Bernard-Kargar, C. & Ktorza, A. Endocrine pancreas plasticity under physiological and pathological conditions. *Diabetes* **50 Suppl 1**, S30-5 (2001).
138. Karaca, M., Magnan, C. & Kargar, C. Functional pancreatic beta-cell mass: involvement in type 2 diabetes and therapeutic intervention. *Diabetes Metab.* **35**, 77–84 (2009).
139. Gregg, B. E. *et al.* Formation of a human beta-cell population within pancreatic islets is set early in life. *J. Clin. Endocrinol. Metab.* **97**, 3197–3206 (2012).
140. Kohler, C. U. *et al.* Cell cycle control of beta-cell replication in the prenatal and postnatal human pancreas. *Am. J. Physiol. Endocrinol. Metab.* **300**, E221-30 (2011).
141. Perl, S. *et al.* Significant human beta-cell turnover is limited to the first three decades of life as determined by in vivo thymidine analog incorporation and radiocarbon dating. *J. Clin. Endocrinol. Metab.* **95**, E234-9 (2010).
142. Krishnamurthy, J. *et al.* p16INK4a induces an age-dependent decline in islet regenerative potential. *Nature* **443**, 453–457 (2006).

143. Zhou, J. X. *et al.* Combined modulation of polycomb and trithorax genes rejuvenates beta cell replication. *J. Clin. Invest.* **123**, 4849–4858 (2013).
144. Chen, H. *et al.* PDGF signalling controls age-dependent proliferation in pancreatic beta-cells. *Nature* **478**, 349–355 (2011).
145. Dirice, E. *et al.* Inhibition of DYRK1A Stimulates Human beta-Cell Proliferation. *Diabetes* **65**, 1660–1671 (2016).
146. Wang, P. *et al.* A high-throughput chemical screen reveals that harmine-mediated inhibition of DYRK1A increases human pancreatic beta cell replication. *Nat. Med.* **21**, 383–388 (2015).
147. Shen, W. *et al.* Small-molecule inducer of beta cell proliferation identified by high-throughput screening. *J. Am. Chem. Soc.* **135**, 1669–1672 (2013).
148. Bonner-Weir, S. *et al.* Beta-cell growth and regeneration: replication is only part of the story. *Diabetes* **59**, 2340–2348 (2010).
149. Baron, M. *et al.* A Single-Cell Transcriptomic Map of the Human and Mouse Pancreas Reveals Inter- and Intra-cell Population Structure. *Cell Syst.* **3**, 346-360.e4 (2016).
150. Dorrell, C. *et al.* Human islets contain four distinct subtypes of beta cells. *Nat. Commun.* **7**, 11756 (2016).
151. Xin, Y. *et al.* RNA Sequencing of Single Human Islet Cells Reveals Type 2 Diabetes Genes. *Cell Metab.* **24**, 608–615 (2016).
152. Segerstolpe, A. *et al.* Single-Cell Transcriptome Profiling of Human Pancreatic Islets in Health and Type 2 Diabetes. *Cell Metab.* **24**, 593–607 (2016).
153. Inada, A. *et al.* Carbonic anhydrase II-positive pancreatic cells are progenitors for both endocrine and exocrine pancreas after birth. *Proc. Natl. Acad. Sci. U. S. A.* **105**, 19915–19919 (2008).
154. Vieira, A. *et al.* Neurog3 misexpression unravels mouse pancreatic ductal cell plasticity. *PLoS One* **13**, e0201536 (2018).
155. Ben-Othman, N. *et al.* Long-Term GABA Administration Induces Alpha Cell-Mediated Beta-like Cell Neogenesis. *Cell* **168**, 73-85.e11 (2017).
156. Al-Hasani, K. *et al.* Adult duct-lining cells can reprogram into beta-like cells able to counter repeated cycles of toxin-induced diabetes. *Dev. Cell* **26**, 86–100 (2013).
157. Thorel, F. *et al.* Conversion of adult pancreatic alpha-cells to beta-cells after extreme beta-cell loss. *Nature* **464**, 1149–1154 (2010).
158. Chera, S. *et al.* Diabetes recovery by age-dependent conversion of pancreatic δ-cells into insulin producers. *Nature* **514**, 503–507 (2014).
159. Matsuoka, T.-A. *et al.* Mafa Enables Pdx1 to Effectively Convert Pancreatic Islet Progenitors and Committed Islet alpha-Cells Into beta-Cells In Vivo. *Diabetes* **66**, 1293–1300 (2017).
160. Bonner-Weir, S. *et al.* In vitro cultivation of human islets from expanded ductal tissue. *Proc. Natl. Acad. Sci. U. S. A.* **97**, 7999–8004 (2000).
161. Chakravarthy, H. *et al.* Converting Adult Pancreatic Islet alpha Cells into beta Cells by Targeting Both Dnmt1 and Arx. *Cell Metab.* **25**, 622–634 (2017).
162. Bouwens, L. & Pipeleers, D. G. Extra-insular beta cells associated with ductules are frequent in adult human pancreas. *Diabetologia* **41**, 629–633 (1998).
163. Li, J. *et al.* Artemisinins Target GABAA Receptor Signaling and Impair alpha Cell Identity. *Cell* **168**, 86-100.e15 (2017).
164. Ackermann, A. M., Moss, N. G. & Kaestner, K. H. GABA and Artesunate Do Not Induce

Pancreatic alpha-to-beta Cell Transdifferentiation In Vivo. *Cell Metab.* **28**, 787-792.e3 (2018).
165. van der Meulen, T. *et al.* Artemether Does Not Turn alpha Cells into beta Cells. *Cell Metab.* **27**, 218-225.e4 (2018).
166. Friedenstein, A. J., Chailakhjan, R. K. & Lalykina, K. S. The development of fibroblast colonies in monolayer cultures of guinea-pig bone marrow and spleen cells. *Cell Tissue Kinet.* **3**, 393–403 (1970).
167. Dominici, M. *et al.* Minimal criteria for defining multipotent mesenchymal stromal cells. The International Society for Cellular Therapy position statement. *Cytotherapy* **8**, 315–317 (2006).
168. Pittenger, M. F. *et al.* Multilineage potential of adult human mesenchymal stem cells. *Science* **284**, 143–147 (1999).
169. Romanov, Y. A., Darevskaya, A. N., Merzlikina, N. V & Buravkova, L. B. Mesenchymal stem cells from human bone marrow and adipose tissue: isolation, characterization, and differentiation potentialities. *Bull. Exp. Biol. Med.* **140**, 138–143 (2005).
170. Muraglia, A., Cancedda, R. & Quarto, R. Clonal mesenchymal progenitors from human bone marrow differentiate in vitro according to a hierarchical model. *J. Cell Sci.* **113 (Pt 7**, 1161–1166 (2000).
171. Fraser, J. K., Wulur, I., Alfonso, Z. & Hedrick, M. H. Fat tissue: an underappreciated source of stem cells for biotechnology. *Trends Biotechnol.* **24**, 150–154 (2006).
172. Chong, P.-P., Selvaratnam, L., Abbas, A. A. & Kamarul, T. Human peripheral blood derived mesenchymal stem cells demonstrate similar characteristics and chondrogenic differentiation potential to bone marrow derived mesenchymal stem cells. *J. Orthop. Res.* **30**, 634–642 (2012).
173. Kassis, I. *et al.* Isolation of mesenchymal stem cells from G-CSF-mobilized human peripheral blood using fibrin microbeads. *Bone Marrow Transplant.* **37**, 967–976 (2006).
174. Lama, V. N. *et al.* Evidence for tissue-resident mesenchymal stem cells in human adult lung from studies of transplanted allografts. *J. Clin. Invest.* **117**, 989–996 (2007).
175. Jarvinen, L. *et al.* Lung resident mesenchymal stem cells isolated from human lung allografts inhibit T cell proliferation via a soluble mediator. *J. Immunol.* **181**, 4389–4396 (2008).
176. Crisan, M. *et al.* A perivascular origin for mesenchymal stem cells in multiple human organs. *Cell Stem Cell* **3**, 301–313 (2008).
177. Young, H. E. *et al.* Human reserve pluripotent mesenchymal stem cells are present in the connective tissues of skeletal muscle and dermis derived from fetal, adult, and geriatric donors. *Anat. Rec.* **264**, 51–62 (2001).
178. Viswanathan, S. *et al.* Mesenchymal stem versus stromal cells: International Society for Cell & Gene Therapy (ISCT(R)) Mesenchymal Stromal Cell committee position statement on nomenclature. *Cytotherapy* **21**, 1019–1024 (2019).
179. Heo, J. S., Choi, Y., Kim, H.-S. & Kim, H. O. Comparison of molecular profiles of human mesenchymal stem cells derived from bone marrow, umbilical cord blood, placenta and adipose tissue. *Int. J. Mol. Med.* **37**, 115–125 (2016).
180. Andrzejewska, A., Lukomska, B. & Janowski, M. Concise Review: Mesenchymal Stem Cells: From Roots to Boost. *Stem Cells* **37**, 855–864 (2019).
181. Ren, J. *et al.* Intra-subject variability in human bone marrow stromal cell (BMSC) replicative senescence: molecular changes associated with BMSC senescence. *Stem Cell*

Res. **11**, 1060–1073 (2013).
182. Zhukareva, V., Obrocka, M., Houle, J. D., Fischer, I. & Neuhuber, B. Secretion profile of human bone marrow stromal cells: Donor variability and response to inflammatory stimuli. *Cytokine* **50**, 317–321 (2010).
183. Phinney, D. G. *et al.* Donor variation in the growth properties and osteogenic potential of human marrow stromal cells. *J. Cell. Biochem.* **75**, 424–436 (1999).
184. Rosen, E. D. & MacDougald, O. A. Adipocyte differentiation from the inside out. *Nat. Rev. Mol. Cell Biol.* **7**, 885–896 (2006).
185. Mackay, A. M. *et al.* Chondrogenic differentiation of cultured human mesenchymal stem cells from marrow. *Tissue Eng.* **4**, 415–428 (1998).
186. He, J. *et al.* Directing the osteoblastic and chondrocytic differentiations of mesenchymal stem cells: matrix vs. induction media. *Regen. Biomater.* **4**, 269–279 (2017).
187. Vizoso, F. J., Eiro, N., Cid, S., Schneider, J. & Perez-Fernandez, R. Mesenchymal Stem Cell Secretome: Toward Cell-Free Therapeutic Strategies in Regenerative Medicine. *Int. J. Mol. Sci.* **18**, (2017).
188. Kean, T. J., Lin, P., Caplan, A. I. & Dennis, J. E. MSCs: Delivery Routes and Engraftment, Cell-Targeting Strategies, and Immune Modulation. *Stem Cells Int.* **2013**, 732742 (2013).
189. Phinney, D. G. & Pittenger, M. F. Concise Review: MSC-Derived Exosomes for Cell-Free Therapy. *Stem Cells* **35**, 851–858 (2017).
190. Cunningham, C. J., Redondo-Castro, E. & Allan, S. M. The therapeutic potential of the mesenchymal stem cell secretome in ischaemic stroke. *J. Cereb. Blood Flow Metab.* **38**, 1276–1292 (2018).
191. Sun, D. Z., Abelson, B., Babbar, P. & Damaser, M. S. Harnessing the mesenchymal stem cell secretome for regenerative urology. *Nat. Rev. Urol.* (2019) doi:10.1038/s41585-019-0169-3.
192. Konala, V. B. R. *et al.* The current landscape of the mesenchymal stromal cell secretome: A new paradigm for cell-free regeneration. *Cytotherapy* **18**, 13–24 (2016).
193. Katagiri, W. *et al.* Angiogenesis in newly regenerated bone by secretomes of human mesenchymal stem cells. *Maxillofac. Plast. Reconstr. Surg.* **39**, 8 (2017).
194. Kupcova Skalnikova, H. Proteomic techniques for characterisation of mesenchymal stem cell secretome. *Biochimie* **95**, 2196–2211 (2013).
195. Ferreira, J. R. *et al.* Mesenchymal Stromal Cell Secretome: Influencing Therapeutic Potential by Cellular Pre-conditioning. *Front. Immunol.* **9**, 2837 (2018).
196. Lee, R. H. *et al.* Multipotent stromal cells from human marrow home to and promote repair of pancreatic islets and renal glomeruli in diabetic NOD/scid mice. *Proc. Natl. Acad. Sci. U. S. A.* **103**, 17438–17443 (2006).
197. Ezquer, F. E. *et al.* Systemic administration of multipotent mesenchymal stromal cells reverts hyperglycemia and prevents nephropathy in type 1 diabetic mice. *Biol. Blood Marrow Transplant.* **14**, 631–640 (2008).
198. Hess, D. *et al.* Bone marrow-derived stem cells initiate pancreatic regeneration. *Nat. Biotechnol.* **21**, 763–770 (2003).
199. Bell, G. I. *et al.* Combinatorial human progenitor cell transplantation optimizes islet regeneration through secretion of paracrine factors. *Stem Cells Dev.* **21**, 1863–1876 (2012).
200. Bell, G. I. *et al.* Transplanted human bone marrow progenitor subtypes stimulate

endogenous islet regeneration and revascularization. *Stem Cells Dev.* **21**, 97–109 (2012).
201. Fiorina, P. *et al.* Immunomodulatory function of bone marrow-derived mesenchymal stem cells in experimental autoimmune type 1 diabetes. *J. Immunol.* **183**, 993–1004 (2009).
202. Si, Y. *et al.* Infusion of mesenchymal stem cells ameliorates hyperglycemia in type 2 diabetic rats: identification of a novel role in improving insulin sensitivity. *Diabetes* **61**, 1616–1625 (2012).
203. Path, G., Perakakis, N., Mantzoros, C. S. & Seufert, J. Stem cells in the treatment of diabetes mellitus - Focus on mesenchymal stem cells. *Metabolism.* **90**, 1–15 (2019).
204. Park, K.-S. *et al.* Trophic Molecules Derived From Human Mesenchymal Stem Cells Enhance Survival, Function, and Angiogenesis of Isolated Islets After Transplantation. *Transplantation* **89**, (2010).
205. Liu, C. *et al.* Mesenchymal stem cell (MSC)-mediated survival of insulin producing pancreatic beta-cells during cellular stress involves signalling via Akt and ERK1/2. *Mol. Cell. Endocrinol.* **473**, 235–244 (2018).
206. de Souza, B. M. *et al.* Effect of co-culture of mesenchymal stem/stromal cells with pancreatic islets on viability and function outcomes: a systematic review and meta-analysis. *Islets* **9**, 30–42 (2017).
207. Kuljanin, M. *et al.* Human Multipotent Stromal Cell Secreted Effectors Accelerate Islet Regeneration. *Stem Cells* **37**, 516–528 (2019).
208. Kuljanin, M., Bell, G. I., Sherman, S. E., Lajoie, G. A. & Hess, D. A. Proteomic characterisation reveals active Wnt-signalling by human multipotent stromal cells as a key regulator of beta cell survival and proliferation. *Diabetologia* (2017) doi:10.1007/s00125-017-4355-7.
209. Kuljanin, M. *et al.* Quantitative Proteomics Evaluation of Human Multipotent Stromal Cell for beta Cell Regeneration. *Cell Rep.* **25**, 2524-2536.e4 (2018).
210. MacDonald, B. T., Tamai, K. & He, X. Wnt/beta-catenin signaling: components, mechanisms, and diseases. *Dev. Cell* **17**, 9–26 (2009).
211. Valenta, T., Hausmann, G. & Basler, K. The many faces and functions of β-catenin. *EMBO J.* **31**, 2714–2736 (2012).
212. Logan, C. Y. & Nusse, R. The Wnt signaling pathway in development and disease. *Annu. Rev. Cell Dev. Biol.* **20**, 781–810 (2004).
213. Martins-Neves, S. R. *et al.* IWR-1, a tankyrase inhibitor, attenuates Wnt/beta-catenin signaling in cancer stem-like cells and inhibits in vivo the growth of a subcutaneous human osteosarcoma xenograft. *Cancer Lett.* **414**, 1–15 (2018).
214. Chen, B. *et al.* Small molecule-mediated disruption of Wnt-dependent signaling in tissue regeneration and cancer. *Nat. Chem. Biol.* **5**, 100–107 (2009).
215. Butler, A. E. *et al.* Beta-cell deficit and increased beta-cell apoptosis in humans with type 2 diabetes. *Diabetes* **52**, 102–110 (2003).
216. Gao, R. *et al.* Characterization of endocrine progenitor cells and critical factors for their differentiation in human adult pancreatic cell culture. *Diabetes* **52**, 2007–2015 (2003).
217. Xu, X. *et al.* Beta cells can be generated from endogenous progenitors in injured adult mouse pancreas. *Cell* **132**, 197–207 (2008).
218. Zhang, M. *et al.* Growth factors and medium hyperglycemia induce Sox9+ ductal cell differentiation into beta cells in mice with reversal of diabetes. *Proc. Natl. Acad. Sci. U. S. A.* **113**, 650–655 (2016).
219. Keenan, H. A. *et al.* Residual insulin production and pancreatic ß-cell turnover after 50

years of diabetes: Joslin Medalist Study. *Diabetes* **59**, 2846–2853 (2010).
220. Fanjul, M. *et al.* Evidence for epithelial-mesenchymal transition in adult human pancreatic exocrine cells. *J. Histochem. Cytochem.* **58**, 807–823 (2010).
221. Means, A. L., Xu, Y., Zhao, A., Ray, K. C. & Gu, G. A CK19(CreERT) knockin mouse line allows for conditional DNA recombination in epithelial cells in multiple endodermal organs. *Genesis* **46**, 318–323 (2008).
222. Madisen, L. *et al.* A robust and high-throughput Cre reporting and characterization system for the whole mouse brain. *Nat. Neurosci.* **13**, 133–140 (2010).
223. Lee, C. J. *et al.* Post-remission strategies for the prevention of relapse following allogeneic hematopoietic cell transplantation for high-risk acute myeloid leukemia: expert review from the Acute Leukemia Working Party of the European Society for Blood and Marrow Transpla. *Bone Marrow Transplant.* **54**, 519–530 (2019).
224. Conget, P. A. & Minguell, J. J. Phenotypical and functional properties of human bone marrow mesenchymal progenitor cells. *J. Cell. Physiol.* **181**, 67–73 (1999).
225. Bell, G. I., Putman, D. M., Hughes-Large, J. M. & Hess, D. A. Intrapancreatic delivery of human umbilical cord blood aldehyde dehydrogenase-producing cells promotes islet regeneration. *Diabetologia* **55**, 1755–1760 (2012).
226. Seneviratne, A. K. *et al.* Expanded Hematopoietic Progenitor Cells Reselected for High Aldehyde Dehydrogenase Activity Demonstrate Islet Regenerative Functions. *Stem Cells* **34**, 873–887 (2016).
227. Iglay, K. *et al.* Prevalence and co-prevalence of comorbidities among patients with type 2 diabetes mellitus. *Curr. Med. Res. Opin.* **32**, 1243–1252 (2016).
228. Ernst, S., Demirci, C., Valle, S., Velazquez-Garcia, S. & Garcia-Ocaña, A. Mechanisms in the adaptation of maternal β-cells during pregnancy. *Diabetes Manag. (Lond).* **1**, 239–248 (2011).
229. Saisho, Y. *et al.* β-cell mass and turnover in humans: effects of obesity and aging. *Diabetes Care* **36**, 111–117 (2013).
230. Dirice, E. *et al.* Human duct cells contribute to β cell compensation in insulin resistance. *JCI insight* **4**, (2019).
231. Reichert, M. *et al.* Isolation, culture and genetic manipulation of mouse pancreatic ductal cells. *Nat. Protoc.* **8**, 1354–1365 (2013).
232. Schmid, I., Uittenbogaart, C. H., Keld, B. & Giorgi, J. V. A rapid method for measuring apoptosis and dual-color immunofluorescence by single laser flow cytometry. *J. Immunol. Methods* **170**, 145–157 (1994).
233. Kobayashi, H. *et al.* Lectin as a marker for staining and purification of embryonic pancreatic epithelium. *Biochem. Biophys. Res. Commun.* **293**, 691–697 (2002).
234. Noë, M. *et al.* Immunolabeling of Cleared Human Pancreata Provides Insights into Three-Dimensional Pancreatic Anatomy and Pathology. *Am. J. Pathol.* **188**, 1530–1535 (2018).
235. Oshima, Y. *et al.* Isolation of mouse pancreatic ductal progenitor cells expressing CD133 and c-Met by flow cytometric cell sorting. *Gastroenterology* **132**, 720–732 (2007).
236. Eberhard, D., Tosh, D. & Slack, J. M. W. Origin of pancreatic endocrine cells from biliary duct epithelium. *Cell. Mol. Life Sci.* **65**, 3467–3480 (2008).
237. Watanabe, M., Muramatsu, T., Shirane, H. & Ugai, K. Discrete Distribution of binding sites for Dolichos biflorus agglutinin (DBA) and for peanut agglutinin (PNA) in mouse organ tissues. *J. Histochem. Cytochem. Off. J. Histochem. Soc.* **29**, 779–780 (1981).
238. Jensen, J. N. *et al.* Recapitulation of elements of embryonic development in adult mouse

pancreatic regeneration. *Gastroenterology* **128**, 728–741 (2005).
239. Dor, Y., Brown, J., Martinez, O. I. & Melton, D. A. Adult pancreatic beta-cells are formed by self-duplication rather than stem-cell differentiation. *Nature* **429**, 41–46 (2004).
240. Reichert, M. *et al.* The Prrx1 homeodomain transcription factor plays a central role in pancreatic regeneration and carcinogenesis. *Genes Dev.* **27**, 288–300 (2013).
241. Eguchi, M., Ozawa, T., Suda, J., Sugita, K. & Furukawa, T. Lectins for electron microscopic distinction of eosinophils from other blood cells. *J. Histochem. Cytochem. Off. J. Histochem. Soc.* **37**, 743–749 (1989).
242. Qin, L. *et al.* Goat uterine DBA+ leukocytes differentiation and cytokines expression respond differently to cloned versus fertilized embryos. *PLoS One* **10**, e0116649 (2015).
243. Zhang, J. H., Yamada, A. T. & Croy, B. A. DBA-lectin reactivity defines natural killer cells that have homed to mouse decidua. *Placenta* **30**, 968–973 (2009).
244. Kasper, M., Haroske, G., Pollack, K., Migheli, A. & Müller, M. Heterogeneous Dolichos biflorus lectin binding to a subset of rat alveolar macrophages in normal and fibrotic lung tissue. *Acta Histochem.* **95**, 1–11 (1993).
245. Austyn, J. M. & Gordon, S. F4/80, a monoclonal antibody directed specifically against the mouse macrophage. *Eur. J. Immunol.* **11**, 805–815 (1981).
246. Hume, D. A. & Gordon, S. Mononuclear phagocyte system of the mouse defined by immunohistochemical localization of antigen F4/80. Identification of resident macrophages in renal medullary and cortical interstitium and the juxtaglomerular complex. *J. Exp. Med.* **157**, 1704–1709 (1983).
247. McKnight, A. J. *et al.* Molecular cloning of F4/80, a murine macrophage-restricted cell surface glycoprotein with homology to the G-protein-linked transmembrane 7 hormone receptor family. *J. Biol. Chem.* **271**, 486–489 (1996).
248. Chen, E. Y. *et al.* Glycogen synthase kinase 3 inhibitors induce the canonical WNT/β-catenin pathway to suppress growth and self-renewal in embryonal rhabdomyosarcoma. *Proc. Natl. Acad. Sci. U. S. A.* **111**, 5349–5354 (2014).
249. Wang, S. *et al.* GSK-3β Inhibitor CHIR-99021 Promotes Proliferation Through Upregulating β-Catenin in Neonatal Atrial Human Cardiomyocytes. *J. Cardiovasc. Pharmacol.* **68**, 425–432 (2016).
250. Romagnani, P., Rinkevich, Y. & Dekel, B. The use of lineage tracing to study kidney injury and regeneration. *Nat. Rev. Nephrol.* **11**, 420–431 (2015).
251. Dahlke, M. H., Larsen, S. R., Rasko, J. E. J. & Schlitt, H. J. The biology of CD45 and its use as a therapeutic target. *Leuk. Lymphoma* **45**, 229–236 (2004).
252. Villmow, T., Kemkes-Matthes, B. & Matzdorff, A. C. Markers of platelet activation and platelet-leukocyte interaction in patients with myeloproliferative syndromes. *Thromb. Res.* **108**, 139–145 (2002).
253. Moghadasali, R. *et al.* Mesenchymal stem cell-conditioned medium accelerates regeneration of human renal proximal tubule epithelial cells after gentamicin toxicity. *Exp. Toxicol. Pathol. Off. J. Gesellschaft fur Toxikologische Pathol.* **65**, 595–600 (2013).
254. Potapova, I. A. *et al.* Mesenchymal stem cells support migration, extracellular matrix invasion, proliferation, and survival of endothelial cells in vitro. *Stem Cells* **25**, 1761–1768 (2007).
255. van Buul, G. M. *et al.* Mesenchymal stem cells secrete factors that inhibit inflammatory processes in short-term osteoarthritic synovium and cartilage explant culture. *Osteoarthr. Cartil.* **20**, 1186–1196 (2012).

256. Chen, Y.-T. *et al.* The superiority of conditioned medium derived from rapidly expanded mesenchymal stem cells for neural repair. *Stem Cell Res. Ther.* **10**, 390 (2019).
257. Lee, T.-J. *et al.* Mesenchymal stem cell-conditioned medium enhances osteogenic and chondrogenic differentiation of human embryonic stem cells and human induced pluripotent stem cells by mesodermal lineage induction. *Tissue Eng. Part A* **20**, 1306–1313 (2014).
258. Ramos-Mejía, V. *et al.* Maintenance of human embryonic stem cells in mesenchymal stem cell-conditioned media augments hematopoietic specification. *Stem Cells Dev.* **21**, 1549–1558 (2012).
259. Nakanishi, C. *et al.* Activation of cardiac progenitor cells through paracrine effects of mesenchymal stem cells. *Biochem. Biophys. Res. Commun.* **374**, 11–16 (2008).
260. Abramson, J., Giraud, M., Benoist, C. & Mathis, D. Aire's partners in the molecular control of immunological tolerance. *Cell* **140**, 123–135 (2010).
261. Mathieu, A.-L. *et al.* PRKDC mutations associated with immunodeficiency, granuloma, and autoimmune regulator-dependent autoimmunity. *J. Allergy Clin. Immunol.* **135**, 1578–88.e5 (2015).
262. Gerling, I. C., Friedman, H., Greiner, D. L., Shultz, L. D. & Leiter, E. H. Multiple low-dose streptozocin-induced diabetes in NOD-scid/scid mice in the absence of functional lymphocytes. *Diabetes* **43**, 433–440 (1994).
263. Seiron, P. *et al.* Characterisation of the endocrine pancreas in type 1 diabetes: islet size is maintained but islet number is markedly reduced. *J. Pathol. Clin. Res.* **5**, 248–255 (2019).
264. Gordon, S. & Martinez-Pomares, L. Physiological roles of macrophages. *Pflugers Arch.* **469**, 365–374 (2017).
265. Lukić, M. L., Stosić-Grujicić, S. & Shahin, A. Effector mechanisms in low-dose streptozotocin-induced diabetes. *Dev. Immunol.* **6**, 119–128 (1998).
266. Lukic, M. L., Stosic-Grujicic, S., Ostojic, N., Chan, W. L. & Liew, F. Y. Inhibition of nitric oxide generation affects the induction of diabetes by streptozocin in mice. *Biochem. Biophys. Res. Commun.* **178**, 913–920 (1991).
267. Kolb-Bachofen, V., Epstein, S., Kiesel, U. & Kolb, H. Low-dose streptozocin-induced diabetes in mice. Electron microscopy reveals single-cell insulitis before diabetes onset. *Diabetes* **37**, 21–27 (1988).
268. Ward, M. G., Li, G. & Hao, M. Apoptotic β-cells induce macrophage reprogramming under diabetic conditions. *J. Biol. Chem.* **293**, 16160–16173 (2018).
269. Niu, S. *et al.* Broad Infiltration of Macrophages Leads to a Proinflammatory State in Streptozotocin-Induced Hyperglycemic Mice. *J. Immunol.* **197**, 3293–3301 (2016).
270. Klinkhammer, C., Dohle, C. & Gleichmann, H. T cell-dependent class II major histocompatibility complex antigen expression in vivo induced by the diabetogen streptozotocin. *Immunobiology* **180**, 1–11 (1989).
271. Cockfield, S. M., Ramassar, V., Urmson, J. & Halloran, P. F. Multiple low dose streptozotocin induces systemic MHC expression in mice by triggering T cells to release IFN-gamma. *J. Immunol.* **142**, 1120–1128 (1989).
272. Reichert, M. & Rustgi, A. K. Pancreatic ductal cells in development, regeneration, and neoplasia. *J. Clin. Invest.* **121**, 4572–4578 (2011).
273. Kamprom, W. *et al.* Effects of mesenchymal stem cell-derived cytokines on the functional properties of endothelial progenitor cells. *Eur. J. Cell Biol.* **95**, 153–163 (2016).
274. Scherzad, A. *et al.* Human mesenchymal stem cells enhance cancer cell proliferation via

IL-6 secretion and activation of ERK1/2. *Int. J. Oncol.* **47**, 391–397 (2015).
275. Kwon, H. M. *et al.* Multiple paracrine factors secreted by mesenchymal stem cells contribute to angiogenesis. *Vascul. Pharmacol.* **63**, 19–28 (2014).
276. Butler, A. E. *et al.* Pancreatic duct replication is increased with obesity and type 2 diabetes in humans. *Diabetologia* **53**, 21–26 (2010).
277. Li, W.-C. *et al.* Activation of pancreatic-duct-derived progenitor cells during pancreas regeneration in adult rats. *J. Cell Sci.* **123**, 2792–2802 (2010).
278. Bonner-Weir, S. *et al.* Transdifferentiation of pancreatic ductal cells to endocrine beta-cells. *Biochem. Soc. Trans.* **36**, 353–356 (2008).
279. Lagies, S. *et al.* Cells grown in three-dimensional spheroids mirror in vivo metabolic response of epithelial cells. *Commun. Biol.* **3**, 246 (2020).
280. Bai, L., Caplan, A., Lennon, D. & Miller, R. H. Human mesenchymal stem cells signals regulate neural stem cell fate. *Neurochem. Res.* **32**, 353–362 (2007).
281. Kretzschmar, K. & Watt, F. M. Lineage tracing. *Cell* **148**, 33–45 (2012).
282. Blanpain, C. & Simons, B. D. Unravelling stem cell dynamics by lineage tracing. *Nat. Rev. Mol. Cell Biol.* **14**, 489–502 (2013).
283. Huh, W. J. *et al.* Tamoxifen induces rapid, reversible atrophy, and metaplasia in mouse stomach. *Gastroenterology* **142**, 21-24.e7 (2012).
284. Lee, M.-H. *et al.* Gene expression profiling of murine hepatic steatosis induced by tamoxifen. *Toxicol. Lett.* **199**, 416–424 (2010).
285. Navarro, J. F. & Mora, C. Role of inflammation in diabetic complications. *Nephrology, dialysis, transplantation : official publication of the European Dialysis and Transplant Association - European Renal Association* vol. 20 2601–2604 (2005).
286. Tsalamandris, S. *et al.* The Role of Inflammation in Diabetes: Current Concepts and Future Perspectives. *Eur. Cardiol.* **14**, 50–59 (2019).
287. Pescovitz, M. D. *et al.* Rituximab, B-lymphocyte depletion, and preservation of beta-cell function. *N. Engl. J. Med.* **361**, 2143–2152 (2009).
288. Pescovitz, M. D. *et al.* B-lymphocyte depletion with rituximab and β-cell function: two-year results. *Diabetes Care* **37**, 453–459 (2014).
289. Mastrandrea, L. *et al.* Etanercept treatment in children with new-onset type 1 diabetes: pilot randomized, placebo-controlled, double-blind study. *Diabetes Care* **32**, 1244–1249 (2009).
290. Gottlieb, P. A. *et al.* α1-Antitrypsin therapy downregulates toll-like receptor-induced IL-1β responses in monocytes and myeloid dendritic cells and may improve islet function in recently diagnosed patients with type 1 diabetes. *J. Clin. Endocrinol. Metab.* **99**, E1418-26 (2014).
291. Dandona, P. *et al.* Insulin inhibits intranuclear nuclear factor kappaB and stimulates IkappaB in mononuclear cells in obese subjects: evidence for an anti-inflammatory effect? *J. Clin. Endocrinol. Metab.* **86**, 3257–3265 (2001).
292. Caballero, A. E. *et al.* The differential effects of metformin on markers of endothelial activation and inflammation in subjects with impaired glucose tolerance: a placebo-controlled, randomized clinical trial. *J. Clin. Endocrinol. Metab.* **89**, 3943–3948 (2004).
293. Hattori, Y., Suzuki, K., Hattori, S. & Kasai, K. Metformin inhibits cytokine-induced nuclear factor kappaB activation via AMP-activated protein kinase activation in vascular endothelial cells. *Hypertens. (Dallas, Tex. 1979)* **47**, 1183–1188 (2006).
294. Vasamsetti, S. B. *et al.* Metformin inhibits monocyte-to-macrophage differentiation via

AMPK-mediated inhibition of STAT3 activation: potential role in atherosclerosis. *Diabetes* **64**, 2028–2041 (2015).
295. de Rotte, M. C. F. J. *et al.* Effect of methotrexate use and erythrocyte methotrexate polyglutamate on glycosylated hemoglobin in rheumatoid arthritis. *Arthritis Rheumatol. (Hoboken, N.J.)* **66**, 2026–2036 (2014).
296. Prasad, V. K. *et al.* Efficacy and safety of ex vivo cultured adult human mesenchymal stem cells (Prochymal™) in pediatric patients with severe refractory acute graft-versus-host disease in a compassionate use study. *Biol. blood marrow Transplant. J. Am. Soc. Blood Marrow Transplant.* **17**, 534–541 (2011).
297. Robles, J. D. *et al.* Immunosuppressive mechanisms of human bone marrow derived mesenchymal stromal cells in BALB/c host graft versus host disease murine models. *Exp. Hematol. Oncol.* **4**, 13 (2015).
298. Kurtzberg, J. *et al.* Allogeneic human mesenchymal stem cell therapy (remestemcel-L, Prochymal) as a rescue agent for severe refractory acute graft-versus-host disease in pediatric patients. *Biol. blood marrow Transplant. J. Am. Soc. Blood Marrow Transplant.* **20**, 229–235 (2014).
299. Zappia, E. *et al.* Mesenchymal stem cells ameliorate experimental autoimmune encephalomyelitis inducing T-cell anergy. *Blood* **106**, 1755–1761 (2005).
300. Bai, L. *et al.* Human bone marrow-derived mesenchymal stem cells induce Th2-polarized immune response and promote endogenous repair in animal models of multiple sclerosis. *Glia* **57**, 1192–1203 (2009).
301. Cohen, J. A. Mesenchymal stem cell transplantation in multiple sclerosis. *J. Neurol. Sci.* **333**, 43–49 (2013).
302. Gerdoni, E. *et al.* Mesenchymal stem cells effectively modulate pathogenic immune response in experimental autoimmune encephalomyelitis. *Ann. Neurol.* **61**, 219–227 (2007).
303. Shultz, L. D. *et al.* Multiple defects in innate and adaptive immunologic function in NOD/LtSz-scid mice. *J. Immunol.* **154**, 180–191 (1995).
304. Richardson, S. J., Willcox, A., Bone, A. J., Foulis, A. K. & Morgan, N. G. Islet-associated macrophages in type 2 diabetes. *Diabetologia* vol. 52 1686–1688 (2009).
305. Esser, N., Legrand-Poels, S., Piette, J., Scheen, A. J. & Paquot, N. Inflammation as a link between obesity, metabolic syndrome and type 2 diabetes. *Diabetes Res. Clin. Pract.* **105**, 141–150 (2014).
306. Shiota, C. *et al.* Gcg (CreERT2) knockin mice as a tool for genetic manipulation in pancreatic alpha cells. *Diabetologia* **60**, 2399–2408 (2017).

Curriculum Vitae

Section 1: University Education Background

Master of Science, Department of Physiology and Pharmacology (2018-Present)
The University of Western Ontario, London, ON
Thesis Title: Developing a model to assess the contribution of cytokeratin 19-expressing cells in multipotent stromal cell-induced islet regeneration

Bachelor of Medical Sciences, Honours Specialization in Physiology (2014-2018)
The University of Western Ontario, London, ON
Thesis Title: Identification of ductal-derived beta cell precursors stimulated by bone marrow multipotent stromal cells

---

Section 2: Research Experience

Master's Student, Dr. David Hess's Lab of Regenerative Medicine, Robarts Research Institute, Department of Physiology and Pharmacology, The University of Western Ontario, London, ON (2018-Present)

- I showed that the secreted contents (conditioned media) of human bone marrow-derived multipotent stromal cells increase proliferation of murine ductal cells *in vitro* and characterized a lineage tracing mouse model to follow the fate of cytokeratin 19-expressing cells following conditioned media injection.
- I performed cell purification preparation, cell culture expansion, immunofluorescence staining, and mouse handling and treatments, as well as analyses using flow cytometry and immunofluorescence/immunohistochemical imaging.

Summer Research Student, Dr. David Hess's Lab of Regenerative Medicine, Robarts Research Institute, London, ON (May 2018-August 2018)

- I digested pancreata from streptozotocin-treated mice to prepare for analysis by fluorescence activated cell sorting and subsequently cultured and stained purified cells by immunofluorescence.
- Cultured and expanded human bone marrow multipotent stromal cells and concentrated their conditioned media for experimental use.
- I cryosectioned and performed histological analysis on pancreatic tissue sections to image various cell markers.
- I reviewed relevant literature to develop experiments and stay up-to-date on the use of stem cells for pancreatic beta cell regeneration.

Physiology Undergraduate Honours Thesis, Dr. David Hess's Lab of Regenerative Medicine, Robarts Research Institute, Department of Physiology and Pharmacology, The University of Western Ontario, London, ON (September 2017-April 2018)

- I cultured and expanded human bone marrow multipotent stromal cells concentrated conditioned media for experimental use.
- I prepared mouse pancreatic ductal cell for isolation using fluorescence-activated cell sorting and subsequently cultured them for immunofluorescence analysis.
- I presented the results of my study and discussed how it impacts the current knowledge in the field on a scientific poster to colleagues and faculty members.

Physiology Laboratory Student, Department of Physiology and Pharmacology, The University of Western Ontario, London, ON (September 2016-April 2017)

- I clearly and concisely wrote a scientific report on the characteristics of conduction in the sciatic nerve of a pithed frog, muscle contraction of the human flexor digitorum superficialis, and interactions between the nervous and muscular systems in response to external stimuli by gathering information from laboratory experiments and relevant literature.
- I clearly articulated background information, methods, results, and the relevance of scientific experiments pertaining to visual smooth pursuit, oxygen consumption, and dexamethasone treatment on embryonic mouse tibiae in oral presentations using posters or PowerPoint presentations.

Summer Student Research Program Volunteer, Brampton Civic Hospital, Brampton, ON (June 2015-August 2015)

- I worked alongside the surgical department's clinical analyst to analyze outcome and efficiency data to brainstorm a new structure for the hospital's endoscopy department based on provincial funding guidelines

---

Section 3: University Research Presentations and Awards

Canada Graduate Scholarship-Master's, Canadian Institutes of Health Research (2019-2020; $17,500)

London Health Research Day Poster Presentation, London, ON (2019)

- I presented my work on the effects of the secreted contents of human-derived stem cells on the growth kinetics and protein expression of isolated mouse pancreatic ductal cells in culture to attendees.

Physiology and Pharmacology Research Day Poster Presentation & Award in New Student Category, Department of Physiology and Pharmacology, The University of Western Ontario, London, ON (2018)

- I presented my work on the planned methodology and preliminary results for my Master's thesis project.
- I received an award in the 'New Student' category for my poster presentation.

Till & McCulloch Meetings Poster Presentation, Ottawa, ON (2018)

- I presented my work on the effects of the secreted contents of human-derived stem cells on the growth kinetics and physical make up of isolated mouse pancreatic ductal cell cultures at a national conference.
- I received a travel award from Stem Cell Network for my work to fund my attendance at the conference.

Dean's Honor List, The University of Western Ontario, London, ON (2015-2018)

Continuing Admission Scholarship, The University of Western Ontario, London, ON (2014-2017)

Section 4: Technical Research Experience

***In vivo* procedures**: mouse subcutaneous injection, mouse intramuscular injection, mouse intraperitoneal injection, rodent anesthesia, rodent aseptic surgical techniques, mouse oral gavage, mouse intracardiac blood collection

***In vitro* procedures**: tissue culture, cell immunotyping using flow cytometry, immunofluorescence/immunohistochemistry

---

Section 5: Teaching Experience

Teaching Assistant, Department of Physiology and Pharmacology, The University of Western Ontario, London, ON (2018-2020)

- I worked with a group of graduate students to plan and lead undergraduate physiology and pharmacology experiments to develop students' reasoning and communication skills, and gave ongoing feedback and support to students to assist in their academic and personal development.
- I participated in regular team meetings to practice ongoing improvement of the performance of teaching roles.

Kaplan MCAT Prep Course Instructor and Live Online 1:1 Tutor, Kaplan Test Prep, Toronto/London, ON (2017-2020)

- I created lesson plans and led interactive learning sessions tailored to student needs to help students develop skills required to be successful on the MCAT.
- I developed study plans for students based on their specific skill sets and goals.
- I communicated with students regularly via email to keep up-to-date on their progress in their study plan and on their well-being, and adapted their study strategies moving forward accordingly.

Leadership and Academic Mentorship Program Peer Mentor, The Student Success Centre, The University of Western Ontario, London, ON (2015-2017)

- I drew on personal experience in my university career to provide guidance and advice to first and second year students in the Medical Sciences program via email and personal meetings.
- I provided first and second year students with up-to-date notices of campus events to help them expand their communication and leadership skills and gain experience by getting involved in the campus community.
- I worked with a team to facilitate a first year Chemistry review session to help first year students prepare for an upcoming exam.

Tutor (Math and Science), Western Young Tutors Club, The University of Western Ontario, London, ON (2014-2017)

- I provided teaching support to high school students to improve their grades and develop a solid foundation of basic knowledge to be used in more advanced courses.
- I created lesson plans tailored to the specific learning styles of each student to aid in their development of the problem-solving skills.